7th International Summer School on Computational Quantum Materials - abridged Lecture notes

André-Marie Tremblay

May 2024

CONTENTS

List of Figures

Part I

Lecture 1 (30 minutes)

1. MAIN RESULTS FROM SECOND QUANTIZATION

One of the most important results of quantum mechanics is that identical particles are indistinguishible: we cannot tell that a specific electron is at a given coordinate, we can just say that one electron is at that coordinate. Even in statistical mechanics, this indistinguishibility is important. This means that the wave function, say $\psi(\mathbf{r}_1, \mathbf{r}_2, \mathbf{r}_3)$ behaves in s specific way if coordinates are interchanged: If $\mathbf{r}_1$ takes any particular value, say $\mathbf{a}$, and $\mathbf{r}_2$ takes another value, say $\mathbf{b}$, then they are indistinguishible, i.e. $\psi(\mathbf{a}, \mathbf{b}, \mathbf{r}_3) = \psi(\mathbf{b}, \mathbf{a}, \mathbf{r}_3)$. But that is not the only possibility since the only thing we know for sure is that if we exchange twice the coordinates of two particles then we should return to the same wave function. This means that under one permutation of two coordinates (exchange), the wave function can not only stay invariant, or have an eigenvalue of $+1$ as in the example we just gave, it can also have an eigenvalue of -1. These two cases are clearly the only possibilities and they correspond respectively to bosons and fermions. There are more possibilities in two dimensions, but that is beyond the scope of this chapter.

When dealing with many identical particles, a basis of single-particle states is most convenient. Given what we just said however, it is clear that a simple direct product such as $|\alpha_1\rangle \otimes |\alpha_2\rangle$ cannot be used without further care because many-particle states must be symmetrized or antisymmetrized depending on whether we deal with bosons or fermions. For example, for two fermions an acceptable wave function would have the form $\sqrt{2}^{-1} \langle \mathbf{r}_1| \otimes \langle \mathbf{r}_2| \left[|\alpha_1\rangle \otimes |\alpha_2\rangle - |\alpha_2\rangle \otimes |\alpha_1\rangle \right]$. Second quantization allows us to take into account these symmetry or antisymmetry properties in a straightforward fashion. To take matrix elements directly between wave functions would be very cumbersome.

The single-particle basis state is a complete basis that is used most often. Note however that a simple wave-function such as

$$\psi(x, y) = (x - y) N e^{-|x-y|/a} \tag{1.1}$$

for two electrons in one dimension, with N and a constants, is a perfectly acceptable antisymmetric wave function. To expand it in a single-particle basis state however requires a sum over many (in general an infinite number of) antisymmetrized one-particle states. There are cases, such as the quantum Hall effect, where working directly with wave functions is desirable, but for our purposes this is not so.

Remark 1 *Second quantization as we introduce it in this chapter looks like just a convenient trick to work with many particles. Second and first quantization are completely equivalent. In first quantization, we start with particles, set up commutation relations between position and momentum, and end up with a wave function. Second quantization can be seen as starting from a wave function, or field , setting up commutation relations with the conjugate field and ending up with particles, or excitations of that field. With the electromagnetic field, in a sense we do not have the choice to do this. The next chapter will introduce the formal way to set up second quantization from first principles.*

Remark 2 *In some ways, second quantization is the perfect formalism to see*

wave-particle duality. A state will be defined by having an integer number of creation operator acting on the vacuum. Each operator creates a particle, but that particle is in a state that can be a plane wave for example. And even "worse". The many-body state can be a superposition of N particles in momentum eigenstates plus N particles in position eigenstates, to take an extreme example.

1.1 Fock space, creation and annihilation operators

As is often the case in mathematics, working in a space that is larger than the one we are interested in may simplify matters. Think of the use of functions of a complex variable to do integrals on the real axis. Here we are interested most of the time in Hamiltonians that conserve the number of particles. Nevertheless, it is easier to work in a space that contains an arbitrary number of particles. That is Fock space. Annihilation and creation operators allow us to change the number of particles while preserving indistinguishability and antisymmetry. In this representation, a three-electron state comes out as three excitations of the same vacuum state $|0\rangle$, a rather satisfactory state of affairs since it looks very much from what we know from the quantized harmonic oscillator. Particles in that context correpond simply to transitions from the ground state to excited states. To go to the third excited state, we need three particles.

It will be very helpful if you review creation-annihilation operators, also called ladder operators, in the context of the harmonic oscillator.

1.1.1 Creation-annihilation operators for fermion wave functions

For the time being our fermions *are spinless, it will be easy to add spin later on.* We assume that the one-particle states $|\alpha_i\rangle$ form an orthonormal basis for one particle, namely $\langle\alpha_i|\,\alpha_j\rangle = \delta_{i,j}$. The notation is that α denotes the basis whose components are labeled by the index. α_1 is the first state, α_2 the second state etc.

What concerns us here are many-body states. The state $|\alpha_1\alpha_2\rangle$ with two fermions is antisymmetrized, namely

$$|\alpha_1\alpha_2\rangle = \frac{1}{\sqrt{2}}\left(|\alpha_1\rangle \otimes |\alpha_2\rangle - |\alpha_2\rangle \otimes |\alpha_1\rangle\right).$$

The first Hilbert space on the right of the above expression can be either in state α_1 or α_2. Antisymmetry means that $|\alpha_1\alpha_2\rangle = -\,|\alpha_2\alpha_1\rangle$.

We define a vaccum $|0\rangle$ that contains no particle. Then, we define $a^\dagger_{\alpha_1}$ that creates a particle from the vacuum to put it in state $|\alpha_1\rangle$ and for fermions it antisymmetrizes that state will all others. In other words, $a^\dagger_{\alpha_1}|0\rangle = |\alpha_1\rangle$. Up to now, there is nothing to antisymmetrize with, but if we add another particle,

$$a^\dagger_{\alpha_1}a^\dagger_{\alpha_2}|0\rangle = |\alpha_1\alpha_2\rangle$$

then that state has to be antisymmetric. In other words, we need to have $|\alpha_2\alpha_1\rangle = -\,|\alpha_1\alpha_2\rangle$, or

$$|\alpha_2\alpha_1\rangle = a^\dagger_{\alpha_2}a^\dagger_{\alpha_1}|0\rangle = -\,|\alpha_1\alpha_2\rangle = -a^\dagger_{\alpha_1}a^\dagger_{\alpha_2}|0\rangle.$$

Clearly this will automatically be the case if we impose that the creation operators anticommute, i.e. $a^\dagger_{\alpha_i} a^\dagger_{\alpha_j} = -a^\dagger_{\alpha_j} a^\dagger_{\alpha_i}$ or

$$\left\{a^\dagger_{\alpha_i}, a^\dagger_{\alpha_j}\right\} \equiv a^\dagger_{\alpha_i} a^\dagger_{\alpha_j} + a^\dagger_{\alpha_j} a^\dagger_{\alpha_i} = 0. \tag{1.2}$$

This property is a property of the operators, independently of the specific state they act on. The anticommutation property garantees the Pauli exclusion principle as we know it, since if $i = j$ then the above leads to

$$a^\dagger_{\alpha_i} a^\dagger_{\alpha_i} = -a^\dagger_{\alpha_i} a^\dagger_{\alpha_i}. \tag{1.3}$$

The only operator that is equal to minus itself is zero. Hence we cannot create two particles in the same state.

If we want the whole formalism to make sense, we want to have a sign change to occur whenever we interchange two fermions, wherever they are in the list. In other words, we want $|\alpha_i\alpha_j \ldots \alpha_k \ldots \alpha_l \ldots \alpha_m\rangle = -|\alpha_i\alpha_j \ldots \alpha_l \ldots \alpha_k \ldots \alpha_m\rangle$. To see that our formalism works, you can write the state to the left in terms of creation operators on the vacuum

$$|\alpha_i\alpha_j \ldots \alpha_k \ldots \alpha_l \ldots \alpha_m\rangle = a^\dagger_{\alpha_i} a^\dagger_{\alpha_j} \ldots a^\dagger_{\alpha_k} \ldots a^\dagger_{\alpha_l} \ldots a^\dagger_{\alpha_m} |0\rangle. \tag{1.4}$$

If there are n operators between $a^\dagger_{\alpha_k}$ and $a^\dagger_{\alpha_l}$, we pay a $(-1)^n$ to place $a^\dagger_{\alpha_k}$ to the left of $a^\dagger_{\alpha_l}$. Then there is a (-1) to interchange $a^\dagger_{\alpha_k}$ and $a^\dagger_{\alpha_l}$, and finally another $(-1)^n$ to take $a^\dagger_{\alpha_l}$ where $a^\dagger_{\alpha_k}$ was. Since $(-1)^{2n} = 1$, there is only the minus sign from the "local" interchange $a^\dagger_{\alpha_k}$ and $a^\dagger_{\alpha_l}$ that is left.

Note that with fermions we need to determine an initial order of operators for the states. That is totally arbitrary because of the phase arbitrariness of quantum mechanics. But then, during the calculations we need to keep track of the minus signs.

Now that we know how to create, let us move to destruction. The destruction operators are the adjoints of $a^\dagger_{\alpha_i}$. Their anticommutation property follows by taking the adjoint of $\left\{a^\dagger_{\alpha_i}, a^\dagger_{\alpha_j}\right\} = 0$:

$$\left\{a_{\alpha_i}, a_{\alpha_j}\right\} \equiv a_{\alpha_i} a_{\alpha_j} + a_{\alpha_j} a_{\alpha_i} = 0. \tag{1.5}$$

These adjoint operators are defined as follows

$$\langle\alpha_1| = \langle 0| a_{\alpha_1}. \tag{1.6}$$

They create and antisymmetrize in bras instead of kets. When they act on kets instead of bras, they remove a particle instead of adding it. In particular,

$$a_{\alpha_1} |0\rangle = 0. \tag{1.7}$$

This is consistent with $\langle\alpha_1|\, 0\rangle = 0 = \langle 0| a_{\alpha_1} |0\rangle$.

Since we also want states to be normalized, we need

$$\langle\alpha_i|\, \alpha_j\rangle = \langle 0| a_{\alpha_i} a^\dagger_{\alpha_j} |0\rangle = \delta_{i,j}. \tag{1.8}$$

Since we already know that $a_{\alpha_1} |0\rangle = 0$, that will automatically be satisfied if we write the following anticommutation relation between creation and annihilation operators

$$\left\{a_{\alpha_i}, a^\dagger_{\alpha_j}\right\} \equiv a_{\alpha_i} a^\dagger_{\alpha_j} + a^\dagger_{\alpha_j} a_{\alpha_i} = \delta_{i,j} \tag{1.9}$$

because then $\langle 0| a_{\alpha_i} a^\dagger_{\alpha_j} |0\rangle = -\langle 0| a^\dagger_{\alpha_j} a_{\alpha_i} |0\rangle + \langle 0| \delta_{i,j} |0\rangle = 0 + \delta_{i,j}$. The above three sets of anticommutation relations are called canonical.

At this point one may ask why anticommutation instead of commutation. Well, two reasons. The first one is that given the previous anticommutation rules, this choice seems elegant. The second one is that with this rule, we can define the very useful operator, the number operator

$$\widehat{n}_{\alpha_i} = a^\dagger_{\alpha_i} a_{\alpha_i}. \tag{1.10}$$

That operator just counts the number of particles in state α_i. To see that this is so and that anticommutation is needed for this to work, we look at a few simple cases. First note that if $\widehat{n}_{\alpha_i}$ acts on a state where α_i is not occupied, then

$$\widehat{n}_{\alpha_i} |\alpha_j\rangle = \widehat{n}_{\alpha_i} a^\dagger_{\alpha_j} |0\rangle = a^\dagger_{\alpha_i} a_{\alpha_i} a^\dagger_{\alpha_j} |0\rangle = -a^\dagger_{\alpha_i} a^\dagger_{\alpha_j} a_{\alpha_i} |0\rangle = 0. \tag{1.11}$$

In an arbitrary many-particle state $|\alpha_j, \alpha_k, \ldots\rangle$, if the state α_i does not appear in the list, then when I compute $\widehat{n}_{\alpha_i} |\alpha_j, \alpha_k, \ldots\rangle$, I will be able to anticommute the destruction operator all the way to the vacuum and obtain zero. On the other hand, if α_i appears in the list then

$$\widehat{n}_{\alpha_i} \left(a^\dagger_{\alpha_j} a^\dagger_{\alpha_k} \ldots a^\dagger_{\alpha_i} \ldots a^\dagger_{\alpha_l} |0\rangle \right) = a^\dagger_{\alpha_j} a^\dagger_{\alpha_k} \ldots \widehat{n}_{\alpha_i} a^\dagger_{\alpha_i} \ldots a^\dagger_{\alpha_l} |0\rangle . \tag{1.12}$$

I have been able to move the operator all the way to the indicated position without any additional minus sign because both the destruction and the annihilation operators anticommute with the creation operators that do not have the same labels. The minus signs from the creation and from the annihilation operators in $a^\dagger_{\alpha_i} a_{\alpha_i}$ cancel each other. This would not have occured if a_{α_i} and $a^\dagger_{\alpha_j}$ had commuted instead of anticommuted while a_{α_i} and a_{α_j} had anticommuted. Now, let us focus on $\widehat{n}_{\alpha_i} a^\dagger_{\alpha_i}$ in the last equation. Using our anticommutation properties, one can check that

$$\widehat{n}_{\alpha_i} a^\dagger_{\alpha_i} = a^\dagger_{\alpha_i} a_{\alpha_i} a^\dagger_{\alpha_i} = a^\dagger_{\alpha_i} \left(1 - a^\dagger_{\alpha_i} a_{\alpha_i} \right). \tag{1.13}$$

Since there are never two fermions in the same state, now the destruction operator in the above equation is free to move and annihilate the vacuum state, and

$$\widehat{n}_{\alpha_i} \left(a^\dagger_{\alpha_j} a^\dagger_{\alpha_k} \ldots a^\dagger_{\alpha_i} \ldots a^\dagger_{\alpha_l} |0\rangle \right) = \left(a^\dagger_{\alpha_j} a^\dagger_{\alpha_k} \ldots a^\dagger_{\alpha_i} \ldots a^\dagger_{\alpha_l} |0\rangle \right). \tag{1.14}$$

This means that $\widehat{n}_{\alpha_i}$ does simply count the number of particles. It gives one or zero depending on whether the state is occupied or not.

Remark 3 *We define the bra* $\langle \alpha_1 \alpha_2 |$ *by*

$$\langle \alpha_1 \alpha_2 | = \left(|\alpha_1 \alpha_2\rangle \right)^\dagger = \left(a^\dagger_{\alpha_1} a^\dagger_{\alpha_2} |0\rangle \right)^\dagger = \langle 0 | a_{\alpha_2} a_{\alpha_1}. \tag{1.15}$$

Notice the change in the order of labels between $\langle \alpha_1 \alpha_2 |$ *and* $\langle 0 | a_{\alpha_2} a_{\alpha_1}$.

1.2 Change of basis

1.2.1 General case

Creation-annihilation operators change basis in a way that is completely determined by the way one changes basis in single-particle states. Suppose one wants to change from the α basis to the μ basis, namely

$$|\mu_m\rangle = \sum_i |\alpha_i\rangle \langle \alpha_i | \mu_m \rangle \tag{1.16}$$

which is found by inserting the completeness relation. Let creation operator $a^\dagger_{\alpha_i}$ create single particle state $|\alpha_i\rangle$ and antisymmetrize while creation operator $c^\dagger_{\mu_m}$ creates single particle state $|\mu_m\rangle$ and antisymmetrize. Then the correspondance between both sets of operators is clearly

$$c^\dagger_{\mu_m} = \sum_i a^\dagger_{\alpha_i} \langle \alpha_i | \, \mu_m \rangle \tag{1.17}$$

with the adjoint

$$c_{\mu_m} = \sum_i \langle \mu_m | \, \alpha_i \rangle \, a_{\alpha_i} \tag{1.18}$$

given as usual that $\langle \alpha_i | \, \mu_m \rangle = \langle \mu_m | \, \alpha_i \rangle^*$. Physically then, creating a particle in a state $|\mu_m\rangle$ is like creating it in a linear combination of states $|\alpha_i\rangle$. We can do the change of basis in the other direction as well.

If we define with $\langle \alpha_i | \, \mu_n \rangle$ a matrix for the change of basis, this matrix is unitary if $\langle \mu_m | \, \mu_n \rangle = \delta_{\mu_m,\mu_n}$. Indeed, inserting a complete set of states, we see that $\sum_i \langle \mu_m | \, \alpha_i \rangle \langle \alpha_i | \, \mu_n \rangle = \langle \mu_m | \, \mu_n \rangle = \delta_{\mu_m,\mu_n}$.

Since we have defined new creation- annihilation operators, it is quite natural to ask what are their commutation or anticommutation relations. It is easy to find using the change of basis formula and the completeness relation. Assuming that the creation-annihilation operators are for fermions, we find

$$\begin{aligned} \left\{ c_{\mu_m}, c^\dagger_{\mu_n} \right\} &= \sum_i \sum_j \langle \mu_m | \, \alpha_i \rangle \left\{ a_{\alpha_i}, a^\dagger_{\alpha_j} \right\} \langle \alpha_j | \, \mu_n \rangle & (1.19) \\ &= \sum_i \sum_j \langle \mu_m | \, \alpha_i \rangle \, \delta_{i,j} \, \langle \alpha_j | \, \mu_n \rangle & (1.20) \\ &= \sum_i \langle \mu_m | \, \alpha_i \rangle \langle \alpha_i | \, \mu_n \rangle = \langle \mu_m | \, \mu_n \rangle \, . & (1.21) \end{aligned}$$

Hence, if the transformation between basis is unitary, the new operators obey canonical anticommutation relations, namely

$$\left\{ c_{\mu_m}, c^\dagger_{\mu_n} \right\} = \delta_{m,n}. \tag{1.22}$$

When the change of basis is unitary, we say that we have made a canonical transformation. The same steps show that a unitary basis change also preserves the canonical commutation relations for bosons.

Remark 4 *The notation c_{μ_m}, a_{α_i} is rather clumsy. In practice, one uses, for example, f_i to label destruction operators for an f electron in a state i, d_i for d electrons, c_i for conduction electrons etc. In other words, the basis is identified by the choice of label for creation-annihilation operators, and the component by the index of that symbol.*

1.2.2 The position and momentum space basis

We recall a strange basis. In this basis, we take continuum notation for space and discrete notation for momentum. Starting from $\langle \mathbf{r} \, | \mathbf{r}' \rangle = \delta \left(\mathbf{r} - \mathbf{r}' \right)$ and $\langle \mathbf{k} \, | \mathbf{k}' \rangle = \delta_{\mathbf{k},\mathbf{k}'}$ it is easy to check by left or right multiplying that the following operators give the completeness relation

$$\sum_{\mathbf{k}} |\mathbf{k}\rangle \langle \mathbf{k}| = 1 = \int d\mathbf{r} \, |\mathbf{r}\rangle \langle \mathbf{r}|$$

To go from one basis to the other, we use plane-waves that are normalized to unity in a volume $\mathcal{V}$, namely

$$\langle \mathbf{r} \,|\mathbf{k}\rangle = \frac{1}{\sqrt{\mathcal{V}}} e^{i\mathbf{k}\cdot\mathbf{r}} \tag{1.23}$$

$$\langle \mathbf{k} \,|\mathbf{r}\rangle = \frac{1}{\sqrt{\mathcal{V}}} e^{-i\mathbf{k}\cdot\mathbf{r}} \tag{1.24}$$

We can check that $\langle \mathbf{r} \,|\mathbf{r}'\rangle$ is normalized in the continuum while $\langle \mathbf{k} \,|\mathbf{k}'\rangle$ is normalized as a discrete set of states

$$\langle \mathbf{r} \,|\mathbf{r}'\rangle = \sum_{\mathbf{k}} \langle \mathbf{r} \,|\mathbf{k}\rangle \langle \mathbf{k} \,|\mathbf{r}'\rangle = \frac{1}{\mathcal{V}} \sum_{\mathbf{k}} e^{i\mathbf{k}\cdot(\mathbf{r}-\mathbf{r}')} = \int \frac{d\mathbf{k}}{(2\pi)^3} e^{i\mathbf{k}\cdot(\mathbf{r}-\mathbf{r}')} = \delta(\mathbf{r}-\mathbf{r}') \tag{1.25}$$

$$\langle \mathbf{k} \,|\mathbf{k}'\rangle = \int d\mathbf{r} \langle \mathbf{k} \,|\mathbf{r}\rangle \langle \mathbf{r} \,|\mathbf{k}'\rangle = \frac{1}{\mathcal{V}} \int d\mathbf{r} e^{-i\mathbf{r}\cdot(\mathbf{k}-\mathbf{k}')} = \delta_{\mathbf{k},\mathbf{k}'} \ . \tag{1.26}$$

To take the continuum limit of the discrete sum over $\mathbf{k}$, one uses eigenstates of momentum in a box where the separation between states is given by $\Delta k_x = 2\pi/L_x$, where L_x is the size of the box in the x direction, and similarly for the other directions.

Creation operators in eigenstates of position are usually denoted, $\psi^\dagger(\mathbf{r})$, while creation operators in eigenstates of momentum are denoted $c^\dagger_{\mathbf{k}}$. The basis change between them leads to

$$\psi^\dagger(\mathbf{r}) = \sum_{\mathbf{k}} c^\dagger_{\mathbf{k}} \langle \mathbf{k} \,|\mathbf{r}\rangle = \frac{1}{\sqrt{\mathcal{V}}} \sum_{\mathbf{k}} c^\dagger_{\mathbf{k}} e^{-i\mathbf{k}\cdot\mathbf{r}} \tag{1.27}$$

$$\psi(\mathbf{r}) = \sum_{\mathbf{k}} \langle \mathbf{r} \,|\mathbf{k}\rangle c_{\mathbf{k}} = \frac{1}{\sqrt{\mathcal{V}}} \sum_{\mathbf{k}} e^{i\mathbf{k}\cdot\mathbf{r}} c_{\mathbf{k}}. \tag{1.28}$$

Given our above convention, the momentum operators obey the algebra of a discrete set of creation operators. Taking fermions as an example, we then have

$$\boxed{\left\{c_{\mathbf{k}}, c^\dagger_{\mathbf{k}'}\right\} = \delta_{\mathbf{k},\mathbf{k}'} \quad ; \quad \{c_{\mathbf{k}}, c_{\mathbf{k}'}\} = \left\{c^\dagger_{\mathbf{k}}, c^\dagger_{\mathbf{k}'}\right\} = 0} \tag{1.29}$$

while the position space creation-annihilation operators obey

$$\boxed{\left\{\psi(\mathbf{r}), \psi^\dagger(\mathbf{r}')\right\} = \sum_{\mathbf{k}} \sum_{\mathbf{k}'} \langle \mathbf{r} \,|\mathbf{k}\rangle \left\{c_{\mathbf{k}}, c^\dagger_{\mathbf{k}'}\right\} \langle \mathbf{k}' \,|\mathbf{r}'\rangle = \sum_{\mathbf{k}} \langle \mathbf{r} \,|\mathbf{k}\rangle \langle \mathbf{k} \,|\mathbf{r}'\rangle = \langle \mathbf{r} \,|\mathbf{r}'\rangle = \delta(\mathbf{r}-\mathbf{r}')} \tag{1.30}$$

$$\boxed{\{\psi(\mathbf{r}), \psi(\mathbf{r}')\} = \left\{\psi^\dagger(\mathbf{r}), \psi^\dagger(\mathbf{r}')\right\} = 0} \tag{1.31a}$$

1.3 Wave functions

With N-particles, the wave function is obtained by projection on a position basis. If we have a single many-body state, $|\Phi\rangle = a^\dagger_{\alpha_1} a^\dagger_{\alpha_2} \ldots a^\dagger_{\alpha_i} \ldots a^\dagger_{\alpha_N} |0\rangle$ then the correspondance between first and second quantized description is in a sense contained in the following expression

$$\langle \mathbf{r}_1 \mathbf{r}_2 ... \mathbf{r}_N| \, \Phi\rangle = \langle \mathbf{r}_1 \mathbf{r}_2 ... \mathbf{r}_N| \, \alpha_1 \alpha_2 ... \alpha_N\rangle = \langle 0| \, \psi(\mathbf{r}_N) \ldots \psi(\mathbf{r}_2) \psi(\mathbf{r}_1) \, a^\dagger_{\alpha_1} a^\dagger_{\alpha_2} \ldots a^\dagger_{\alpha_i} \ldots a^\dagger_{\alpha_N} |0\rangle$$

which is proportional to a so-called Slater determinant if we have fermions. Indeed, using our change of basis formula,

$$\psi(\mathbf{r}) = \sum_i \langle \mathbf{r} | \alpha_i \rangle a_{\alpha_i} = \sum_i \phi_{\alpha_i}(\mathbf{r}) a_{\alpha_i} \tag{1.32}$$

any of the positions $\mathbf{r}$ can be in a state α_i, or vice versa the position $\mathbf{r}$ has amplitudes on all states, so you can check that the (unnormalized) wave function is equal to

$$\sum_p \varepsilon_p \phi_{\alpha_{p(1)}}(\mathbf{r}_1) \phi_{\alpha_{p(2)}}(\mathbf{r}_2) ... \phi_{\alpha_{p(N)}}(\mathbf{r}_N) = \text{Det} \begin{bmatrix} \phi_{\alpha_1}(\mathbf{r}_1) & \phi_{\alpha_1}(\mathbf{r}_2) & ... & \phi_{\alpha_1}(\mathbf{r}_N) \\ \phi_{\alpha_2}(\mathbf{r}_1) & \phi_{\alpha_2}(\mathbf{r}_2) & ... & \phi_{\alpha_2}(\mathbf{r}_N) \\ ... & ... & ... & \\ \phi_{\alpha_N}(\mathbf{r}_1) & \phi_{\alpha_N}(\mathbf{r}_2) & & \phi_{\alpha_N}(\mathbf{r}_N) \end{bmatrix} \tag{1.33}$$

where the sum is over all permutations $p(i)$ of the set i and ε_p is the signature of the permutation, given by $+1$ if the number of transpositions (interchanges) of pairs of creation operators to get back to the original order is even and -1 if the number of transpositions is odd.

Remark 5 *Closure relation and normalization:*

$$\boxed{\frac{1}{N!} \int d\mathbf{r}_1 d\mathbf{r}_2 ... d\mathbf{r}_N |\mathbf{r}_1 \mathbf{r}_2 ... \mathbf{r}_N\rangle \langle \mathbf{r}_1 \mathbf{r}_2 ... \mathbf{r}_N|} \tag{1.34}$$

This closure relation implies that if we want to recover the usual expression for normalized wave functions, $\langle \Phi | \Phi \rangle = 1$, the determinant above should be multiplied by $1/\sqrt{N!}$. We recover our example with two particles where the normalization is $1/\sqrt{2}$.

Remark 6 *Many-Body wave function and basis states: It is very important to note that the most general state must be written as a linear combination of the states $a^\dagger_{\alpha_1} a^\dagger_{\alpha_2} \dots a^\dagger_{\alpha_i} \dots a^\dagger_{\alpha_N} |0\rangle$ or of the above Slater determinants. In other words, a general many body state $|\Phi\rangle$ must be expanded as*

$$|\Phi\rangle = \sum_{i,j,...\ell,...} C^{i,j,...\ell,...} \left(a^\dagger_{\alpha_i} a^\dagger_{\alpha_j} \dots a^\dagger_{\alpha_\ell} \dots |0\rangle \right) \tag{1.35}$$

where $C^{i,j,...\ell,...}$ are expansion coefficients. In a way, the Feynman diagrams that we will encounter are a way to write the various components of a general state.

Remark 7 *Wave functions live in Hilbert space: It is important to note that the (unnormalized) wave function*

$$\psi_{\alpha_1 \alpha_2 ... \alpha_N}(\mathbf{r}_1 \mathbf{r}_2 ... \mathbf{r}_N) = \langle \mathbf{r}_1 \mathbf{r}_2 ... \mathbf{r}_N | \, \alpha_1 \alpha_2 ... \alpha_N \rangle$$

propagates, so to speak, in Hilbert space, not in ordinary space. The waves that we are familiar with in the classical world are functions of only the three spatial coordinates. Not so for the Schrödinger wave, unless there is a single particle to describe.

Remark 8 *One-particle wave function: The quantity $\psi_{\alpha_1 \alpha_2 ... \alpha_N}(\mathbf{r}_1 \mathbf{r}_2 ... \mathbf{r}_N)$ is often-called a one-particle wave function in the sense that it is just one member of a complete set of states where all particles are independent. The most general state $|\Phi\rangle$ above contains correlations, in addition to those induced by symmetrization or antisymmetrization.*

Remark 9 *Particles and waves: In $\psi_{\alpha_1 \alpha_2 ... \alpha_N}(\mathbf{r}_1 \mathbf{r}_2 ... \mathbf{r}_N)$ we see the wave, but we also see that there are N particles. And we need all this information to describe the system. The continuous and discrete aspects are present all at once.*

Remark 10 *For bosons, the expression is similar, but we compute the determinant without the signs coming from the permutations. This is called a permanent. The normalization will also have the* $1/\sqrt{N!}$ *coming from the closure relation in addition to the prefactor* $1/\sqrt{\prod_i n_{\alpha_i}!}$.

1.4 One-body operators

The matrix elements of an arbitrary one-body operator $\widehat{U}$ (in the $N-$particle case) may be computed in the many-body basis made of one-body states where $\widehat{U}$ is diagonal. As an example of one-body operator, the operator $\widehat{U}$ could be an external potential so that the diagonal basis is position space. In the diagonal basis,

$$\widehat{U}\left|\alpha_i\right\rangle = U_{\alpha_i}\left|\alpha_i\right\rangle = \left\langle\alpha_i\right|\widehat{U}\left|\alpha_i\right\rangle\left|\alpha_i\right\rangle \tag{1.36}$$

where U_{α_i} is the eigenvalue. In this basis, one sees that the effect of the one-body operator is to produce the same eigenvalue, whatever the particular order of the states on which the first-quantized operator acts. In general then when we have N particles in a many-body state, the action of the one-body operator is

$$\sum_{\mu=1}^{N}\widehat{U}_\mu\left|\alpha_i,\alpha_j,\alpha_k\ldots\right\rangle = \left(U_{\alpha_i}+U_{\alpha_j}+U_{\alpha_k}+\ldots\right)\left|\alpha_i,\alpha_j,\alpha_k\ldots\right\rangle \tag{1.37}$$

Knowing the action of the number operator, we can write the same result differently

$$\sum_{\mu=1}^{N}\widehat{U}_\mu\left|\alpha_i,\alpha_j,\alpha_k\ldots\right\rangle = \sum_{m=1}^{\infty}U_{\alpha_m}\widehat{n}_{\alpha_m}\left|\alpha_i,\alpha_j,\alpha_k\ldots\right\rangle \tag{1.38}$$

in other words, there will be a contribution as long as α_i appears in the state. And if α_i occurs more than once, the corresponding eigenvalue U_{α_i} will appear more than once. Note also that I have assumed that there there is an infinite number of basis states $\left|\alpha_m\right\rangle$.

We hold a very elegant result. The one-body operator $\sum_m U_{\alpha_m}\widehat{n}_{\alpha_m}$ in second quantized notation makes no reference to the total number of particles nor to whether we are dealing with bosons or fermions. Note that in first quantization the sum extends over all particle coordinates whereas in second quantization the sum over m extends over all *states*.

Using the change of basis formula explained above, we have that

$$\sum_i\left\langle\alpha_i\right|\widehat{U}\left|\alpha_i\right\rangle a^\dagger_{\alpha_i}a_{\alpha_i} = \sum_i\sum_m\sum_n c^\dagger_{\mu_m}\left\langle\mu_m\right.\left|\alpha_i\right\rangle\left\langle\alpha_i\right|\widehat{U}\left|\alpha_i\right\rangle\left\langle\alpha_i\right.\left|\mu_n\right\rangle c_{\mu_n}. \tag{1.39}$$

Since U is diagonal, we can add a sum over α_j and use the closure relation to arrive at the final result

$$\boxed{\sum_i U_{\alpha_i}\widehat{n}_{\alpha_i} = \sum_m\sum_n c^\dagger_{\mu_m}\left\langle\mu_m\right|\widehat{U}\left|\mu_n\right\rangle c_{\mu_n}.} \tag{1.40}$$

Let us give examples in the position and momentum representation. A one-body scattering potential in the continuum would be represented in second quantized version[1] by

$$\boxed{\widehat{U} = \int d\mathbf{r}U\left(\mathbf{r}\right)\psi^\dagger\left(\mathbf{r}\right)\psi\left(\mathbf{r}\right)} \tag{1.41}$$

[1] We have denoted by $\widehat{U}$ the operator in both first and second quantization. Strictly speaking the operators are different. One needs to specify which representation one is working in.

which looks similar to the usual Schrödinger average. Similarly, the kinetic energy operator in the momentum representation is diagonal and it can be rewritten in the position basis using the change of variables of the previous section.

$$\widehat{T} = \sum_{\mathbf{k}} \langle \mathbf{k} | \frac{k^2}{2m} | \mathbf{k} \rangle c_{\mathbf{k}}^{\dagger} c_{\mathbf{k}} = \sum_{\mathbf{k}} \int d\mathbf{r} \int d\mathbf{r}' \psi^{\dagger}(\mathbf{r}) \langle \mathbf{r} | \mathbf{k} \rangle \langle \mathbf{k} | \frac{k^2}{2m} | \mathbf{k} \rangle \langle \mathbf{k} | \mathbf{r}' \rangle \psi(\mathbf{r}') \tag{1.42}$$

$$= \frac{1}{\mathcal{V}} \sum_{\mathbf{k}} \int d\mathbf{r} \int d\mathbf{r}' \psi^{\dagger}(\mathbf{r}) e^{i\mathbf{k}\cdot(\mathbf{r}-\mathbf{r}')} \frac{k^2}{2m} \psi(\mathbf{r}') \tag{1.43}$$

$$= \int \frac{d^3\mathbf{k}}{(2\pi)^3} \int d\mathbf{r} \int d\mathbf{r}' \psi^{\dagger}(\mathbf{r}) \left(-\frac{1}{2m} \nabla_{\mathbf{r}'}^2 e^{i\mathbf{k}\cdot(\mathbf{r}-\mathbf{r}')} \right) \psi(\mathbf{r}') \tag{1.44}$$

$$= \int d\mathbf{r} \int d\mathbf{r}' \psi^{\dagger}(\mathbf{r}) \left(-\frac{1}{2m} \nabla_{\mathbf{r}'}^2 \delta(\mathbf{r}-\mathbf{r}') \right) \psi(\mathbf{r}') \tag{1.45}$$

Using partial integration and assuming that everything vanishes at infinity or is periodic, we obtain,

$$\boxed{\widehat{T} = \left(-\tfrac{1}{2m}\right) \int d\mathbf{r} \psi^{\dagger}(\mathbf{r}) \left(\nabla^2 \psi(\mathbf{r}) \right) = \tfrac{1}{2m} \int d\mathbf{r} \boldsymbol{\nabla} \psi^{\dagger}(\mathbf{r}) \cdot \nabla \psi(\mathbf{r})}. \tag{1.46}$$

Again notice that second-quantized operators look like simple Schrödinger averages over wave functions.

1.5 Number operator and the nature of states in second quantization

This section is nothing new compared with what we already know, but it gives a different perspective on the whole formalism. Once an operator (the "single-particle" Hamiltonian for example) is in the diagonal form $\sum_i H_{\alpha_i} \widehat{n}_{\alpha_i}$, the theorem on commutators of ladder operators can be used to find its eigenstates. Indeed, this theorem tells that if $|n\rangle$ is an eigenstate of $\widehat{n}_{\alpha_i}$, then $a_{\alpha_i}^{\dagger} |n\rangle$ is an eigenstate with eigenvalue $n+1$. If a ground state exists, this means that there is a state (the vacuum) which is such that $a_{\alpha_i} |0\rangle = 0$, in other words we cannot decrease the eigenvalue indefinitely if U_{α_i} for example is the Hamiltonian. Hence, the eigentates are of the form $a_{\alpha_1}^{\dagger} a_{\alpha_2}^{\dagger} \ldots a_{\alpha_i}^{\dagger} \ldots a_{\alpha_N}^{\dagger} |0\rangle$ for N particles. This is analogous to what we have discussed for the harmonic oscillator.

It is important to note that these states form a complete set of many-body states. The most general eigenstate will be a linear combination of such states.

Remark 11 *The need to diagonalize: Note that to find the eigenstates of* $\sum_m \sum_n c_{\mu_m}^{\dagger} \langle \mu_m | \widehat{H} | \mu_n \rangle c_{\mu_n}$, *we need to diagonalize the matrix* $\langle \mu_m | \widehat{H} | \mu_n \rangle$. *The rules have not changed!*

1.6 Two-body operators.

A two-body operator involves the coordinates of two particles. An example is the Coulomb potential with position basis where $\widehat{V}_{1,2} = \widehat{V}(\mathbf{R}_1, \mathbf{R}_2)$ which is diagonal in position space, namely $\widehat{V}(\mathbf{R}_1, \mathbf{R}_2) |\mathbf{r}'\rangle \otimes |\mathbf{r}\rangle = V(\mathbf{r}', \mathbf{r}) |\mathbf{r}'\rangle \otimes |\mathbf{r}\rangle$.

Let us return to the general discussion. If we let the indices in $\widehat{V}_{1,2}$ refer to the potential energy between the first and second particles in the direct product, and if we are in the diagonal basis, we have in first quantization that

$$\widehat{V}_{1,2}\left|\alpha_i\right\rangle \otimes \left|\alpha_j\right\rangle = V_{\alpha_i\alpha_j}\left|\alpha_i\right\rangle \otimes \left|\alpha_j\right\rangle \tag{1.47}$$

$$\widehat{V}_{1,3}\left|\alpha_i\right\rangle \otimes \left|\alpha_j\right\rangle \otimes \left|\alpha_k\right\rangle = V_{\alpha_i\alpha_k}\left|\alpha_i\right\rangle \otimes \left|\alpha_j\right\rangle \otimes \left|\alpha_k\right\rangle \tag{1.48}$$

The abreviation $\widehat{V}_{1,3}$ in the position basis means $\widehat{V}\left(\mathbf{R}_1, \mathbf{R}_3\right)$ where $\mathbf{R}_1$ acts on the first one-particle Hilbert space and $\mathbf{R}_3$ acts on the third. In this basis, one sees that again the eigenvalue does not depend on the order in which the states are when the first-quantized operator acts. This means that

$$\frac{1}{2}\sum_{\mu=1}^{N}\sum_{\substack{\nu=1\\ \nu\neq\mu}}^{N}\widehat{V}_{\mu,\nu}\left|\alpha_i, \alpha_j, \alpha_k \ldots\right\rangle = \left(V_{\alpha_i\alpha_j} + V_{\alpha_i\alpha_k} + V_{\alpha_j\alpha_k} + \ldots\right)\left|\alpha_i, \alpha_j, \alpha_k \ldots\right\rangle \tag{1.49}$$

where now on the right-hand side every interaction is counted only once. As above, $\widehat{V}_{\mu,\nu}$ refers to the potential energy between the μ and ν particles. If $\left|\alpha_i\right\rangle \neq \left|\alpha_j\right\rangle$, then the number of times that $V_{\alpha_i\alpha_j}$ occurs in the double sum is equal to $n_{\alpha_i}n_{\alpha_j}$. However, when $\left|\alpha_i\right\rangle = \left|\alpha_j\right\rangle$, then the number of times that $V_{\alpha_i\alpha_j}$ occurs is equal to $n_{\alpha_i}(n_{\alpha_i} - 1)$ because we are not counting the interaction of the particle with itself, as specified by $\nu \neq \mu$ in the sum. In general then,

$$\frac{1}{2}\sum_{\mu=1}^{N}\sum_{\substack{\nu=1\\ \nu\neq\mu}}^{N}\widehat{V}_{\mu,\nu}\left|\alpha_i, \alpha_j, \alpha_k \ldots\right\rangle = \frac{1}{2}\sum_{m=1}^{\infty}\sum_{n=1}^{\infty}V_{\alpha_m\alpha_n}\left(\widehat{n}_{\alpha_m}\widehat{n}_{\alpha_n} - \delta_{m,n}\widehat{n}_{\alpha_n}\right)\left|\alpha_i, \alpha_j, \alpha_k \ldots\right\rangle. \tag{1.50}$$

Again the expression for the operator to the right is independent of the state it acts on. It is valid in general. I assumed that the basis α has an infinite number of states.

We can simplify the expression further. Defining

$$\boxed{\zeta = -1 \quad \text{for} \quad \text{fermions}} \tag{1.51}$$

$$\boxed{\zeta = 1 \quad \text{for} \quad \text{bosons}} \tag{1.52}$$

we can rewrite $\widehat{n}_{\alpha_i}\widehat{n}_{\alpha_j} - \delta_{i,j}\widehat{n}_{\alpha_i}$ in terms of creation and annihilation operators in such a way that the form is valid for both fermions and bosons

$$\widehat{n}_{\alpha_i}\widehat{n}_{\alpha_j} - \delta_{i,j}\widehat{n}_{\alpha_i} = a^\dagger_{\alpha_i}a_{\alpha_i}a^\dagger_{\alpha_j}a_{\alpha_j} - \delta_{i,j}a^\dagger_{\alpha_i}a_{\alpha_i} = a^\dagger_{\alpha_i}\zeta a^\dagger_{\alpha_j}a_{\alpha_i}a_{\alpha_j} = a^\dagger_{\alpha_i}a^\dagger_{\alpha_j}a_{\alpha_j}a_{\alpha_i}. \tag{1.53}$$

Second quantized operators are thus written in the simple form

$$\boxed{\tfrac{1}{2}\textstyle\sum_i\sum_j V_{\alpha_i\alpha_j}\left(\widehat{n}_{\alpha_i}\widehat{n}_{\alpha_j} - \delta_{i,j}\widehat{n}_{\alpha_i}\right) \equiv \tfrac{1}{2}\sum_i\sum_j\left(\alpha_i\alpha_j\right|V\left|\alpha_i\alpha_j\right)a^\dagger_{\alpha_i}a^\dagger_{\alpha_j}a_{\alpha_j}a_{\alpha_i}}} \tag{1.54}$$

where

$$\left|\alpha_i\alpha_j\right) \equiv \left|\alpha_i\right\rangle \otimes \left|\alpha_j\right\rangle. \tag{1.55}$$

Under unitary transformation to an arbitrary basis we have

$$\boxed{\widehat{V} = \tfrac{1}{2}\textstyle\sum_m\sum_n\sum_p\sum_q\left(\mu_m\mu_n\right|V\left|\mu_p\mu_q\right)c^\dagger_{\mu_m}c^\dagger_{\mu_n}c_{\mu_q}c_{\mu_p}}. \tag{1.56}$$

Definition 1 *When a series of creation and annihilation operators are placed in such an order where all destruction operators are to the right, one calls this "normal order".*

Remark 12 *Note the inversion in the order of μ_p and μ_q in the annihilation operators compared with the order in the matrix elements (This could have been for the creation operator instead).*

Remark 13 *Note that the first state $(\alpha_i\alpha_j|\,V\,|\alpha_i\alpha_j)$ in both the bra and the ket is associated with the first coordinate in V, and the second state with the second label in V. This means that the notation $(\mu_m\mu_n|\,V\,|\mu_p\mu_q)$ for the two-body matrix element stands for, in the coordinate representation for example,*

$$\int d\mathbf{r}_1 d\mathbf{r}_2 \phi^*_{\mu_m}(\mathbf{r}_1)\,\phi^*_{\mu_n}(\mathbf{r}_2)\,V(\mathbf{r}_1-\mathbf{r}_2)\,\phi_{\mu_p}(\mathbf{r}_1)\,\phi_{\mu_q}(\mathbf{r}_2)\,. \tag{1.57}$$

Example 2 *In the case of a potential, such as the Coulomb potential, which acts on the densities, we have*

$$\boxed{\widehat{V} = \tfrac{1}{2}\int d\mathbf{x}\int d\mathbf{y} v(\mathbf{x}-\mathbf{y})\,\psi^\dagger(\mathbf{x})\,\psi^\dagger(\mathbf{y})\,\psi(\mathbf{y})\,\psi(\mathbf{x})}\,. \tag{1.58}$$

Part II

Lecture 2 (45 minutes)
Time-ordered product, Green functions

2. PERTURBATION THEORY AND TIME-ORDERED PRODUCTS

In the grand canonical ensemble, we want to evaluate

$$e^{-\beta\left(\widehat{H}-\mu\widehat{N}\right)} \tag{2.1}$$

where H is the Hamiltonian, N the number of particles and μ the chemical potential. For convenience, define

$$\widehat{K} = \widehat{H} - \mu\widehat{N}. \tag{2.2}$$

In general you will be facing a situation where

$$\widehat{K} = \widehat{H}_0 + \widehat{H}_1 - \mu\widehat{N} \equiv \widehat{K}_0 + \widehat{K}_1 \tag{2.3}$$

where $\widehat{K}_0 = H_0 - \mu N$ can easily be diagonalized but not $\widehat{K}$ because $\widehat{K}_0$ and $\widehat{K}_1$ do not commute. In that case, perturbation theory can help. We now prove

$$\boxed{e^{-\beta\widehat{K}} = e^{-\beta\widehat{K}_0}\widehat{U}(\beta)} \tag{2.4}$$

$$\boxed{\widehat{U}(\beta) \equiv T_\tau \left[e^{-\int_0^\beta \widehat{K}_1(\tau)d\tau}\right]} \tag{2.5}$$

$$\boxed{\widehat{K}_1(\tau) \equiv e^{\widehat{K}_0\tau}\widehat{K}_1 e^{-\widehat{K}_0\tau}}. \tag{2.6}$$

In the above expression, T_τ is the so-called time-ordering operator. It orders operators from left to right in increasing order of τ. Note that if $\widehat{K}_0$ and $\widehat{K}_1$ commute, then $\widehat{K}_1$ is independent of τ, $\widehat{U}(\beta) = e^{-\beta\widehat{K}_1}$ and $e^{-\beta\widehat{K}} = e^{-\beta\widehat{K}_0}e^{-\beta\widehat{K}_1}$ as expected.

Remark 14 *Imaginary time: The quantity, τ, is called imaginary time because the ordinary time evolution operator is e^{-iHt} and in the Heisenberg representation, operators evolve as follows: $\widehat{K}_1(t) = e^{i\widehat{K}_0 t/\hbar}\widehat{K}_1 e^{-i\widehat{K}_0 t/\hbar}$.*

To prove the above very important result is not difficult. It suffices to find a differential equation for $\widehat{U}$. Start from

$$\begin{aligned}
\frac{\partial}{\partial\tau}e^{-\widehat{K}\tau} &= \left(-\widehat{K}_0 - \widehat{K}_1\right)e^{-\widehat{K}\tau} \\
\frac{\partial}{\partial\tau}\left(\widehat{U}(\tau)\right) &= \frac{\partial}{\partial\tau}\left(e^{\widehat{K}_0\tau}e^{-\widehat{K}\tau}\right) && (2.7)\\
&= e^{\widehat{K}_0\tau}\left(\widehat{K}_0 - (\widehat{K}_0 + K_1)\right)e^{-\widehat{K}\tau} && (2.8)
\end{aligned}$$

where in the second equation, we have used the definition of $\widehat{U}$, Eq.(2.4) and the chain rule. We are left with

$$\begin{aligned}
\frac{\partial}{\partial\tau}\widehat{U}(\tau) &= -\left(e^{\widehat{K}_0\tau}\widehat{K}_1 e^{-\widehat{K}_0\tau}\right)\widehat{U}(\tau) && (2.9)\\
&= -\widehat{K}_1(\tau)\,\widehat{U}(\tau) && (2.10)
\end{aligned}$$

where $\widehat{K}_1(\tau)$ takes the form advertized in Eq.(2.6).

To find $\widehat{U}(\beta)$, integrate both sides of the equation, remembering that $\widehat{U}(0) = 1$. Then

$$\widehat{U}(\beta) = 1 - \int_0^\beta \widehat{K}_1(\tau)\,\widehat{U}(\tau)\,d\tau. \tag{2.11}$$

To solve in powers of $\widehat{K}_1$, which is the whole idea behind perturbation theory after all, we just iterate the above equation

$$\begin{aligned}\widehat{U}(\beta) &= 1 - \int_0^\beta d\tau \widehat{K}_1(\tau) + (-1)^2 \int_0^\beta d\tau \widehat{K}_1(\tau) \int_0^\tau d\tau' \widehat{K}_1(\tau') \\ &\quad + (-1)^3 \int_0^\beta d\tau \widehat{K}_1(\tau) \int_0^\tau d\tau' \widehat{K}_1(\tau') \int_0^{\tau'} d\tau'' \widehat{K}_1(\tau'') + \cdots \end{aligned} \tag{2.12}$$

Note that the operators are always ordered from right to left in increasing order of τ. This means that with the help of the time-ordering operator T_τ, the above equation can be rearranged in the form

$$\begin{aligned}\widehat{U}(\beta) &= 1 - \int_0^\beta d\tau \widehat{K}_1(\tau) + \frac{(-1)^2}{2!} T_\tau \left[\int_0^\beta d\tau \widehat{K}_1(\tau) \int_0^\beta d\tau' \widehat{K}_1(\tau') \right] \\ &\quad + \frac{(-1)^3}{3!} T_\tau \left[\int_0^\beta d\tau \widehat{K}_1(\tau) \int_0^\beta d\tau' \widehat{K}_1(\tau') \int_0^\beta d\tau'' \widehat{K}_1(\tau'') \right] + \cdot \end{aligned} \tag{2.13}$$

where the factorial takes care of the fact that by completing all the integrals so that the upper bound is β for all of them, operators will come in all possible orders in τ so they will need to be rearranged in the proper order $\widehat{K}!$ times for the term of order $\widehat{K}$. The series can now be resummed in an exponential, as written in Eq.(2.5).

2.1 Measuring a two-point correlation function (ARPES)

In a photoemission experiment, a photon ejects an electron from a solid. This is nothing but the old familiar photoelectric effect. In the angle-resolved version of this experiment (ARPES), the energy and the direction of the outgoing electron are measured. This is illustrated in Fig.(2-1). The outgoing electron energy can be measured. Because it is a free electron, this measurement gives the value of the wave vector through $k^2/2m$. Using energy conservation, the energy of the outgoing electron is equal to the energy of the incident photon E_{ph}, minus the work function W plus the energy of the electron in the system, ω, measured relative to the Fermi level.

The energy of the electron in the system ω will be mostly negative. The value of $\mathbf{k}_{||}$ may be extracted by simple geometric considerations from the value of k. Since in this experiment there is translational invariance only in the direction parallel to the plane, this means that in fact it is only the value of $\mathbf{k}_{||}$ that is conserved. Hence, it is only for layered systems that we really have access to both energy ω and total momentum $\mathbf{k}_{||}$ of the electron when it was in the system.

We can give a sketchy derivation of the calculation of the cross-section as follows. The cross-section we will find below neglects, amongst other things, processes where energy is transferred from the outgoing electron to phonons or other excitations before it is detected (multiple scattering of outgoing electron). Such processes are referred to as "inelastic background". We start from Fermi's Golden rule. The

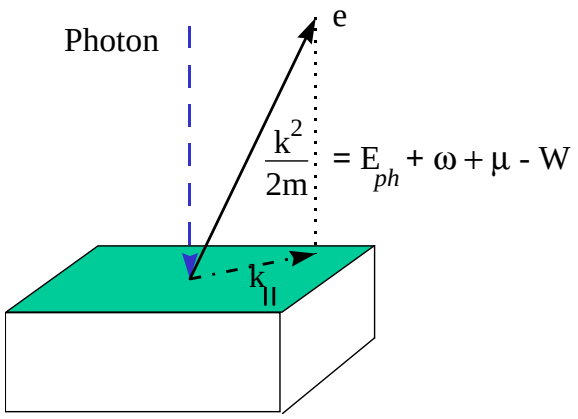

Figure 2-1 Schematic representation of an angle-resolved photoemission experiment. W is the work function.

initial state is a direct product $|m\rangle \otimes |0\rangle \otimes |1_{\mathbf{q}}\rangle_{em}$ of the state of the system $|m\rangle$, with the state $|0\rangle$ with no electron far away from the detector and with the state of the electromagnetic field that has one incoming photon $|1_{\mathbf{q}}\rangle_{em}$. The final state $|n\rangle \otimes |\mathbf{k}\rangle \otimes |0\rangle_{em}$ has the system in state $|n\rangle$ with one less electron, the detector with one electron in state $|\mathbf{k}\rangle$ and the electromagnetic field in state $|0\rangle_{em}$ with no photon. Strictly speaking, the electrons in the system should be antisymmetrized with the electrons in the detector, but when they are far enough apart and one electron is detected, we can assume that it is distinguishible from electrons in the piece of material. The coupling of matter with electromagnetic field that produces this transition from initial to final state is $-\mathbf{j} \cdot \mathbf{A}$ as we saw previously. Hence, the transition rate will be proportional to the square of the following matrix element

$$-\sum_{\mathbf{k}'} \langle n| \otimes \langle \mathbf{k}| \otimes \langle 0|_{em} \mathbf{j}_{\mathbf{k}'} \cdot \mathbf{A}_{-\mathbf{k}'} |m\rangle \otimes |0\rangle \otimes |1_{\mathbf{q}}\rangle_{em}. \tag{2.14}$$

$$= -\sum_{\mathbf{k}'} \langle n| \otimes \langle \mathbf{k}| \mathbf{j}_{\mathbf{k}'} |m\rangle \otimes |0\rangle \cdot \langle 0|_{em} \mathbf{A}_{-\mathbf{k}'} |1_{\mathbf{q}}\rangle_{em} \tag{2.15}$$

The vector potential is the analog of the position operator for harmonic vibration of the electromagnetic field. Hence, it is proportionnal to $a^{\dagger}_{-\mathbf{k}'} + a_{\mathbf{k}'}$, like for the harmonic oscillator excep that this time the particles involved are photons. The term with $\mathbf{k}' = \mathbf{q}$ with the destruction operator will lead to a non-zero value of $\langle 0|_{em} \mathbf{A}_{-\mathbf{k}'} |1_{\mathbf{q}}\rangle$. For the range of energies of interest, the wave vector of the photon $\mathbf{k}' = \mathbf{q}$ can be considered in the center of the Brillouin zone, $\mathbf{k}' \approx \mathbf{0}$. The current operator is a one-body operator. In the continuum, it is then given by

$$\mathbf{j}_{\mathbf{k}'=\mathbf{0}} = e \sum_{\mathbf{p}} \frac{\mathbf{p}}{m} c^{\dagger}_{\mathbf{p}} c_{\mathbf{p}}. \tag{2.16}$$

The value $\mathbf{p} = \mathbf{k}_{||}$ will lead to a non-zero matrix element. Overall then, the matrix element is

$$-\langle n| c_{\mathbf{k}_{||}} |m\rangle \left(\langle \mathbf{k}| c^{\dagger}_{\mathbf{k}_{||}} |0\rangle \, e \frac{\mathbf{k}_{||}}{m} \cdot \langle 0|_{em} \mathbf{A}_{\mathbf{k}'=\mathbf{q}\sim\mathbf{0}} |1_{\mathbf{q}}\rangle_{em} \right). \tag{2.17}$$

The term in large parenthesis is a matrix element that does not depend on the state of the system. Without going into more details of the assumptions going into the derivation then, Fermi's golden rule suggests, (see first section of Chapter

2) that the cross section for ejecting an electron of momentum $\mathbf{k}_{||}$ and energy ω (measured with respect to μ) is proportional to

$$\begin{aligned}
\frac{\partial^2\sigma}{\partial\Omega\partial\omega} &\propto \sum_{mn} e^{-\beta K_m} \left|\langle n| c_{\mathbf{k}_{||}} |m\rangle\right|^2 \delta\left(\omega+\mu-(E_m-E_n)\right) && (2.18)\\
&\propto \sum_{mn} e^{-\beta K_m} \left|\langle n| c_{\mathbf{k}_{||}} |m\rangle\right|^2 \delta\left(\omega-(K_m-K_n)\right) && (2.19)\\
&\propto \int dt e^{i\omega t} \sum_{mn} e^{-\beta K_m} \langle m| c^\dagger_{\mathbf{k}_{||}} |n\rangle \langle n| e^{iK_n t} c_{\mathbf{k}_{||}} e^{-iK_m t} |m\rangle && (2.20)\\
&\propto \int dt e^{i\omega t} \left\langle c^\dagger_{\mathbf{k}_{||}} c_{\mathbf{k}_{||}}(t)\right\rangle . && (2.21)
\end{aligned}$$

In the above equations, note that there is one more particle in state $|m\rangle$ than in state $|n\rangle$. This means that the minimum change in energy that we can have is $E_m - E_n = \mu$. With some extra energy, we can eject an electron that is farther away below the Fermi surface. Measuring energies with respect to the chemical potential, we define $K_m = E_m - N_m\mu$. For the last line, we have followed van Hove and used the integral representation of the Dirac delta function and the fact that the states are energy eigenstates. We have achieved our goal of expressing the cross section in terms of a correlation function.

In the case of electron scattering that we related to density fluctuations, there was a relation between the correlation function and the spectral weight that could be established with the fluctuation-dissipation theorem. We will be able to achieve the same thing below. More specifically, we will be able to rewrite this result in terms of the spectral weight $A\left(\mathbf{k}_{||},\omega\right)$ as follows,

$$\frac{\partial^2\sigma}{\partial\Omega\partial\omega} \propto f(\omega)\, A\left(\mathbf{k}_{||},\omega\right) \tag{2.22}$$

where $f(\omega)$ is the Fermi function.

Remark 15 *Time-evolution operator: It is very important to note that in the above expression for the cross section, Eq.(2.21), it is $K = H - \mu N$ that is the time evolution operator. This is what we will generally use, as soon as we go to the Matsubara formalism. The μN represents the effect of a particle reservoir. It comes in naturally above and represents the time evolution operator when we control the chemical potential instead of the number of particles. It makes the time-evolution operator in imaginary time more similar to the density matrix $e^{-\beta K_m}/Z$. More simply, this just corresponds to a choice of the zero of energy, namely ω is equal to zero for energies at the chemical potential. This can be seen from the above equations. Since we have by definition of K_n the equalities $e^{iK_n t} c_{\mathbf{k}_{||}} e^{-iK_m t} = e^{i(E_n-\mu N_n)t} c_{\mathbf{k}_{||}} e^{-i(E_m-\mu N_m)t}$ and $N_m - N_n = 1$, the phase factor $e^{i\mu t}$ can just be added to ω in the Fourier transform over time, illustrating why this choice of time evolution operator is related to the choice of zero of energy for ω.*

3. DEFINITION OF THE MATSUBARA GREEN FUNCTION

The most useful fermion correlation function, which can be used to obtain directly the above cross section as you will see, is the Matsubara Green function

$$\boxed{\mathcal{G}_{\alpha\beta}(\tau) = -\left\langle T_\tau c_\alpha(\tau)\, c_\beta^\dagger(0)\right\rangle} \tag{3.1}$$

$$= -\left\langle c_\alpha(\tau)\, c_\beta^\dagger(0)\right\rangle \theta(\tau) + \left\langle c_\beta^\dagger(0)\, c_\alpha(\tau)\right\rangle \theta(-\tau). \tag{3.2}$$

The last equation above defines the time ordering operator for fermions. It is very important to notice the minus sign associated with interchanging two fermion operators. This time-ordering operator is thus a slight generalization of the time-ordering operator we encountered before. One of the motivations for defining the Green function with a time-ordering operator is that T_τ appears naturally in perturbation theory as we have seen above. The time-ordering operator makes the perturbative evaluation of $\mathcal{G}_{\alpha\beta}$ natural.

Remark 16 *The time-ordering operator for quantities that are quadratic in fermions, i.e. bosonic quantities, such as $\widehat{K}_1$ that appeared in the perturbation expansion, never have a minus sign associated with the exchange of bosonic operators.*

Remark 17 *Physically, $\mathcal{G}_{\alpha\beta}(\tau)$ represents the amplitude that an excitation in a state β shows up as an excitation in state α after a "time" τ.*

We still need to specify a few things. First, the thermodynamic average is in the grand-canonical ensemble

$$\langle \mathcal{O}\rangle \equiv \frac{Tr\left[e^{-\beta\widehat{K}}\mathcal{O}\right]}{Tr\left[e^{-\beta\widehat{K}}\right]} \tag{3.3}$$

while the time evolution of the operators is defined by

$$\boxed{c_\alpha(\tau) \equiv e^{\widehat{K}\tau} c_\alpha e^{-\widehat{K}\tau}} \tag{3.4}$$

$$\boxed{c_\alpha^\dagger(\tau) \equiv e^{\widehat{K}\tau} c_\alpha^\dagger e^{-\widehat{K}\tau}} \tag{3.5}$$

Remark 18 *Note that $c_\alpha^\dagger(\tau)$ is not the Hermitian conjugate of $c_\alpha(\tau)$. The notation is somewhat abusive, but justified by the fact that if you replace immaginary time by real time, $\tau \to it/\hbar$, then we recover the usual case.*

Remark 19 *From now on, I set $\hbar = 1$. Sorry for the lazyness.*

3.1 The Matsubara frequency representation is convenient: antiperiodicity

Since we are working in time-translationally invariant systems, it is natural to think for Fourier transforms and enquire about a frequency representation. Since

we work on a finite imaginary-time interval contained between $-\beta$ and β, it is in fact Fourier series that will come to the rescue.

The first thing to notice are the Kubo-Martin-Schwinger boundary conditions that tell us that $\mathcal{G}_{\alpha\beta}(\tau)$ is antiperiodic in imaginary time. What this means is the following.

$$\mathcal{G}_{\alpha\beta}(\tau) = -\mathcal{G}_{\alpha\beta}(\tau - \beta). \tag{3.6}$$

Proof: Take $\tau > 0$ for example.

$$\mathcal{G}_{\alpha\beta}(\tau) = -\frac{1}{Z}\,\mathrm{Tr}\left[e^{-\beta\widehat{K}} e^{\widehat{K}\tau} c_\alpha e^{-\widehat{K}\tau} c_\beta^\dagger\right] \tag{3.7}$$

The cyclic property of the trace then tells us that

$$\begin{aligned}
\mathcal{G}_{\alpha\beta}(\tau) &= -\frac{1}{Z}\,\mathrm{Tr}\left[c_\beta^\dagger e^{-\beta\widehat{K}} e^{\widehat{K}\tau} c_\alpha e^{-\widehat{K}\tau}\right] &(3.8)\\
&= -\frac{1}{Z}\,\mathrm{Tr}\left[e^{-\beta\widehat{K}} c_\beta^\dagger e^{-\beta\widehat{K}} e^{\widehat{K}\tau} c_\alpha e^{-\widehat{K}\tau} e^{\beta\widehat{K}}\right]\\
&= -\frac{1}{Z}\,\mathrm{Tr}\left[e^{-\beta\widehat{K}} c_\beta^\dagger c_\alpha(\tau - \beta)\right]\\
&= -\mathcal{G}_{\alpha\beta}(\tau - \beta). &(3.9)
\end{aligned}$$

where we have used $\tau - \beta < 0$ and the definition of the Green function.

The antiperiodicity that we just proved can be used in conjunction with the theorems on Fourier series to arrive to the useful representation

$$\boxed{\mathcal{G}_{\alpha\beta}(\tau) = \tfrac{1}{\beta}\textstyle\sum_{n=-\infty}^{\infty} e^{-ik_n\tau}\mathcal{G}_{\alpha\beta}(ik_n)} \tag{3.10}$$

where the so-called Matsubara frequencies for fermions are odd, namely

$$\boxed{k_n = (2n+1)\,\pi T = \tfrac{(2n+1)\pi}{\beta}} \quad ; \quad n \quad \text{integer} \tag{3.11}$$

The antiperiodicity property will be automatically fulfilled because $e^{-ik_n\beta} = e^{-i(2n+1)\pi} = -1$.

Choice of units Here and from now on, we have taken Boltzmann's constant k_B to be equal to unity.

The expansion coefficients are obtained as usual for Fourier series of antiperiodic functions from

$$\boxed{\mathcal{G}_{\alpha\beta}(ik_n) = \textstyle\int_0^\beta d\tau e^{ik_n\tau}\mathcal{G}_{\alpha\beta}(\tau)} \tag{3.12}$$

3.2 $\mathcal{G}_{\mathbf{k}}(ik_n)$ for the non-interacting case $U = 0$

Before we see how the Green function is related to the photoemission cross section in general, it is useful to have a look at the non-interacting case to develop some intuition. This is our first occasion to write down the equation of motion for $\mathcal{G}_{\alpha\beta}$. You will notice that it is the kind of equation that one encounters with Green functions in general. Since we are considering the non-interacting case, take

$$\widehat{K}_0 = \sum_{\mathbf{p}} \zeta_{\mathbf{p}} c_{\mathbf{p}}^\dagger c_{\mathbf{p}} \tag{3.13}$$

where $\zeta_{\mathbf{p}} = \varepsilon_{\mathbf{p}} - \mu$. Using the definition

$$\mathcal{G}_{\mathbf{k}}(\tau) = -\left\langle T_\tau c_{\mathbf{k}}(\tau)\, c_{\mathbf{k}}^\dagger(0)\right\rangle \tag{3.14}$$

then

$$\frac{\partial \mathcal{G}_{\mathbf{k}}(\tau)}{\partial \tau} = -\delta(\tau)\left\langle\left\{c_{\mathbf{k}}, c_{\mathbf{k}}^\dagger\right\}\right\rangle - \left\langle T_\tau \frac{\partial c_{\mathbf{k}}(\tau)}{\partial \tau} c_{\mathbf{k}}^\dagger(0)\right\rangle. \tag{3.15}$$

Since $\left\{c_{\mathbf{k}}, c_{\mathbf{k}}^\dagger\right\} = 1$ and using

$$\begin{aligned}[AB, C] &= ABC - CAB = ABC + (ACB - ACB) - CAB \\ &= A\{B, C\} - \{A, C\} B\end{aligned}$$

which yields

$$\frac{\partial c_{\mathbf{k}}(\tau)}{\partial \tau} = \left[\widehat{K}_0, c_{\mathbf{k}}(\tau)\right] \tag{3.16}$$

$$= -\zeta_{\mathbf{k}} c_{\mathbf{k}}(\tau) \tag{3.17}$$

we are left with

$$\frac{\partial \mathcal{G}_{\mathbf{k}}(\tau)}{\partial \tau} = -\delta(\tau) - \zeta_{\mathbf{k}} \mathcal{G}_{\mathbf{k}}(\tau). \tag{3.18}$$

Using Matsubara frequencies, as in Eq.(3.10) you find

$$(-ik_n + \zeta_{\mathbf{k}})\, \mathcal{G}_{\mathbf{k}}(ik_n) = -1 \tag{3.19}$$

so that

$$\mathcal{G}_{\mathbf{k}}(ik_n) = \frac{1}{ik_n - \zeta_{\mathbf{k}}}. \tag{3.20}$$

The replacement

$$ik_n \to \omega + i\eta \tag{3.21}$$

where ω is a real frequency and η is a positive infinitesimal, is called analytic continuation. We are about to see why we do this and why this is useful. But for now, let us just look at the result. Upon analytic continuation, $\mathcal{G}_{\mathbf{k}}(ik_n)$ becomes the so-called retarded Green function

$$\boxed{G^R(\omega) = \frac{1}{\omega + i\eta - \zeta_{\mathbf{k}}}.} \tag{3.22}$$

Using the identity

$$\lim_{\eta \to 0} \frac{1}{x + i\eta} = \lim_{\eta \to 0} \frac{x - i\eta}{x^2 + \eta^2} = P\frac{1}{x} - i\pi\delta(x) \tag{3.23}$$

with P the principal part, we find

$$-2\,\mathrm{Im}\, G^R(\omega) = 2\pi\delta(\omega - \zeta_{\mathbf{k}}), \tag{3.24}$$

which tells us that in a non-interacting system, in an eigenstate of momentum $\mathbf{k}$, the energy ω is $\zeta_{\mathbf{k}}$.

Remark 20 *When bands are calculated within DFT, one obtains $\zeta_{\mathbf{k},n}$ for each of the Bloch bands labeled by ν. In that case we have a band index so states must be labeled by both quantum numbers and*

$$A_{\mathbf{k},\nu}(\omega) = 2\pi\delta\left(\omega - \zeta_{\mathbf{k},\nu}\right). \tag{3.25}$$

3.3 Time ordered product in practice

Suppose I want to compute

$$\left\langle T_\tau \psi(\tau_1)\,\psi^\dagger(\tau_3)\,\psi(\tau_2)\,\psi^\dagger(\tau_4)\right\rangle. \tag{3.26}$$

We drop space indices to unclutter the equations. The time ordered product for fermions keeps tract of permutations, so if I exchange the first two operators for example, I find

$$\left\langle T_\tau \psi(\tau_1)\,\psi^\dagger(\tau_3)\,\psi(\tau_2)\,\psi^\dagger(\tau_4)\right\rangle = -\left\langle T_\tau \psi^\dagger(\tau_3)\,\psi(\tau_1)\,\psi(\tau_2)\,\psi^\dagger(\tau_4)\right\rangle \tag{3.27}$$

I need not worry about delta functions at equal time or anything but the number of fermion exchanges. Indeed, whichever of the above two expressions I start with, if $\tau_1 < \tau_2 < \tau_3 < \tau_4$, I will find at the end that

$$\left\langle T_\tau \psi(\tau_1)\,\psi^\dagger(\tau_3)\,\psi(\tau_2)\,\psi^\dagger(\tau_4)\right\rangle = -\left\langle \psi^\dagger(\tau_4)\,\psi^\dagger(\tau_3)\,\psi(\tau_2)\,\psi(\tau_1)\right\rangle. \tag{3.28}$$

We cannot, however, have two of the times equal. We have to specify that one is infinitesimally larger or smaller than the other to know in which order to place the operators.

4. SUMS OVER MATSUBARA FREQUENCIES

In the derivation above, we went from imaginary-time to Matsubara frequencies. We can also do the reverse, from Matsubara frequencies to imaginary time. So you need to learn about sums over Matsubara frequencies. This will be necessary in doing practical calculations even when we are not trying to go back to imaginary time. When we have products of Green's functions, we will use contour integration tricks that are the same as those in this section. Also, we may use partial fractions in such a way that the only sums to evaluate will basically look like

$$T\sum_n \frac{1}{ik_n - \zeta_{\mathbf{k}}}. \tag{4.1}$$

where $T = \beta^{-1}$. We have however to be careful since the result of this sum is ambiguous. Indeed, returning back to the motivation for these sums, recall that

$$\mathcal{G}(\mathbf{k};\tau) = T\sum_n \frac{e^{-ik_n\tau}}{ik_n - \zeta_{\mathbf{k}}} \tag{4.2}$$

We already know that the Green's function has a jump at $\tau = 0$. In other words,

$$\left[\lim_{\tau\to 0^+} \mathcal{G}(\mathbf{k};\tau) = -\left\langle c_{\mathbf{k}} c_{\mathbf{k}}^+ \right\rangle\right] \neq \left[\lim_{\tau\to 0^-} \mathcal{G}(\mathbf{k};\tau) = \left\langle c_{\mathbf{k}}^+ c_{\mathbf{k}} \right\rangle\right] \tag{4.3}$$

This inequality in turn means that

$$T\sum_n \frac{e^{-ik_n 0^-}}{ik_n - \zeta_{\mathbf{k}}} \neq T\sum_n \frac{e^{-ik_n 0^+}}{ik_n - \zeta_{\mathbf{k}}} \neq T\sum_n \frac{1}{ik_n - \zeta_{\mathbf{k}}} \tag{4.4}$$

The sum does not converge uniformly in the interval including $\tau = 0$ because the $1/n$ decrease for $n \to \infty$ is too slow. Even if we can obtain a finite limit for the last sum by combining positive and negative Matsubara frequencies, what makes physical sense is only one or the other of the two limits $\tau \to 0^{\pm}$.

Remark 21 *The jump,* $\lim_{\tau\to 0^-} \mathcal{G}(\mathbf{k};\tau) - \lim_{\tau\to 0^+} \mathcal{G}(\mathbf{k};\tau)$ *is always equal to unity because of the anticommutation relations. The slow convergence in* $1/ik_n$ *is thus a reflection of the anticommutation relations and will remain true even in the interacting case. If the* $(ik_n)^{-1}$ *has a coefficient different from unity, the spectral weight is not normalized and the jump is not unity. This will be discussed shortly.*

Let us evaluate the Matsubara frequency sums. Considering again the case of fermions I will show as special cases that

$$\boxed{T\textstyle\sum_n \frac{e^{-ik_n 0^-}}{ik_n - \zeta_{\mathbf{k}}} = \frac{1}{e^{\beta\zeta_{\mathbf{k}}}+1} = f(\zeta_{\mathbf{k}}) = \mathcal{G}_0(\mathbf{k};0^-)} \tag{4.5}$$

$$\boxed{T\textstyle\sum_n \frac{e^{-ik_n 0^+}}{ik_n - \zeta_{\mathbf{k}}} = \frac{-1}{e^{-\beta\zeta_{\mathbf{k}}}+1} = -1 + f(\zeta_{\mathbf{k}}) = \mathcal{G}_0(\mathbf{k};0^+)} \tag{4.6}$$

Obviously, the non-interacting Green's function has the correct jump $\mathcal{G}_0(\mathbf{k};0^-) - \mathcal{G}_0(\mathbf{k};0^+) = 1$.In addition, since $\mathcal{G}_0(\mathbf{k};0^-) = \left\langle c_{\mathbf{k}}^\dagger c_{\mathbf{k}} \right\rangle$ and $\mathcal{G}_0(\mathbf{k};0^+) = -\left\langle c_{\mathbf{k}} c_{\mathbf{k}}^\dagger \right\rangle$

the above results just tell us that $\left\langle c_{\mathbf{k}}^{\dagger} c_{\mathbf{k}} \right\rangle = f(\zeta_{\mathbf{k}})$ that we know from elementary statistical mechanics. The anticommutation relations immediately give $-\left\langle c_{\mathbf{k}} c_{\mathbf{k}}^{\dagger} \right\rangle = -1 + f(\zeta_{\mathbf{k}})$. So these sums over Matsubara frequencies better behave as advertized.

Proof: [?] [1] To perform the sum over Matsubara frequencies, the standard trick is to go to the complex plane. The following function

$$-\beta \frac{1}{e^{\beta z}+1} \tag{4.7}$$

has poles for z equal to any fermionic Matsubara frequency: $z = ik_n$. Its residue at these poles is unity since for

$$z = ik_n + \delta z \tag{4.8}$$

we have

$$-\beta \frac{1}{e^{\beta z}+1} = -\beta \frac{1}{e^{ik_n\beta + \beta\delta z}+1} = -\beta \frac{1}{-1e^{\beta\delta z}+1} \tag{4.9}$$

$$\lim_{z-ik_n\to 0} \delta z \left[-\beta \frac{1}{e^{\beta z}+1}\right] = 1 \tag{4.10}$$

Similarly the following function has the same poles and residues:

$$\lim_{z-ik_n\to 0} \delta z \left[\beta \frac{1}{e^{-\beta z}+1}\right] = 1 \tag{4.11}$$

To evaluate the $\tau < 0$ case by contour integration, we use the residue theorem on the contour C_1, which is a sum of circles going counterclockwise around the points where z is equal to the Matsubara frequencies. Using Eq.(4.10), this allows us to establish the equality

$$-\frac{1}{2\pi i}\int_{C_1} \frac{dz}{e^{\beta z}+1} \frac{e^{-z\tau}}{z-\zeta_{\mathbf{k}}} = \frac{1}{\beta}\sum_n \frac{e^{-ik_n\tau}}{ik_n - \zeta_{\mathbf{k}}}. \tag{4.12}$$

This contour can then be deformed, as illustrated in Fig. (4-1), into C_1' and then into $C_2 + C_3$. There is no contribution from C_3 at $\mathrm{Re}(z) = \infty$ because the denominator of $\frac{e^{-z\tau}}{e^{\beta z}+1}$ makes the integrand converge exponentially since in $e^{-z(\tau+\beta)}$, $\tau + \beta$ is always positive ($\tau > -\beta$). Similarly, there is no contribution from C_2 at $\mathrm{Re}(z) = -\infty$ because in that case $\frac{e^{-z\tau}}{e^{\beta z}+1} \to e^{-z\tau}$ and $-z\tau < 0$. So finally, we have

$$\boxed{\frac{1}{\beta}\sum_n \frac{e^{-ik_n\tau}}{ik_n - \zeta_{\mathbf{k}}} = \frac{e^{-\zeta_{\mathbf{k}}\tau}}{e^{\beta\zeta_{\mathbf{k}}}+1} = e^{-\zeta_{\mathbf{k}}\tau} f(\zeta_{\mathbf{k}})} \tag{4.13}$$

which is the value of $\mathcal{G}_0(\mathbf{k};\tau)$ when $\tau < 0$. In particular, when $\tau = 0^-$ we have proven the identity (4.6) .

To evaluate the $\tau > 0$ case we use the same contour but with the other form of auxiliary function Eq.(4.11). We can again check that the integral over the circle at infinity vanishes because this time $e^{-z\tau}$ insures convergence when $\mathrm{Re}(z) = \infty$, $\tau > 0$ and $\frac{1}{e^{-\beta z}+1}$ ensures convergence when $\mathrm{Re}(z) = -\infty$ despite $e^{-z\tau}$ in the numerator. We then obtain,

$$\frac{1}{\beta}\sum_n \frac{e^{-ik_n\tau}}{ik_n - \zeta_{\mathbf{k}}} = \frac{1}{2\pi i}\int_{C_1} \frac{dz}{e^{-\beta z}+1} \frac{e^{-z\tau}}{z-\zeta_{\mathbf{k}}}. \tag{4.14}$$

[1] I thank Yan Wang, 2018, for this version of the proof.

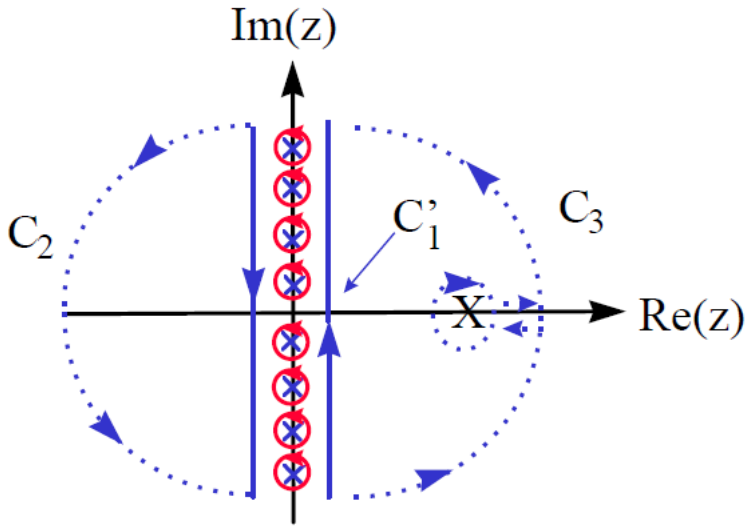

Figure 4-1 Evaluation of fermionic Matsubara frequency sums in the complex plane.

Again, from $C_2 + C_3$, only the contribution from the pole in the clockwise directions survives so that we have,

$$\boxed{\frac{1}{\beta}\sum_n \frac{e^{-ik_n\tau}}{ik_n-\zeta_{\mathbf{k}}} = -\frac{e^{-\zeta_{\mathbf{k}}\tau}}{e^{-\beta\zeta_{\mathbf{k}}}+1} = -\frac{e^{-\zeta_{\mathbf{k}}\tau}e^{\beta\zeta_{\mathbf{k}}}}{e^{\beta\zeta_{\mathbf{k}}}+1} = -e^{-\zeta_{\mathbf{k}}\tau}\left(1-f\left(\zeta_{\mathbf{k}}\right)\right).} \quad (4.15)$$

This is the value of $\mathcal{G}_0\left(\mathbf{k};\tau\right)$ when $\tau > 0$. In particular, when $\tau = 0^+$ we have proven the identity (4.5).

Remark 22 *Branch cut: When there is a branch cut all the way to infinity, the above proof is easy to generalize. For example, for a branch cut from $\zeta_{\mathbf{k}}$ to ∞, there are three integrals to do. Two of them extend from ∞ in two directions above and below the real axis and another one is an open circle around the end of the branch cut.*

Remark 23 *When there is a sum over Matsubara frequencies for a product of Green's function, the same trick as above applies. There are just more poles to go around when the contour is deformed.*

Part III

Lecture 3 (45 minutes)
Spectral weight, Self-energy, Quasiparticles

5. SPECTRAL WEIGHT AND HOW IT IS RELATED TO $\mathcal{G}_{\mathbf{K}}(IK_N)$ AND TO PHOTOEMISSION: LEHMANN REPRESENTATION

The quantity $-2\,\mathrm{Im}\,G^R(\omega)$ is called the spectral weight. To understand its general meaning, it suffices to start from the definition of the Matsubara Green function and to use a complete sets of states. More specifically,

$$\mathcal{G}_{\mathbf{k}}(ik_n) = -\int_0^\beta d\tau e^{ik_n\tau}\left\langle c_{\mathbf{k}}(\tau)\, c_{\mathbf{k}}^\dagger(0)\right\rangle \tag{5.1}$$

$$= -\int_0^\beta d\tau e^{ik_n\tau}\sum_{n,m}\frac{e^{-\beta K_n}}{Z}\langle n|\, e^{K_n\tau}c_{\mathbf{k}}e^{-K_m\tau}\,|m\rangle\,\langle m|\, c_{\mathbf{k}}^\dagger\,|n\rangle\,. \tag{5.2}$$

The integral over imaginary time is now easy to do,

$$\boxed{\mathcal{G}_{\mathbf{k}}(ik_n)=\sum_{n,m}\frac{e^{-\beta K_n}}{Z}\frac{e^{\beta(K_n-K_m)}+1}{ik_n+K_n-K_m}\langle n|\, c_{\mathbf{k}}\,|m\rangle\,\langle m|\, c_{\mathbf{k}}^\dagger\,|n\rangle.} \tag{5.3}$$

We have used $e^{ik_n\beta}=-1$. This is the so-called Lehmann representation of $\mathcal{G}_{\mathbf{k}}(ik_n)$. This last result may be written in the so-called spectral representation

$$\boxed{\mathcal{G}_{\mathbf{k}}(ik_n)=\int\frac{d\omega}{2\pi}\frac{A_{\mathbf{k}}(\omega)}{ik_n-\omega}} \tag{5.4}$$

if we define the spectral weight by

$$A_{\mathbf{k}}(\omega) \equiv \sum_{n,m}\frac{1}{Z}\left(e^{-\beta K_m}+e^{-\beta K_n}\right)\langle n|\, c_{\mathbf{k}}\,|m\rangle\,\langle m|\, c_{\mathbf{k}}^\dagger\,|n\rangle \tag{5.5}$$

$$\times 2\pi\delta\left(\omega-(K_m-K_n)\right) \tag{5.6}$$

$$= \sum_{n,m}\frac{e^{-\beta K_m}}{Z}\left(1+e^{\beta\omega}\right)\langle n|\, c_{\mathbf{k}}\,|m\rangle\,\langle m|\, c_{\mathbf{k}}^\dagger\,|n\rangle\, 2\pi\delta\left(\omega-(K_m-K_n)\right).$$

Given this result, the differential photoemission cross section may be obtained from

$$\frac{\partial^2\sigma}{\partial\Omega\partial\omega}\propto A_{\mathbf{k}}(\omega)\, f(\omega) \tag{5.7}$$

with $f(\omega)=\left(1+e^{\beta\omega}\right)^{-1}$ the Fermi function.

To find the physical meaning of the spectral weight, exchange the dummy summation indices m,n in the first term of Eq.(5.5) and you find

$$A_{\mathbf{k}}(\omega) \equiv \sum_{n,m}\frac{1}{Z}e^{-\beta K_n}\langle n|\, c_{\mathbf{k}}^\dagger\,|m\rangle\,\langle m|\, c_{\mathbf{k}}\,|n\rangle\, 2\pi\delta\left(\omega-(K_n-K_m)\right)$$

$$+\frac{1}{Z}e^{-\beta K_n}\langle n|\, c_{\mathbf{k}}\,|m\rangle\,\langle m|\, c_{\mathbf{k}}^\dagger\,|n\rangle\, 2\pi\delta\left(\omega-(K_m-K_n)\right) \tag{5.8}$$

This quantity is normalized since

$$\begin{aligned}\int \frac{d\omega}{2\pi} A_{\mathbf{k}}(\omega) &= \sum_{n,m} \frac{1}{Z} e^{-\beta K_n} \left(\langle n| c_{\mathbf{k}}^{\dagger} |m\rangle \langle m| c_{\mathbf{k}} |n\rangle + \langle n| c_{\mathbf{k}} |m\rangle \langle m| c_{\mathbf{k}}^{\dagger} |n\rangle \right) \\ &= \left\langle \left\{ c_{\mathbf{k}}^{\dagger}(0), c_{\mathbf{k}}(0) \right\} \right\rangle = 1. \end{aligned} \tag{5.9}$$

Clearly then, $A_{\mathbf{k}}(\omega)/(2\pi)$ can be interpreted as the probability that the state formed by adding to an eigenstate $|n\rangle$ a particle of momentum $\mathbf{k}$, i.e. $c_{\mathbf{k}}^{\dagger}|n\rangle$ or a hole $c_{\mathbf{k}}|n\rangle$, yields an eigenstate $\langle m|$ whose grand potential K has an energy ω compared with the original state $|n\rangle$. In the non-interacting case, for any given $\mathbf{k}$ there is only one frequency ω where there will be a non-zero contribution since $c_{\mathbf{k}}^{\dagger}|n\rangle$ or $c_{\mathbf{k}}|n\rangle$ are eigenstates. This is no-longer the case when there are interactions. Then, $c_{\mathbf{k}}^{\dagger}|n\rangle$ or $c_{\mathbf{k}}|n\rangle$ are not eigenstates and there are many states $\langle m|$ with different excitation energies ω whose overlap with $c_{\mathbf{k}}^{\dagger}|n\rangle$ or with $c_{\mathbf{k}}|n\rangle$ is non-vanishing (in other words where the quantum mechanical probability $|\langle m| c_{\mathbf{k}} |n\rangle|^2$ is non-vanishing). This is equivalent to saying that in the presence of interactions, the momentum $\mathbf{k}$ of a single particle is not conserved (or no-longer a good quantum number).

Remark 24 *It is important to recall once again that all the physical information is in the spectral weight* $A_{\mathbf{k}}(\omega)$.

5.1 Obtaining the spectral weight from $\mathcal{G}_{\mathbf{k}}(ik_n)$: the problem of analytic continuation

If we can compute $\mathcal{G}_{\mathbf{k}}(ik_n)$ by any means, we can obtain the spectral weight from its analytic continuation since, using the spectral representation Eq.(5.4) of $\mathcal{G}_{\mathbf{k}}(ik_n)$ we can simply do the analytic continuation $ik_n \to \omega + i\eta$ and find

$$\boxed{G_{\mathbf{k}}^{R}(\omega) = \int \frac{d\omega'}{2\pi} \frac{A_{\mathbf{k}}(\omega')}{\omega + i\eta - \omega'}.} \tag{5.10}$$

From this, the spectral weight $A_{\mathbf{k}}(\omega')$ is easy to find from

$$\boxed{A_{\mathbf{k}}(\omega) = -2 \operatorname{Im} G_{\mathbf{k}}^{R}(\omega).} \tag{5.11}$$

All this is very easy analytically, but with numerical data it turns into a nightmare. There are two methods that are widely used, Padé approximants and Maximum Entropy analytic continuation. These are whole subjects in themselves.

Remark 25 *We already mentioned that the physical information is in* $A_{\mathbf{k}}(\omega)$. *An equivalent way of saying this is that it is in the poles of* $G_{\mathbf{k}}^{R}(\omega)$.

6. SELF-ENERGY AND THE EFFECT OF INTERACTIONS

6.1 A first phenomenological encounter with self-energy

In this short Chapter, we want to develop an intuition for the concept of self-energy. The concept is simplest to understand if we start from a non-interacting system and assume that we add interactions with a potential or whatever that changes the situation a little. We will be guided by simple ideas about the harmonic oscillator.

Let us start then from the Green function for a non-interacting particle

$$\langle \mathbf{k}| \, \widehat{G}_0^R(\omega) \, |\mathbf{k}'\rangle = G_0^R(\mathbf{k},\omega) = \langle \mathbf{k}| \, \frac{1}{\omega + i\eta - \widehat{H}} \, |\mathbf{k}'\rangle = \frac{\langle \mathbf{k}| \, \mathbf{k}'\rangle}{\omega + i\eta - \varepsilon_{\mathbf{k}}}. \tag{6.1}$$

Since the momentum states are orthogonal, it is convenient to define $G_0^R(\mathbf{k},\omega)$ by

$$G_0^R(\mathbf{k},\omega) = \frac{1}{\omega + i\eta - \varepsilon_{\mathbf{k}}}.$$

The corresponding spectral weight is particularly simple,

$$A_0(\mathbf{k},\omega) = -2\,\mathrm{Im}\, G_0^R(\mathbf{k},\omega) = 2\pi\delta(\omega - \varepsilon_{\mathbf{k}}). \tag{6.2}$$

We should think of the frequency as the energy. It is only for a non-interacting particle that specifying the energy specifies the wave vector, since it is only in that case that $\omega = \varepsilon_{\mathbf{k}}$.

In general, if momentum is not conserved, the spectral representation

$$G^R(\mathbf{k};\omega) = \int \frac{d\omega'}{2\pi} \frac{A(\mathbf{k};\omega')}{\omega + i\eta - \omega'} \tag{6.3}$$

and the explicit expression for the spectral weight

$$A(\mathbf{k};\omega') = \sum_n \langle \mathbf{k}| \, n\rangle \langle n \, |\mathbf{k}\rangle \, 2\pi\delta(\omega' - E_n) \tag{6.4}$$

tells us that a momentum eigenstate has non-zero projection on several true eigenstates and hence $A(\mathbf{k};\omega')$ is not a delta function.

Intuitively, for weak perturbations, we simply expect that $A(\mathbf{k};\omega')$ will broaden in frequency around $\omega = \widetilde{\varepsilon}_{\mathbf{k}}$ where $\widetilde{\varepsilon}_{\mathbf{k}}$ is close to $\varepsilon_{\mathbf{k}}$.We take this intuition from the damped harmonic oscillator where the resonance is broadened and shifted by damping. If we take a Lorentzian as a phenomenological form for the spectral weight

$$A(\mathbf{k};\omega') = \frac{2\Gamma}{(\omega - \widetilde{\varepsilon}_{\mathbf{k}})^2 + \Gamma^2} \tag{6.5}$$

then the Green's function can be computed from the spectral representation Eq.(6.3) by using Cauchy's residue theorem. The result is

$$G^R(\mathbf{k},\omega) = \frac{1}{\omega - \widetilde{\varepsilon}_{\mathbf{k}} + i\Gamma}. \tag{6.6}$$

We have neglected $i\eta$ in front of $i\Gamma$. It is easy to verify that $-2\,\mathrm{Im}\,G^R(\mathbf{k},\omega)$ gives the spectral weight we started from.

With a jargon that we shall explain momentarily, we define the one-particle irreducible self-energy by

$$G^R(\mathbf{k},\omega)=\frac{1}{\omega+i\eta-\varepsilon_{\mathbf{k}}-\Sigma^R(\mathbf{k},\omega)}=\frac{1}{G_0^R(\mathbf{k},\omega)^{-1}-\Sigma^R(\mathbf{k},\omega)}. \tag{6.7}$$

Its physical meaning is clear. The imaginary part $\mathrm{Im}\,\Sigma^R(\mathbf{k},\omega)=-\Gamma$ corresponds to the scattering rate, or inverse lifetime, whereas the real part, $\mathrm{Re}\,\Sigma^R(\mathbf{k},\omega)=\widetilde{\varepsilon}_{\mathbf{k}}-\varepsilon_{\mathbf{k}}$ leads to the shift in the position of the resonance in the spectral weight. In other words, $\Sigma^R(\mathbf{k},\omega)$ contains all the information about the interactions.

With the simple approximation that we did for the self-energy,

$$\Sigma^R(\mathbf{k},\omega)=\widetilde{\varepsilon}_{\mathbf{k}}-\varepsilon_{\mathbf{k}}-i\Gamma, \tag{6.8}$$

one notices that the second moment $n=2$ diverges because the second moment of a Lorentzian does. Hence, the high-frequency expansion becomes incorrect already at order $1/\omega^3$. We need to improve the approximation to recover higher frequency moments. Nevertheless, in the form

$$G^R(\mathbf{k},\omega)^{-1}=G_0^R(\mathbf{k},\omega)^{-1}-\Sigma^R(\mathbf{k},\omega) \tag{6.9}$$

equivalent to that given above, there is no loss in generality. The true self-energy is defined as the difference between the inverse of the non-interacting propagator and the inverse of the true propagator. Lifetimes and shifts must in general be momentum and frequency dependent.

Remark 26 *The time dependence of the retarded Green's function shows the damping: Indeed, note that the Fourier transform of $G^R(\mathbf{k},\omega)$ is, for $t>0$,*

$$G^R(\mathbf{k},t)=\int_{-\infty}^{\infty}\frac{d\omega}{2\pi}e^{-i\omega t}\frac{1}{\omega-\widetilde{\varepsilon}_{\mathbf{k}}+i\Gamma}=-i\theta(t)\,e^{-i\widetilde{\varepsilon}_{\mathbf{k}}t-\Gamma t} \tag{6.10}$$

which shows that when Γ tends to zero, then we have the expected oscillatory behavior in time for the evolution of an eigenstate of renormalized energy $\widetilde{\varepsilon}_{\mathbf{k}}$. Taking the square gives a time-independent result (apart from the $\theta(t)$) for the probability. On the other hand, a finite Γ means that the amplitude to stay in state $\mathbf{k}$ decays with time, as does the probability (twice as fast). That probability can be constructed as follows. By construction, the operator $\widehat{G}^R(t)$ allows us to find the wave function at time t, given the initial condition $|\mathbf{k}\rangle$ at time zero, or as an equation, $\langle\mathbf{k}|\,\widehat{G}^R(t)\,|\mathbf{k}\rangle=\langle\mathbf{k}|\,\psi(t)\rangle$. Using the Born rule, the probatility that there is still a particle in state $|\mathbf{k}\rangle$ at time t is the absolute value of the projection of the state at time t on the state $|\mathbf{k}\rangle$, or in other words,

$$|\langle\mathbf{k}|\,\psi(t)\rangle|^2=\left|G^R(\mathbf{k},t)\right|^2=\theta(t)\,e^{-2\Gamma t}. \tag{6.11}$$

I begin by solving the Hubbard Hamiltonian when there are only interactions, no hopping. This is the so-called atomic limit. You will see that in this case the Green function takes a structure very different from the non-interacting case. This will be a natural occasion to introduce the notion of self-energy as a representation of the effect of interactions and to show that the self-energy is singular in the atomic limit, and more generally for Mott insulators. Also, we will see that in the case of a single interacting site in a sea of non-interacting electrons, the self-energy comes only from the interacting site. This is the Anderson impurity model, that happens to be very important in the context of Dynamical Mean-Field Theory. We will see Dyson's equation and a few general properties of the self-energy.

6.2 A few properties of the self-energy

Given the spectral representation Eq.(5.10)

$$G^R_{\mathbf{k}\sigma}(\omega) = \int \frac{d\omega'}{2\pi} \frac{A_{\mathbf{k}\sigma}(\omega')}{\omega + i\eta - \omega'} \tag{6.12}$$

and the positivity of $A_{\mathbf{k}\sigma}$, which can easily be seen from Eq.(5.5), it is clear that $G^R_{\mathbf{k}\sigma}(\omega)$ has poles only in the lower-half complex plane. It can be shown that this is a general consequence of causality. This implies that

$$\mathrm{Im}\,\Sigma^R_{\mathbf{k}\sigma}(\omega) < 0, \tag{6.13}$$

as follows also from the positivity of $A_{\mathbf{k}\sigma}$ and its representation in terms of the self-energy.

Also, the self-energy cannot grow with frequency since

$$\lim_{\omega\to\infty} \omega G^R_{\mathbf{k}\sigma}(\omega) = \omega \int \frac{d\omega'}{2\pi} \frac{A_{\mathbf{k}\sigma}(\omega')}{\omega} = \int \frac{d\omega'}{2\pi} A_{\mathbf{k}\sigma}(\omega') = 1. \tag{6.14}$$

We have used the fact that $A_{\mathbf{k}\sigma}$ has to vanish at large frequency, as follows from Eq.(5.5) and the fact that the matrix elements between a true eigenstate and an eigenstate obtained from adding one excitation in a low energy state must vanish. In practice, the real part of the self-energy can at most be a constant at infinite frequency (This is the Hartree-Fock result).

6.3 Some experimental results from ARPES

The state of technology and historical coincidences have conspired so that the first class of layered (quasi-two-dimensional) compounds that became available for ARPES study around 1990 were high temperature superconductors. These materials have properties that make them non-conventional materials that are not yet understood using standard approaches of solid-state Physics. Hence, people started to look for two-dimensional materials that would behave as expected from standard models. Such a material, semimetallic $TiTe_2$ was finally found around 1992. For our purposes, quasi-two-dimensional just means here that the Fermi velocity perpendicular to the planes is much smaller than the Fermi velocity in the planes. The results of this experiment[**?**] appear in Fig.(6-1).

We have to remember that the incident photon energy is $21.2eV$ while the variation of ω is on a scale of $200meV$ so that, for all practical purposes, the momentum vector in Fig.(2-1) is a fixed length vector. Hence, the angle with respect to the incident photon suffices to define the value of $\mathbf{k}_{||}$. Each curve in Fig.(6-1) is for a given $\mathbf{k}_{||}$, in other words for a given angle measured from the direction of incidence of the photon. The intensity is plotted as a function of the energy of the outgoing electron. Hence these plots are often called EDC (energy distribution curves). The zero corresponds to an electron extracted from the Fermi level. Electrons with a smaller kinetic energy come from states with larger binding energy. In other words, each of the curves above is basically a plot of the hole-like part of $A(\mathbf{k}_{||}, \omega)$, or if you want $f(\omega) A(\mathbf{k}_{||}, \omega)$. From band structure calculations, one knows that the angle $\theta = 14.75^0$ corresponds to the Fermi level (marked k_F on the plot) of a $Ti - 3d$ derived band. It is for this scattering

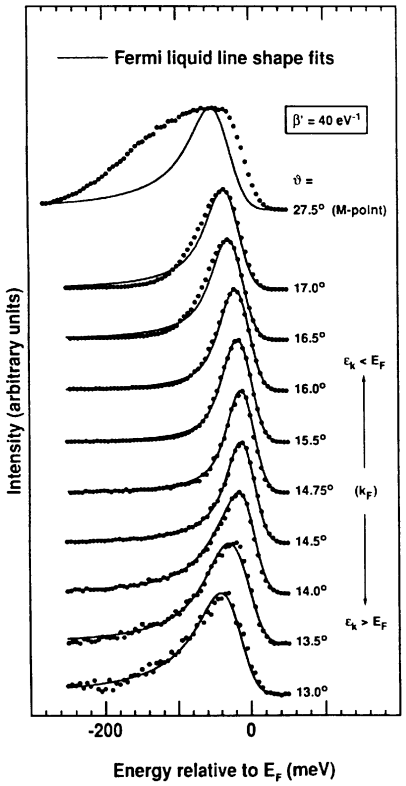

Figure 6-1 ARPES spectrum of $1-T-TiTe_2$, after R. Claessen, R.O. Anderson, J.W. Allen, C.G. Olson, C. Janowitz, W.P. Ellis, S. Harm, M. Kalning, R. Manzke, and M. Skibowski, Phys. Rev. Lett **69**, 808 (1992).

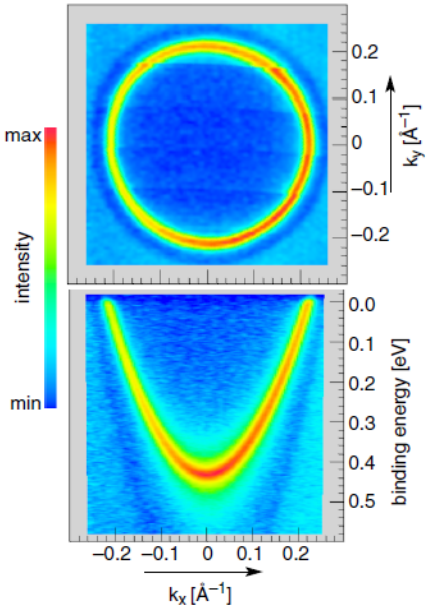

Figure 6-2 This ARPES spectrum is taken on the (1 1 1) surface of Cu. The top plot is the MDC for the projection of a part of the bulk Fermi surface projected on the (1 1 1) surface. The lower panel shows the EDC with the nearly parabolic dispersion below the Fermi level,

angle that the agreement between experiment and Fermi liquid theory is best (see Sec.(7.1) below). The plots for angles $\theta < 14.75^0$ correspond to wave vectors above the Fermi level. There, the intensity is *much* smaller than for the other peaks. For $\theta = 13^0$, the experimental results are scaled up by a factor 16. The intensity observed for wave-vectors above $\omega = 0$ comes from the Fermi function and also from the non-zero projection of the state with a given $\mathbf{k}$ on several values of ω in the spectral weight.

The energy resolution is $35meV$. Nevertheless, it is clear that the line shapes are larger than the energy resolution: Clearly the spectral weight is not a delta function and the electrons in the system are not free particles. Nevertheless, there is a definite maximum in the spectra whose position changes with $\mathbf{k}_{||}$. It is tempting to associate the width of the line to a lifetime. In other words, a natural explanation of these spectra is that the electrons inside the system are "quasiparticles" whose energy disperses with wave vector and that have a lifetime. We try to make these concepts more precise below.

One can also make plots of the probability of having a certain momentum at the Fermi level $\omega = 0$. This is usually represented by a color plot called MDC, momentum distribution curve. This is represented on the top of Fig. (6-2). This is for a specific portion of the Fermi surface of Cu, with the corresponding dependence of energy on momentum (EDC) on the lower part of Fig. (6-2). A theorist's dream.

A more complicated but also spectacular case, shown in Fig. (6.3), is that of strontium ruthenate Sr_2RuO_4 [19], also interesting because it was proposed to be a topological superconductor, a proposal that is still subject of research at the time of writing:

Fig. (6-3) shows some beautiful experimental and theoretical recent work on this compound. [84] On the left is the Fermi surface and on the right various

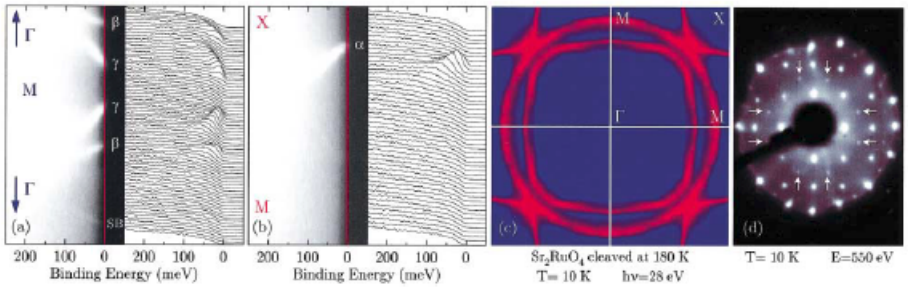

FIG. 4 (color). EDC's and intensity plot $I(\mathbf{k}, \omega)$ along Γ-M-Γ and M-X [panels (a) and (b), respectively]. Panel (c): E_F intensity map. Panel (d): LEED pattern recorded at the end of the FS mapping. All data were taken at 10 K on Sr_2RuO_4 cleaved at 180 K.

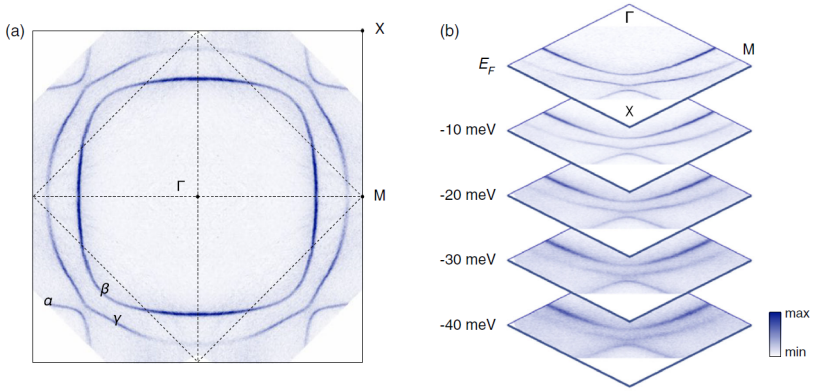

Figure 6-3 Momentum distribution curves. a) at the Fermi level, and b) at various energies below the Fermi surface. From Phys. Rev. X, **2**, 021048 (2019).

MDC's at energies below the Fermi surface. This should be contrasted with high-temperature superconductors in Fig. 6.3. The Fermi surface seems to vanish in thin air ([57]).Getting back to strontium ruthenate [84], Fig. (6-4) shows some detailed comparisons between experiment and theory. The theory is based on density-functional theory, augmented by dynamical mean-field calculations, topics we will address in subsequent chapters. The calculation shows that the effect of spin-orbit interactions is crucial. The red dots are the measurements and the color curves the calculations.

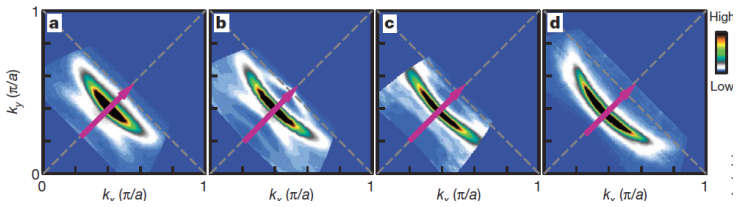

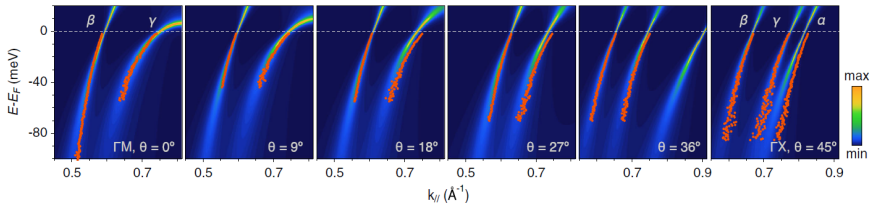

Figure 6-4 Comparison between theory and experiment for strontium ruthenate. The theory is from electronic structure including spin-orbit interactions and supplemented with the effect of interactions using Dynamical Mean-Field theory. From Phys. Rev. X, **2**, 021048 (2019).

7. QUASIPARTICLES

The intuitive notions we may have about lifetime and effective mass of an electron caused by interactions in a solid can all be extracted from the self-energy, as I will show. As we discussed in Chapter 6.1, for a general interacting system, the one-particle Green's function takes the form,

$$G^R(\mathbf{k},\omega) = \frac{1}{\omega + i\eta - \zeta_{\mathbf{k}} - \sum^R(\mathbf{k},\omega)} \tag{7.1}$$

We can drop $i\eta$ since $\mathrm{Im}\sum^R(\mathbf{k},\omega)$ is negative to preserve causality and always larger than $i\eta$ that should anyway be taken to zero at the end.[1] The spectral weight corresponding to $G^R(\mathbf{k},\omega)$ then is,

$$\begin{aligned} A(\mathbf{k},\omega) &= -2\,\mathrm{Im}\,G^R(\mathbf{k},\omega) && (7.2)\\ &= \frac{-2\,\mathrm{Im}\sum^R(\mathbf{k},\omega)}{\left(\omega - \zeta_{\mathbf{k}} - \mathrm{Re}\sum^R(\mathbf{k},\omega)\right)^2 + \left(\mathrm{Im}\sum^R(\mathbf{k},\omega)\right)^2}. && (7.3)\end{aligned}$$

If the imaginary part of the self-energy, the scattering rate, is not too large and varies smoothly with frequency, conditions I will refine when I discuss Fermi liquids soon, the spectral weight will have a maximum whenever, at fixed **k,** there is a value of ω that satisfies

$$\boxed{\omega - \zeta_{\mathbf{k}} - \mathrm{Re}\,\Sigma^R(\mathbf{k},\omega) = 0.} \tag{7.4}$$

We assume the solution of this equation exists. Let $E_{\mathbf{k}} - \mu$ be the value of ω for which this equation is satisfied. $E_{\mathbf{k}}$ is the so-called *quasiparticle energy* [**?**]. This energy is clearly in general different from the results of band structure calculations that are usually obtained by neglecting the frequency dependence of the self-energy. Expanding $\omega - \zeta_{\mathbf{k}} - \mathrm{Re}\,\Sigma^R(\mathbf{k},\omega)$ around $\omega = E_{\mathbf{k}} - \mu = 0$ where $A(\mathbf{k},\omega)$ is a maximum, we find

$$\begin{aligned} \omega - \zeta_{\mathbf{k}} - \mathrm{Re}\,\Sigma^R(\mathbf{k},\omega) &\approx 0 + \frac{\partial}{\partial\omega}\left[\omega - \zeta_{\mathbf{k}} - \mathrm{Re}\,\Sigma^R(\mathbf{k},\omega)\right]_{\omega=E_{\mathbf{k}}-\mu}(\omega - E_{\mathbf{k}} + \mu) + \dots \\ &\approx \left(1 - \left.\frac{\partial\,\mathrm{Re}\,\Sigma^R(\mathbf{k},\omega)}{\partial\omega}\right|_{E_{\mathbf{k}}-\mu}\right)(\omega - E_{\mathbf{k}} + \mu) + \dots \end{aligned} \tag{7.5}$$

If we define the "quasiparticle weight" or square of the wave function renormalization by

$$\boxed{Z_{\mathbf{k}} = \frac{1}{1 - \frac{\partial}{\partial\omega}\,\mathrm{Re}\,\Sigma^R(\mathbf{k},\omega)\big|_{\omega=E_{\mathbf{k}}-\mu}}} \tag{7.6}$$

then in the vicinity of the maximum, the spectral weight takes the following simple form in the vicinity of the Fermi level, where the peak is sharpest

$$\begin{aligned} A(\mathbf{k},\omega) &\approx 2\pi Z_{\mathbf{k}}\frac{1}{\pi}\frac{-Z_{\mathbf{k}}\,\mathrm{Im}\sum^R(\mathbf{k},\omega)}{(\omega - E_{\mathbf{k}} + \mu)^2 + \left(Z_{\mathbf{k}}\,\mathrm{Im}\sum^R(\mathbf{k},\omega)\right)^2} + inc && (7.7)\\ &= 2\pi Z_{\mathbf{k}}\left[\frac{1}{\pi}\frac{\Gamma_{\mathbf{k}}(\omega)}{(\omega - E_{\mathbf{k}} + \mu)^2 + (\Gamma_{\mathbf{k}}(\omega))^2}\right] + inc. && (7.8)\end{aligned}$$

[1] In exact diagonalizations where the self-energy is still represented by a set of delta functions, the $i\eta$ should be kept everywhere.

The last equation needs some explanation. First, it is clear that I have defined the scattering rate

$$\boxed{\Gamma_{\mathbf{k}}(\omega) = -Z_{\mathbf{k}} \operatorname{Im} \Sigma^R(\mathbf{k},\omega)} \tag{7.9}$$

Second, the quantity in square brackets looks, as a function of frequency. At least if we can neglect the frequency dependence of the scattering rate. The integral over frequency of the square bracket is unity. Since $A(\mathbf{k},\omega)/2\pi$ is normalized to unity, this means both that

$$Z_{\mathbf{k}} \leq 1 \tag{7.10}$$

and that there are additional contributions to the spectral weight that we have denoted *inc* in accord with the usual terminology of "incoherent background". The equality in the last equation holds only if the real part of the self-energy is frequency independent.

It is also natural to ask how the quasiparticle disperses, in other words, what is its effective Fermi velocity compared with that of the bare particle. Let us define the bare velocity by

$$v_{\mathbf{k}} = \nabla_{\mathbf{k}} \zeta_{\mathbf{k}} \tag{7.11}$$

and the renormalized velocity by

$$v^*_{\mathbf{k}} = \nabla_{\mathbf{k}} E_{\mathbf{k}} \tag{7.12}$$

Then the relation between both quantities is obtained by taking the gradient of the quasiparticle equation Eq.(7.4).

$$\nabla_{\mathbf{k}} \left[E_{\mathbf{k}} - \mu - \zeta_{\mathbf{k}} - \operatorname{Re} \Sigma^R(\mathbf{k}, E_{\mathbf{k}} - \mu) \right] = 0 \tag{7.13}$$

$$v^*_{\mathbf{k}} - v_{\mathbf{k}} - \nabla_{\mathbf{k}} \operatorname{Re} \Sigma^R(\mathbf{k}, E_{\mathbf{k}} - \mu) - \left. \frac{\partial \operatorname{Re} \Sigma^R(\mathbf{k},\omega)}{\partial \omega} \right|_{E_{\mathbf{k}} - \mu} v^*_{\mathbf{k}} = 0 \tag{7.14}$$

where $\nabla_{\mathbf{k}}$ in the last equation acts only on the first argument of $\operatorname{Re} \Sigma^R(\mathbf{k}, E_{\mathbf{k}} - \mu)$. The last equation is easily solved if we can write that $\mathbf{k}$ dependence of Σ^R as a function of $\zeta_{\mathbf{k}}$ instead, something that is always possible for spherical Fermi surfaces. In such a case, $\nabla_{\mathbf{k}} \to (\nabla_{\mathbf{k}} \zeta_{\mathbf{k}})\, \partial/\partial \zeta_{\mathbf{k}}$ as we can see for example when $\zeta_{\mathbf{k}} = \mathbf{k}^2/2m$ and we have

$$\boxed{v^*_{\mathbf{k}} = v_{\mathbf{k}} \frac{1 + \frac{\partial}{\partial \zeta_{\mathbf{k}}} \operatorname{Re} \Sigma^R(\mathbf{k}, E_{\mathbf{k}} - \mu)}{1 - \frac{\partial}{\partial \omega} \operatorname{Re} \Sigma^R(\mathbf{k},\omega)\big|_{\omega = E_{\mathbf{k}} - \mu = 0}}.} \tag{7.15}$$

In cases where the electronic (band) structure has correctly treated the $\mathbf{k}$ dependence of the self-energy, or when the latter is negligible, then the renormalized Fermi velocity differs from the bare one only through the famous quasiparticle renormalization factor. In other words, $v^*_{\mathbf{k}} = Z_{\mathbf{k}} v_{\mathbf{k}}$. The equation for the renormalized velocity is also often written in terms of a mass renormalization instead. Indeed, we will discuss later the fact that the Fermi wave vector k_F is unmodified by interactions for spherical Fermi surfaces (Luttinger's theorem). Defining then $m^* v^*_{k_F} = k_F = m v_{k_F}$ means that our equation for the renormalized velocity gives us

$$\boxed{\frac{m}{m^*} = \lim_{\mathbf{k} \to \mathbf{k}_F} \frac{1 + \frac{\partial}{\partial \zeta_{\mathbf{k}}} \operatorname{Re} \Sigma^R(\mathbf{k}, E_{\mathbf{k}} - \mu)}{1 - \frac{\partial}{\partial \omega} \operatorname{Re} \Sigma^R(\mathbf{k},\omega)\big|_{\omega = E_{\mathbf{k}} - \mu}}} \tag{7.16}$$

Remark 27 *In the jargon, the quasiparticle piece of the spectral weight Eq. (7.3) is called the "coherent" piece of the spectral weight, by contrast with the incoherent contribution that I mentionned above.*

7.1 Fermi liquid interpretation of ARPES

Let us see how to interpret the experiments of the previous subsection in light of the quasiparticle model just described. First of all, the wave vectors studied are all close to the Fermi surface as measured on the scale of k_F. Hence, every quantity appearing in the quasiparticle spectral weight Eq.(7.8) that depends on the self-energy is evaluated at the Fermi wave vector, which can however be angle dependent. The frequency dependence of the self-energy then is most important. The experiments were carried out at $T = 20K$ where the resistivity has a T^2 temperature dependence. This is the regime dominated by electron-electron interactions, where so-called Fermi liquid theory applies. What is Fermi liquid theory?[2]

It would require more than the few lines that we have to explain it, but roughly speaking, for our purposes, let us say that it uses the fact that phase space for electron-electron scattering vanishes at zero temperature and at the Fermi surface, to argue that the quasiparticle model applies to interacting electrons. Originally the model was developed by Landau for liquid ^3He which has fermionic properties, hence the name Fermi Liquid theory. It is a very deep theory that in a sense justifies all the successes of the almost-free electron picture of electrons in solids. I cannot do it justice here. A simple way to make its main ingredients plausible, [**?**] is to assume that near the Fermi surface in the limit of zero temperature, the self-energy is *i)* analytic and *ii)* has an imaginary part that vanishes at zero frequency. The latter result follows from general considerations on the Pauli exclusion principle and available phase space that are briefly summarized in Fig. (7-1). I will give an alternate derivation in the section on the electron-gas.

Let us define real and imaginary parts of the retarded self-energy by

$$\Sigma^R = \Sigma' + i\Sigma'' \tag{7.17}$$

Our two hypothesis imply that Σ'' has the Taylor expansion

$$\Sigma''(\mathbf{k}_F;\omega) = \alpha\omega - \gamma\omega^2 + \dots \tag{7.18}$$

The imaginary part of the retarded self-energy must be negative to insure that the retarded Green's function has poles in the lower half-plane, as is clear from the general relation between Green function and self-energy Eq. (7.1). This means that we must have $\alpha = 0$ and $\gamma > 0$. Fermi liquid theory keeps only the leading term

$$\Sigma'' = -\gamma\omega^2$$

We will verify for simple models that this quadratic frequency dependence is essentially correct in $d \geq 3$.

We know that the imaginary part of the self-energy must vanish at infinite frequency where free-particle behavior is expected, as in the harmonic oscillator case. Following Refs. [60], we take the following smooth cutoff model, neglecting impurity scattering and temperature

$$\Sigma''(\omega) = \begin{cases} -s\frac{\omega^2}{\omega^{*2}} & \text{for } \omega < \omega^* \\ -sF\left(\frac{\omega}{\omega^*}\right) & \text{for } \omega > \omega^* \end{cases}, \tag{7.19}$$

where ω^* is the frequency at which ω^2 behavior stops, $2s$ is the electron-electron scattering rate (in units $\hbar = 1$) without many-body effects, and the cutoff function

[2] A short summary on internet by Ross McKenzie
https://docs.google.com/viewer?a=v&pid=sites&srcid=ZGVmYXVsdGRvbWFpbnxjb25kZW5zZWRjb25jZXB0czN8Z

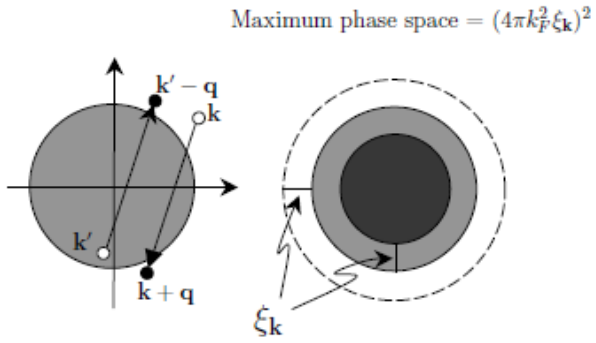

Figure 15.1: The two-particle scattering event that gives rise to a finite life time of the quasiparticles. Both momentum and energy have to be conserved. This together with the Pauli principle cause the phase space available for the scattering to be very limited, which is illustrated on the right hand figure. The dashed circle indicates the energy of the initial state. Since the particle can only loose energy, the other particle which is scattered out of state $\mathbf{k}'$ can only gain energy. Furthermore, because of the Pauli principle the final states of both particles have to lie outside the Fermi surface and therefore the phase space volume for the final state $\mathbf{k}+\mathbf{q}$ (white area) and for the initial state $\mathbf{k}'$ (gray area) both scale with $\xi_{\mathbf{k}}$ giving rise to a maximum total phase proportional to $\xi_{\mathbf{k}}^2$.

Figure 7-1 Taken from H. Bruus and K. Flensberg, "Introduction to Many-body theory in condensed matter physics".

$F(y)$ takes the value unity at $y = 1$ and then decreases monotonically to zero afterwards[3]. A more realistic model, as we will see, crosses over from ω^2 behavior while continuing to increase in absolute value before decreasing. But that does not modify the result that we are looking for, namely that the real-part of the self-energy obtained by Kramers-Kronig gives a value of Z consistent with quasiparticle behavior. So let us forge ahead.

The real part is then obtained from the Kramers-Kronig relation that must be obeyed by the self-energy. We make the additional assumption that $\Sigma''(\omega)$ is even in frequency. Another way to state that is that we assume particle-hole symmetry. Following the same arguments as those used for damping of the harmonic oscillator, the Kramers-Kronig relation give us for small ω

$$\left[\Sigma'(\mathbf{k}_F;\omega) - \Sigma'(\mathbf{k}_F;\infty)\right] = \mathcal{P}\int \frac{d\omega'}{\pi}\frac{\Sigma''(\mathbf{k}_F;\omega')}{\omega'-\omega} \tag{7.20}$$

$$= -\frac{s}{(\omega^*)^2}\mathcal{P}\int_{-\omega^*}^{\omega^*}\frac{d\omega'}{\pi}\frac{\left(\omega'^2-\omega^2+\omega^2\right)}{\omega'-\omega} - 2s\mathcal{P}\int_{\omega^*}^{\infty}\frac{d\omega'}{\pi}\frac{F\left(\frac{\omega}{\omega^*}\right)}{\omega'-\omega} \tag{7.21}$$

[3] Σ'' in this model has a discontinuous first derivative at $\omega = \omega^*$, which is why it is not a quite realistic model, even though it is better than a sharp cutoff model.

Let us focus on the first integral. It can be evaluated as follows

$$-\frac{s}{(\omega^*)^2}\mathcal{P}\int_{-\omega^*}^{\omega^*}\frac{d\omega'}{\pi}\frac{(\omega'-\omega)(\omega'+\omega)}{\omega'-\omega}-\frac{s}{(\omega^*)^2}\omega^2\mathcal{P}\int_{-\omega^*}^{\omega^*}\frac{d\omega'}{\pi}\frac{1}{\omega'-\omega} \tag{7.22}$$

$$= -\frac{s}{\pi}-\frac{2s}{\pi}\left(\frac{\omega}{\omega^*}\right)-\frac{s}{\pi}\left(\frac{\omega}{\omega^*}\right)^2\ln\left|\frac{\omega^*-\omega}{\omega^*+\omega}\right|. \tag{7.23}$$

The constant term is added to $\Sigma'(\mathbf{k}_F;\infty)$ to give the total contribution to the zero-frequency limit of the real-part of the self-energy, which leads to the renormalization of the chemical potential. Since $\ln[(1-x)/(1+x)]\sim -2x$, in the limit $\omega \ll \omega^*$ there is no linear in ω contribution from the logarithm. The remaining term involving F can be expanded in a power series in ω/ω^*. So there is term linear in ω coming from that. We are finally left with

$$\frac{\partial}{\partial\omega}\Sigma'(\mathbf{k}_F,\omega)\Big|_{\omega=0}=-\frac{2s\zeta}{\pi\omega^*} \tag{7.24}$$

where ζ is a number of less than 2 when estimated with the above model for the cutoff (as discussed in a remark below). Hence

$$\frac{\partial}{\partial\omega}\Sigma'(\mathbf{k},\omega)\Big|_{\omega=0}<0 \tag{7.25}$$

This in turn means that the corresponding value of Z_{k_F} is less than unity, as we had concluded in Eqs.(7.6) and (7.10) above. In summary, the analyticity hypothesis along with the vanishing of $\Sigma''(0)$ implies the existence of quasiparticles.

Remark 28 *Warning: there are subtleties. The above results assume that there is a cutoff to $\Sigma''(\mathbf{k}_F;\omega')$. The argument just mentioned in Eq.(7.24) fails when the integral diverges. Then, the low frequency expansion for the self-energy in Eq.(7.21) cannot be done. Expanding under the integral sign is no longer valid. One must do the principal part integral first. In fact, even for a Fermi liquid at finite temperature, $\Sigma''(\mathbf{k}_F;\omega)\sim\omega^2+(\pi T)^2$ so that the $(\pi T)^2$ appears to lead to a divergent integral in Eq.(7.24). Returning to the original Kramers-Krönig expression for Σ' however, the principal part integral shows that the constant term $(\pi T)^2$ for $\Sigma''(\mathbf{k}_F;\omega)$ does not contribute at all to Σ' if the cutoff in Σ'' is symmetric at positive and negative frequencies. In practice one can encounter situations where $\partial\Sigma/\partial\omega>0$. In that case, we do not have a Fermi liquid since $Z>1$ is inconsistent with the normalization of the spectral weight. One can work out an explicit example in the renormalized classical regime of spin fluctuations in two dimensions. (Appendix D of [97]).*

Remark 29 *To estimate the contribution from the cutoff, note that the denominator can be expanded in powers of ω/ω' because by construction, $\omega<\omega^*$ and we assume that $F\left(\frac{\omega}{\omega^*}\right)$ decreases at least as a power law starting from unity, making the integral convergent. So, recalling that this all started with F an even function of its argument,*

$$-2s\int_{\omega^*}^{\infty}\frac{d\omega'}{\pi}\frac{F\left(\frac{\omega}{\omega^*}\right)}{\omega'}\sum_{n=0}^{\infty}\left(\frac{\omega}{\omega'}\right)^{2n+1} \tag{7.26}$$

the linear in ω contribution from this term is

$$-2s\int_{\omega^*}^{\infty}\frac{d\omega'}{\pi}\frac{F\left(\frac{\omega}{\omega^*}\right)}{\omega'}\left(\frac{\omega}{\omega'}\right)\leq-\frac{2s}{\pi}\frac{\omega}{\omega^*}\int_1^{\infty}dy\frac{1}{y^2}=-\frac{2s}{\pi}\frac{\omega}{\omega^*} \tag{7.27}$$

which must be added to the linear in ω contribution, leading to the above estimate for the value of ζ.

The solid lines in Fig.(6-1) are two-parameter fits that also take into account the wave vector and energy resolution of the experiment [**?**]. One parameter is $E_k - \mu$ while the other one is γ', a quantity defined by substituting the Fermi liquid approximation in the equation for damping Eq.(7.9)

$$\Gamma_{k_F}(\omega) = Z_{k_F}\gamma\omega^2 = \gamma'\omega^2. \tag{7.28}$$

Contrary to E_k, the damping parameter γ' is the same for all curves. The solid-line fits are obtained with $\gamma' = 40eV^{-1}$ (β' on the figure). The fits become increasingly worse as one moves away from the Fermi surface, as expected. It is important to notice, however, that even the small left-over weight for wave-vectors above the Fermi surface $\left(\theta < 14.75^0\right)$ can be fitted with the same value of γ. This weight is the tail of a quasiparticle that could be observed at positive frequencies in inverse photoemission experiments (so-called BIS). The authors compared the results of their fits to the theoretical estimate, [**?**] $\gamma = 0.067\omega_p/\varepsilon_F^2$. Using $\omega_p = 18.2eV$, $\varepsilon_F = 0.3eV$ and the extrapolated value of Z_{k_F} obtained by putting[4] $r_s = 10$ in electron gas results, [**?**] they find $\gamma' < 5\,(eV)^{-1}$ while their experimental results are consistent with $\gamma' = 40 \pm 5\,(eV)^{-1}$. The theoretical estimate is almost one order of magnitude smaller than the experimental result. This is not so bad given the crudeness of the theoretical model (electron gas with no lattice effect). In particular, this system is a semimetal so that there are other decay channels than just the one estimated from a single circular Fermi surface. Furthermore, electron gas calculations are formally correct only for small r_s while there we have $r_s = 10$.

More recent experiments have been performed by Grioni's group [**?**]. Results are shown in Fig. (7-2). In this work, authors allow for a constant damping $\Gamma_0 = 17\ meV$ coming from the temperature and from disorder and then they fit the rest with a Fermi velocity $\hbar v_F = 0.73 \pm 0.1eV\ \dot{A}$ close to band structure calculations, $\hbar v_F = 0.68\ eV\ \dot{A}$ and γ' that varies between 0.5 eV^{-1} (16^0) and 0.9 eV^{-1} (14.5^0). The Fermi liquid fit is just as good, but the interpretation of the origin of the broadening terms is different. This shows that it is not always easy to interpret ARPES data, even for Fermi liquids. But we saw in Fig. (6-4) that modern electronic structure calculations that include the effect of correlations can be quite successful.

Theoretical estimates for high-temperature superconductors are two orders of magnitude smaller than the observed result [**?**].

Remark 30 *What allows the existence of the Fermi liquid is the vanishing of the imaginary part of the self-energy at $\omega = 0$. Electrons at the Fermi energy have an infinite lifetime at zero temperature. In addition, their lifetime vanishes faster than their energy ω so that "quasiparticles" survive in the vicinity of the Fermi surface. I will show that at finite temperature and $\omega = 0$, their lifetime is proportional to T^2. As a consequence, their width is sufficiently small that it makes sense to populate the quasiparticle states following the Fermi function.*

Remark 31 *Asymmetry of the lineshape: The line shapes are asymmetrical, with a tail at energies far from the Fermi surface (large binding energies). This is consistent with the fact that the "inverse lifetime" $\Gamma_{k_F}(\omega) = Z_{k_F}\gamma\omega^2$ is not a constant, but is instead larger at larger binding energies.*

Remark 32 *Failure of Fermi liquid at high-frequency: Clearly the Fermi liquid expression for the self-energy fails at large frequencies since we know from its spectral representation that the real-part of the self-energy goes to a frequency-independent constant at large frequency, the first correction being proportional to $1/\omega$. Conversely, there is always a cutoff in the imaginary part of the self-energy.*

[4] r_s is the average electron spacing expressed in terms of the Bohr radius.

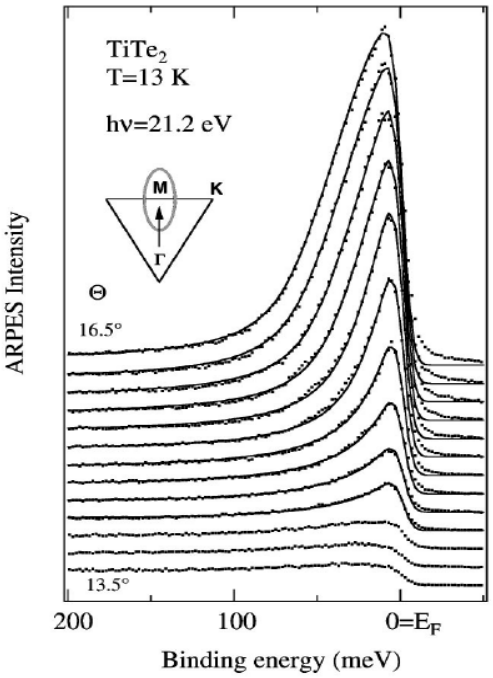

Figure 7-2 Figure 1 from Ref.[?] for the ARPES spectrum of 1*T*-$TiTe_2$ measured near the Fermi surface crossing along the high-symmetry ΓM direction ($\theta = 0$ is normal emission). The lines are results of Fermi liquid fits and the inset shows a portion of the Brillouin zone with the relevant ellipsoidal electron pocket.

This is not apparent in the Fermi liquid form above but we had to assume its existence for convergence. The cutoff on the imaginary part is analogous to the cutoff in χ''. Absorption cannot occur at arbitrary high frequency.

Remark 33 *Destruction of quasiparticles by critical fluctuations in two dimensions: Note that it is only if Σ'' vanishes fast enough at low frequency that it is correct to expand the Kramers-Kronig expression in powers of the frequency to obtain Eq.(7.24). When $\Sigma''(\omega)$ vanishes slower than ω^2, then Eq.(7.24) for the slope of the real part is not valid. The integral does not converge uniformly and it is not possible to interchange the order of differentiation and integration. In such a case it is possible to have the opposite inequality for the slope of the real part $\frac{\partial}{\partial\omega}\Sigma'(\mathbf{k},\omega)\big|_{\omega=0} > 0$. This does not lead to any contradiction, such as $Z_{k_F} > 1$, because there is no quasiparticle solution at $\omega = 0$ in this case. This situation occurs for example in two dimensions when classical thermal fluctuations create a pseudogap in the normal state before a zero-temperature phase transition is reached [?].*

Part IV

Lecture 4 (90 minutes)
Coherent states for fermions

8. COHERENT STATES FOR FERMIONS

Let us go back momentarily to first quantization: the Feynman path integral is an integral over all coordinates. The coordinates are operators in the Hamiltonian formalism. In the path integral case, the argument of the exponential is the action in units of $\hbar$.

By analogy, in second quantization, we want a path integral where the argument of the exponential is the action and the integrals are over fields. For bosons, it suffices to work in the coherent state basis. Coherent states for bosons are the analogs of classical fields. What are coherent states for fermions? This is what we set to do first. Then the functional integral follows naturally. An excellent reference is J.W. Negele and H. Orland, "Quantum Many-Particle Systems" (Addison-Wesley, Redwood city, 1988).

8.1 Grassmann variables for fermions

We wish to compute the partition function for time-ordered products with imaginary-time dependent Hamiltonians. This situation occurs for example when one does perturbation theory, obtains an effective Hamiltonian, or with source fields. Fermion coherent states are defined by analogy with the bosonic case. For simplicity, we work with spinless fermions. It is easy to introduce spins afterwards.

Let c be a fermion destruction operator, then $c\,|0\rangle = 0$ while the fermion coherent state $|\eta\rangle$ is an eigenstate of the destruction operator, by analogy with bosons.

$$c\,|\eta\rangle = \eta\,|\eta\rangle\,. \tag{8.1}$$

Since $c_1 c_2\,|\eta_1,\eta_2\rangle = -c_2 c_1\,|\eta_1,\eta_2\rangle$ the eigenvalues η must be numbers that anticommute. Namely,

$$\{\eta_1,\eta_2\} = 0. \tag{8.2}$$

Since Grassmann numbers occur only inside time-ordered products, it turns out that it suffices to define the adjoint in such a way that it also anticommutes, there is no delta function:

$$\left\{\eta,\eta^\dagger\right\} = 0. \tag{8.3}$$

Note that if we multiply η by a complex number α, then the adjoint of $\alpha\eta$ is given by $(\alpha\eta)^\dagger = \alpha^*\eta^\dagger$ where α^* is the complex conjugate of α.

Given the definition of Grassmann numbers, one can write an explicit definition of fermion coherent states in the Fock basis if we add the definition that Grassmann numbers and fermion operators also anticommute:

$$|\eta\rangle = \left(1-\eta c^\dagger\right)|0\rangle \tag{8.4}$$

Given that $\eta^2 = 0$, one can verify the defining property $c\,|\eta\rangle = \eta\,|\eta\rangle$ Eq.(8.1):

$$c\,|\eta\rangle = c\,|0\rangle + \eta c c^\dagger\,|0\rangle = \eta\,|0\rangle = \eta\left(1-\eta c^\dagger\right)|0\rangle = \eta\,|\eta\rangle\,. \tag{8.5}$$

Also, again since $\eta^2 = 0$, we can use the definition

$$|\eta\rangle = e^{-\eta c^\dagger} |0\rangle \tag{8.6}$$

that has the same structure as a boson coherent state.

Note that while η and $\eta^\dagger$ must be considered independent, the same way that z and z^* must be considered independent, they are nevertheless adjoint from each other. Namely, we have that

$$\langle\eta| = \langle 0| \left(1 - c\eta^\dagger\right). \tag{8.7}$$

8.2 Grassmann Calculus

In the case of bosons, the amplitude of a coherent state is arbitrary. For fermions, we imagine something analog. We must define then Grassmann integrals. To have meaning as integrals, these must satisfy properties such as

$$\int d\eta f(\eta + \xi) = \int d\eta f(\eta) \tag{8.8}$$

where ξ is another Grassmann number. The most general function of a Grassmann variable is $f(\eta) = a + b\eta$ since $\eta^2 = 0$. Hence, the above property is satisfied if $\int d\eta b\xi = 0$, which implies

$$\boxed{\int d\eta = 0.} \tag{8.9}$$

For derivatives and integrals to be consistent, the formula for integration by parts is also satisfied with the above definition (as if f vanished at infinity) because $\frac{df}{d\eta}$ can only be an ordinary number ($f(\eta)$ can only be linear in η).

$$\int d\eta \frac{df}{d\eta} = 0. \tag{8.10}$$

This definition is thus consistent with the natural definition of a derivative

$$\boxed{\frac{df}{d\eta} = \frac{d(a+b\eta)}{d\eta} = b} \tag{8.11}$$

with a and b ordinary C numbers.

Linearity

$$\int d\eta \left(af(\eta) + bg(\eta)\right) = \int d\eta af(\eta) + \int d\eta bg(\eta) \tag{8.12}$$

will be satisfied as long as $\int d\eta\eta$ is a number. The choice

$$\boxed{\int d\eta\eta = 1} \tag{8.13}$$

is convenient. The last property is consistent with the fact that the product of two Grassmann numbers is an ordinary number. Note that derivatives also anticommute. For example

$$\eta^\dagger \frac{\partial}{\partial\eta} = -\frac{\partial}{\partial\eta}\eta^\dagger. \tag{8.14}$$

In the end, note that the formula for integration looks the same as the formula for differentiation. The two rules Eqs.8.9 and 8.13 are all we need to remember.

Grassmann calculus is much easier than ordinary calculus. Not many things to remember!

One more thing. The analog of the Dirac delta function is well defined:

$$\int d\eta \delta\left(\eta' - \eta\right) F(\eta) = \int d\eta(\eta - \eta')(a + b\eta) = (a + b\eta') = F(\eta'). \tag{8.15}$$

Note that the order of η and η' in the argument is important.

8.3 Change of variables in Grassmann integrals

With integrals of ordinary complex variables, changes of variables are relected in the integration volume through a Jacobian. Let us take a single variable

$$\int_{-\infty}^{\infty} dx \exp\left(-x^2/2\right) = \sqrt{2\pi}. \tag{8.16}$$

With the change of variable $x = y/a$ then $dx = dy/a$ so that

$$\frac{1}{a}\int_{-\infty}^{\infty} dy \exp\left(-y^2/2a^2\right) = \frac{1}{a}\sqrt{2\pi a^2} = \sqrt{2\pi}. \tag{8.17}$$

Here, $\frac{1}{a}$ turns into a Jacobian when several variables are present.

Grassman variables behave differently. Indeed, let $F\left(\eta\right) = a + b\eta$ where a and b are complex numbers. Then,

$$\int d\eta F\left(\eta\right) = b \tag{8.18}$$

and if we change variable to $\eta = \eta'/\alpha$ then if we assume the usual Jacobian, namely $d\eta = d\eta'/\alpha$, then we obtain

$$\int d\eta F\left(\eta\right) = \frac{1}{\alpha}\int d\eta' F\left(\eta'/\alpha\right) = \frac{1}{\alpha}\frac{b}{\alpha}, \tag{8.19}$$

which clearly shows that something went wrong. The solution is that we need the inverse of the Jacobian when we do the change of variables

$$\int d\eta F\left(\eta\right) = \alpha\int d\eta' F\left(\eta'/\alpha\right) = b. \tag{8.20}$$

In the many-variable case, consider the following change of variable

$$\psi_i = \sum_{j=1}^{N} U_{ij}\eta_j \tag{8.21}$$

Then

$$\prod_{i=1}^{N}\int d\psi_i = \prod_{i=1}^{N}\sum_{j_i=1}^{N} U_{ij_i}\int d\eta_{j_i}. \tag{8.22}$$

All the j_i indices need to be different because of the properties of the Grassmann numbers. In addition, if you rearrange all the $d\eta_{j_i}$ in increasing order of index, $j_1 =$

1, $j_2 = 2$ etc, the signature of the permutation appears. This can be summarized with the help of the completely antisymmetric (Levi-Civita) tensor $\varepsilon^{j_1 j_2 \cdots j_N}$,

$$\begin{aligned}
\prod_{i=1}^{N} \sum_{j_i=1}^{N} U_{ij_i} \int d\eta_{j_i} &= \sum_{j_1=1}^{N} \sum_{j_2=1}^{N} \cdots \sum_{j_N=1}^{N} U_{1j_1} U_{2j_2} \cdots U_{Nj_N} \int d\eta_{j_1} \int d\eta_{j_2} \cdots \int d\eta_{jN} \\
&= \sum_{j_1=1}^{N} \sum_{j_2=1}^{N} \cdots \sum_{j_N=1}^{N} U_{1j_1} U_{2j_2} \cdots U_{Nj_N} \varepsilon^{j_1 j_2 \cdots j_N} \int d\eta_1 \int d\eta_2 \cdots \int d\eta_N \\
&= \det[U] \prod_{k=1}^{N} \int d\eta_k \qquad (8.23)
\end{aligned}$$

This will be an integral over Grassmann variables and we know that only the part $\psi_{j_1} \psi_{j_2} \cdots \psi_{jN}$ of the function of many variables will contribute. The change of variables will lead to the same determinant. For the same reasons as above then, we should use $\det[U]^{-1}$ instead of $\det[U]$ for the Jacobian.

Remark 34 *Note that the change of variables between imaginary time and Matsubara frequencies is almost unitary, but not quite since*

$$\mathcal{G}(\tau) = T \sum_n e^{-i\omega_n \tau} \mathcal{G}(i\omega_n) \qquad (8.24)$$

$$\mathcal{G}(i\omega_n) = \int_0^\beta d\tau e^{i\omega_n \tau} \mathcal{G}(\tau) \qquad (8.25)$$

gives a transformation matrix $Te^{-i\omega_n \tau}$ whose inverse is $d\tau e^{i\omega_n \tau}$ is not just the complex conjugate of the transpose. There is a numerical factor that comes in. This will lead to subtleties in the expression for the partition function below. Contrast this with the unitary transformation $\frac{1}{\sqrt{N}} e^{i\mathbf{k}\cdot\mathbf{r}_i}$ that allows one to go from discrete momentum space to discrete lattice sites. We can nevertheless relate the Matsubara variables by changing definitions

$$\widetilde{\mathcal{G}}(\tau) = \frac{1}{\sqrt{N_\tau}} \sum_n e^{-i\omega_n \tau} \widetilde{\mathcal{G}}(i\omega_n) \qquad (8.26)$$

$$\widetilde{\mathcal{G}}(i\omega_n) = \sqrt{N_\tau} T \int_0^\beta d\tau e^{i\omega_n \tau} \widetilde{\mathcal{G}}(\tau). \qquad (8.27)$$

with N_τ going to infinity being the number of Matsubara frequencies and the number of imaginay-time points. A discretization of $\sqrt{N_\tau} T d\tau e^{i\omega_n \tau}$ into $e^{i\omega_n \tau}/\sqrt{N_\tau}$ by using $Td\tau = T\beta/N_\tau$ yields a transformation formula that looks unitary.

8.4 Grassmann Gaussian integrals

Let us practice with the integral we will meet all the time, the analog of the Gaussian integral. With the above rules for integration, and $e^{-\eta^\dagger \eta} = 1 - \eta^\dagger \eta$ that follows from $\eta^2 = 0$, we find

$$\int d\eta^\dagger \int d\eta e^{-\eta^\dagger a \eta} = \int d\eta^\dagger \int d\eta \left(1 - \eta^\dagger a \eta\right) = a = \exp(\log(a)) \qquad (8.28)$$

where a is an ordinary number. We used,

$$\int d\eta^\dagger \int d\eta \left(-\eta^\dagger a \eta\right) = \int d\eta^\dagger \eta^\dagger \int d\eta \eta a = a.$$

Note the order of $\int d\eta^\dagger \int d\eta$. We have to keep this order for the rest of our calculations. This is a mere convention, but since Grassmann variables anticommute, we should stick with one convention.

If we have two Grassman variables, notice first by expanding to linear order

$$\begin{aligned}\int d\eta_1^\dagger \int d\eta_1 e^{-\eta_1^\dagger a_1 \eta_1} \int d\eta_2^\dagger \int d\eta_2 e^{-\eta_2^\dagger a_2 \eta_2} &= \\ \int d\eta_1^\dagger \int d\eta_1 \int d\eta_2^\dagger \int d\eta_2 e^{-\eta_1^\dagger a_1 \eta_1} e^{-\eta_2^\dagger a_2 \eta_2} &= a_1 a_2 \qquad (8.29)\\ &= \exp\left[\ln a_1 + \ln a_2\right] \qquad (8.30)\end{aligned}$$

The quantity $a_1 a_2$ is the determinant of the diagonal matrix with a_1 and a_2 on the diagonal. Since it can easily be proven by power series expansion (or from the fact that $\eta_1^\dagger \eta_1$ commutes with $\eta_2^\dagger \eta_2$) that exponentials of sums of quadratic Grassmann expressions behave as classical objects, namely

$$e^{-\eta_1^\dagger a_1 \eta_1} e^{-\eta_2^\dagger a_2 \eta_2} = e^{-\eta_1^\dagger a_1 \eta_1 - \eta_2^\dagger a_2 \eta_2}, \qquad (8.31)$$

we can write in matrix notation for a general basis

$$\boxed{\prod_i \int d\eta_i^\dagger \int d\eta_i e^{-\boldsymbol{\eta}^\dagger \mathbf{A} \boldsymbol{\eta}} = \det(A) = \exp\left[\mathrm{Tr} \ln(A)\right].} \qquad (8.32)$$

The last equalities follow by using the fact that the determinant and the trace are both basis independent. We abbreviate further the notation with the definition of the integration measure

$$\boxed{\int \mathcal{D}\eta^\dagger \int \mathcal{D}\eta e^{-\boldsymbol{\eta}^\dagger \mathbf{A} \boldsymbol{\eta}} \equiv \prod_i \int d\eta_i^\dagger \int d\eta_i e^{-\boldsymbol{\eta}^\dagger \mathbf{A} \boldsymbol{\eta}}.} \qquad (8.33)$$

There is another gaussian integral to do that is simple and that will allow us to use source fields to our benefit. Defining the Grassman source fields J and $J^\dagger$, we can use what we know about shifting the origin of integration, Eq.(8.8), and obtain

$$\begin{aligned}\int d\eta^\dagger \int d\eta e^{-\eta^\dagger a \eta - \eta^\dagger J - J^\dagger \eta} &= \int d\eta \int d\eta^\dagger e^{-\left(\eta^\dagger + J^\dagger a^{-1}\right) a \left(\eta + a^{-1} J\right) + J^\dagger a^{-1} J} \qquad (8.34)\\ &= a \exp\left(J^\dagger a^{-1} J\right). \qquad (8.35)\end{aligned}$$

The generalization to integrals over many Grassmann variables gives

$$\int \mathcal{D}\eta^\dagger \int \mathcal{D}\eta e^{-\boldsymbol{\eta}^\dagger \mathbf{A} \boldsymbol{\eta} - \boldsymbol{\eta}^\dagger \mathbf{J} - \mathbf{J}^\dagger \boldsymbol{\eta}} = \int \mathcal{D}\eta^\dagger \int \mathcal{D}\eta e^{-\left(\boldsymbol{\eta}^\dagger + \mathbf{J}^\dagger \mathbf{A}^{-1}\right) \mathbf{A} \left(\boldsymbol{\eta} + \mathbf{A}^{-1} \mathbf{J}\right) + \left(\mathbf{J}^\dagger \mathbf{A}^{-1} \mathbf{J}\right)}$$

$$\boxed{\int \mathcal{D}\eta^\dagger \int \mathcal{D}\eta e^{-\boldsymbol{\eta}^\dagger \mathbf{A} \boldsymbol{\eta} - \boldsymbol{\eta}^\dagger \mathbf{J} - \mathbf{J}^\dagger \boldsymbol{\eta}} = \det(A) \exp\left(\mathbf{J}^\dagger \mathbf{A}^{-1} \mathbf{J}\right)} \qquad (8.36)$$

We will be able to use this result to obtain Green's functions or multipoint functions from functional derivatives with respect to J.

8.5 Closure, overcompleteness and trace formula

To find the expression for the partition function, we will need the completeness relation. From the last result of the previous section, you can verify the following closure formula by applying it successively on $|0\rangle$ and on $c^\dagger |0\rangle$:

$$\boxed{\int d\eta^\dagger \int d\eta e^{-\eta^\dagger \eta} |\eta\rangle \langle\eta| = \int d\eta^\dagger \int d\eta \left(1 - \eta^\dagger \eta\right) |\eta\rangle \langle\eta| = I.} \qquad (8.37)$$

Indeed, recalling that only terms of the form $\int d\eta^\dagger \int d\eta \eta^\dagger \eta = -1$ survive, we are left with

$$\begin{aligned} & \int d\eta^\dagger \int d\eta \left(1-\eta^\dagger\eta\right)\left(1-\eta c^\dagger\right)|0\rangle\langle 0|\left(1-c\eta^\dagger\right) \\ = & \int d\eta^\dagger \int d\eta \left[\left(-\eta^\dagger\eta\right)|0\rangle\langle 0| + \eta c^\dagger|0\rangle\langle 0| c\eta^\dagger\right] \\ = & |0\rangle\langle 0| + |1\rangle\langle 1| \end{aligned}$$

Take a single state that can be empty or occupied, as above. The trace of an operator O can be written as follows,

$$\boxed{\mathrm{Tr}[O] = \int d\eta^\dagger \int d\eta e^{-\eta^\dagger\eta}\langle -\eta| O |\eta\rangle.} \tag{8.38}$$

The minus sign reflects the antiperiodicity that we encounter with fermions. To prove the above formula, it suffices to use the definition of the fermionic coherent state Eq.(8.4). Indeed,

$$\begin{aligned} \int d\eta^\dagger \int d\eta e^{-\eta^\dagger\eta}\langle -\eta| O |\eta\rangle &= \int d\eta^\dagger \int d\eta e^{-\eta^\dagger\eta}\langle 0|\left(1+c\eta^\dagger\right) O \left(1-\eta c^\dagger\right)|0\rangle \\ &= \int d\eta^\dagger \int d\eta \left(1-\eta^\dagger\eta\right)\langle 0|\left(1+c\eta^\dagger\right) O \left(1-\eta c^\dagger\right)|0\rangle \\ &= \int d\eta^\dagger \int d\eta \left(1-\eta^\dagger\eta\right)\left(\langle 0| O |0\rangle - \langle 0| c\eta^\dagger O \eta c^\dagger |0\rangle\right) \\ &= \int d\eta^\dagger \int d\eta \left(1-\eta^\dagger\eta\right)\left(\langle 0| O |0\rangle - \eta^\dagger\eta\langle 0| cOc^\dagger |0\rangle\right) \\ &= \langle 0| O |0\rangle + \langle 1| O |1\rangle . \end{aligned} \tag{8.39}$$

In the next to last equation, we assumed that O contains an even number of fermion operators so that

$$\eta O = O\eta. \tag{8.40}$$

The set is overcomplete since using the definition in terms of Fock states Eq.(8.4), one finds

$$\boxed{\langle \eta_1 |\eta_2\rangle = \langle 0|\left(1-c\eta_1^\dagger\right)\left(1-\eta_2 c^\dagger\right)|0\rangle = 1+\eta_1^\dagger\eta_2 = e^{\eta_1^\dagger\eta_2}.} \tag{8.41}$$

9. COHERENT STATE FUNCTIONAL INTEGRAL FOR FERMIONS

9.1 A simple example for a single fermion without interactions

For spinless fermions whose Hamiltonian is given by $H = \sum_i \varepsilon_i c_i^\dagger c_i$, the partition function is

$$Z = \mathrm{Tr}\left(\exp\left(-\beta H\right)\right) = \prod_i \left(1 + e^{-\beta\varepsilon_i}\right) = \det\left(1 + e^{-\beta\boldsymbol{\varepsilon}}\right) \tag{9.1}$$

where $\boldsymbol{\varepsilon}$ is the diagonal matrix. The expression remains valid in an arbitrary basis. What is the generalization of this result when H depends on τ and we want a time-ordered product

$$Z = \mathrm{Tr}\left(T_\tau \exp\left(-\int_0^\beta d\tau H\left(\tau\right)\right)\right)? \tag{9.2}$$

We can work this out in the usual operator formalism. With Grassmann variables, we need to suffer first, but then the calculations are easy and formally very close to those for bosons.

Let us start with a single fermion state, so that

$$H = \varepsilon c^\dagger c.$$

Then, we express the trace in the coherent fermion basis. In that basis, we do not know how to compute $e^{-\beta H}\left|\eta\right\rangle$ since the expansion of the exponential gives an infinite number of terms. We can however use the Trotter decomposition to do a Taylor expansion that will be easy to evaluate in the coherent state basis. The Trotter decomposition is given by

$$e^{-\beta H} = \lim_{N_\tau\to\infty} \prod_{i=1}^{N_\tau} e^{-\Delta\tau_i H} = \lim_{N_\tau\to\infty} \prod_{i=1}^{N_\tau} \left(1 - \Delta\tau_i H\right). \tag{9.3}$$

with $\Delta\tau = \beta/N_\tau$. The index i on $\Delta\tau$ is just to allow us to keep track of the different terms. Even if H was time dependent, we could use this approximation in the limit $\Delta\tau \to 0$ because $\left[\Delta\tau H\left(\tau_1\right), \Delta\tau H\left(\tau_2\right)\right] = \mathcal{O}\left(\Delta\tau\right)^2$ and we will neglect terms of that order. In other words, for $\Delta\tau \to 0$ we can assume that exponentials of sums of operators can be rewritten as a product of exponentials.[1] To linear

[1] There is one subtlety. We have many time-slices. Since $N_\tau\left(\Delta\tau\right)^2 = \beta\Delta\tau$, it looks as if the error is of order $\Delta\tau$, not $\left(\Delta\tau\right)^2$. Fye has shown that the prefactor of $\beta\Delta\tau$ vanishes when one is interested in expectation values of certain kinds of operators. This is basically because the operator in front of $\Delta\tau$ is a commutator and is thus anti-Hermitian. The trace of that anti-hermitian operator vanishes.

order in $\Delta\tau$ then, we have that

$$\langle\eta_2|\, e^{-\Delta\tau_i H[c^\dagger,c]}\, |\eta_1\rangle = e^{-\Delta\tau_i H[\eta_2^\dagger,\eta_1]}\, \langle\eta_2\, |\eta_1\rangle \tag{9.4}$$

In this expression, we have assumed that all destruction operators were on the right and all creation operators on the left so that they can be replaced by the corresponding Grassmann variable when acting on coherent states. This order of creation-annihilation operators is known as normal order.

Back to our task. Using the trace formula in the coherent state basis Eq.(8.38) and inserting the completeness relation Eq.(8.37) between each term of the product, we can evaluate the exponential in the coherent-state basis. We find, with the definitions $\eta_\beta = \eta_{N_\tau} = -\eta_0$ and

$$\boxed{\int \mathcal{D}\eta^\dagger \int \mathcal{D}\eta = \int d\eta_0^\dagger \int d\eta_0 \prod_{i=1}^{N_\tau} \int d\eta_i^\dagger \int d\eta_i}$$

that

$$\begin{aligned} Z &= \lim_{N_\tau\to\infty} \int \mathcal{D}\eta^\dagger \int \mathcal{D}\eta e^{-\eta_\beta^\dagger\eta_\beta} \left\langle\eta_\beta\right| e^{-\Delta\tau_{N_\tau}\varepsilon\eta_\beta^\dagger\eta_{N_\tau-1}} \left|\eta_{N_\tau-1}\right\rangle\, e^{-\eta_{N_\tau-1}^\dagger\eta_{N_\tau-1}} \left\langle\eta_{N_\tau-1}\right| \\ &\quad \ldots\, |\eta_1\rangle\, e^{-\eta_1^\dagger\eta_1}\, \langle\eta_1|\, e^{-\Delta\tau_1\varepsilon\eta_1^\dagger\eta_0}\, |\eta_0\rangle \qquad (9.5) \\ &= \lim_{N_\tau\to\infty} \int \mathcal{D}\eta^\dagger \int \mathcal{D}\eta e^{-\eta_\beta^\dagger\eta_\beta} e^{(1-\Delta\tau_{N_\tau}\varepsilon)\eta_\beta^\dagger\eta_{N_\tau-1}}\; e^{-\eta_{N_\tau-1}^\dagger\eta_{N_\tau-1}} e^{\left(1-\Delta\tau_{N_\tau-1}\varepsilon\right)\eta_{N_\tau-1}^\dagger\eta_{N_\tau-2}} \\ &\quad \ldots |\eta_1\rangle\; e^{-\eta_1^\dagger\eta_1} e^{(1-\varepsilon\Delta\tau)\eta_1^\dagger\eta_0}. \qquad (9.6) \end{aligned}$$

which is a time-ordered product. In the second line, we have used, $e^{-\eta_1^\dagger\eta_1}\, \langle\eta_1\, |\eta_0\rangle = e^{-\eta_1^\dagger\eta_1+\eta_1^\dagger\eta_0}$ and applied repeatedly formulas such as

$$\left\langle\eta_\beta\right| e^{-\Delta\tau_{N_\tau}\varepsilon\eta_\beta^\dagger\eta_{N_\tau-1}} \left|\eta_{N_\tau-1}\right\rangle = e^{\eta_\beta^\dagger\eta_{N_\tau-1}} e^{-\Delta\tau_{N_\tau}\varepsilon\eta_\beta^\dagger\eta_{N_\tau-1}} = e^{(1-\Delta\tau_{N_\tau}\varepsilon)\eta_\beta^\dagger\eta_{N_\tau-1}}. \tag{9.7}$$

The above formula is obviously generalizable to a time-dependent Hamiltonian that appears in a time-ordered product.

To evaluate this quantity on a computer, we need to first do the integrals over Grassmann variables and express the result in terms of matrices, remembering that the definition of the matrices must be read off the above formula. There is no ambiguity. The matrix A that appeared in the Gaussian Grassmann integral Eq.(8.32) $Z = \lim_{N_\tau\to\infty} \int \mathcal{D}\eta^\dagger \int \mathcal{D}\eta\; e^{-\boldsymbol{\eta}^\dagger \mathbf{A} \boldsymbol{\eta}}$ can be written down, assuming that $\Delta\tau$ is the same for all imaginary-time slices, as

$$\boxed{A = \begin{bmatrix} 1 & 0 & 0 & \ldots & 0 & (1-\varepsilon\Delta\tau) \\ -(1-\varepsilon\Delta\tau) & 1 & 0 & \ldots & 0 & 0 \\ 0 & -(1-\varepsilon\Delta\tau) & 1 & \ldots & 0 & 0 \\ 0 & 0 & -(1-\varepsilon\Delta\tau) & \ldots & 0 & 0 \\ 0 & 0 & 0 & \ldots & 1 & 0 \\ 0 & 0 & 0 & \ldots & -(1-\varepsilon\Delta\tau) & 1 \end{bmatrix} \equiv -\mathcal{G}^{-1}.} \tag{9.8}$$

The above matrix has dimension $N_\tau \times N_\tau$. Labels 0 to $N_\tau - 1$ or 1 to N_τ can be used. In other words, either time $\tau = 0$ or $\tau = \beta$ can be present as independent labels, but not both. They are related by antiperiodicity. The matrix element in the upper right corner comes from

$$\left\langle\eta_\beta\, \left|\eta_{N_\tau-1}\right\rangle e^{-\varepsilon\eta_\beta^\dagger\eta_{N_\tau-1}\Delta\tau} = \left\langle-\eta_0\, \left|\eta_{N_\tau-1}\right\rangle e^{\varepsilon\eta_0^\dagger\eta_{N_\tau-1}\Delta\tau} = e^{(-1+\varepsilon\Delta\tau)\eta_0^\dagger\eta_{N_\tau-1}}. \right.\right. \tag{9.9}$$

Note that in actual computations, it is more accurate to replace $-1+\varepsilon\Delta\tau$ by $-e^{\varepsilon\Delta\tau}$. If ε is time dependent, it suffices to replace its value at the appropriate time slice. If ε is time independent, the determinant of the matrix A is equal, when N_τ tends to infinity, to $\left(1+(1-\varepsilon\Delta\tau)^{N_\tau}\right)=\left(1+e^{-\beta\varepsilon}\right)$, as we would expect from the free fermion formula Eq.(9.1) when there is a single fermion state.

9.2 Generalization to a continuum and to a time dependent one-body Hamiltonian

The continuum limit can also be taken formally. We can combine the exponentials coming from the completeness relation and from the overlap of fermion coherent states as follows

$$e^{-\eta_1^\dagger\eta_1}\left\langle\eta_1\right|\left.\eta_0\right\rangle=e^{-\eta_1^\dagger\eta_1+\eta_1^\dagger\eta_0}=e^{-\eta_1^\dagger(\eta_1-\eta_0)}=e^{-\eta_1^\dagger\frac{\partial}{\partial\tau}\eta_1\Delta\tau}. \tag{9.10}$$

Also, to leading order in $\Delta\tau$, we approximate terms such as $\eta_1^\dagger\eta_0\Delta\tau$ by $\eta_0^\dagger\eta_0\Delta\tau$. If we take the limit and impose the $\eta_\beta=-\eta_0$ on the last matrix element to the left, we can rewrite the partition function as

$$Z=\int\mathcal{D}\eta^\dagger\int\mathcal{D}\eta\exp\left(-S\right) \tag{9.11}$$

where, by analogy with the Lagrangian formalism, we define the following quantity

$$S=\int_0^\beta d\tau\left(\eta^\dagger\left(\tau\right)\frac{\partial}{\partial\tau}\eta\left(\tau\right)+\varepsilon\left(\tau\right)\eta^\dagger\left(\tau\right)\eta\left(\tau\right)\right) \tag{9.12}$$

as the action S. In writing this, the $\varepsilon\left(\tau\right)$ shows that we have generalized also to a time-dependent Hamiltonian. The integrand is like a Lagrangian when $\eta^\dagger\left(\tau\right)$ and $\eta\left(\tau\right)$ are taken as conjugate variables.

Thinking of the η at different times as different variables, we can use our formula for Gaussian integrals over Grassmann variables Eq.(8.32) the partition funciton can be written as

$$Z=\det\left(\frac{\partial}{\partial\tau}+\varepsilon\left(\tau\right)\right)=\exp\left[\mathrm{Tr}\log\left(\frac{\partial}{\partial\tau}+\varepsilon\left(\tau\right)\right)\right]. \tag{9.13}$$

The matrix entering determinant and trace above is defined by returning to the discrete representation.

In the case of a *time-independent* Hamiltonian, the determinant can be formally evaluated as follows. Go to the basis where the time derivative is diagonal, namely the Matsubara-frequency basis, which has the correct antiperiodicity imposed by the trace formula Eq. 8.38:

$$\eta\left(\tau\right) = \sqrt{T}\sum_n e^{-ik_n\tau}\eta\left(ik_n\right) \tag{9.14}$$

$$\eta^\dagger\left(\tau\right) = \sqrt{T}\sum_m e^{ik'_m\tau}\eta^\dagger\left(ik_m\right). \tag{9.15}$$

This leads to the following formula for the action

$$\begin{aligned} S &= \int_0^\beta d\tau \left(\eta^\dagger(\tau) \frac{\partial}{\partial \tau} \eta(\tau) + \varepsilon\, \eta^\dagger(\tau) \eta(\tau) \right) && (9.16) \\ &= T \int_0^\beta d\tau \sum_n \sum_m e^{-i\left(k_n - k'_m\right)\tau} \eta^\dagger(ik'_m) (-ik_n + \varepsilon) \eta(ik_n) && (9.17) \\ &= \sum_n \eta^\dagger(ik_n) (-ik_n + \varepsilon) \eta(ik_n) && (9.18) \\ &= \sum_n \eta^\dagger(ik_n) \left(-\mathcal{G}^{-1}(ik_n)\right) \eta(ik_n). && (9.19) \end{aligned}$$

The determinant accompanying this change of variables is unity in the following sense:

$$\begin{aligned} \det U^\dagger \det U &= \det U^\dagger U = \det \left(T \sum_n \sum_m e^{-i\left(k_n - k'_m\right)\tau} \right) && (9.20) \\ &= \det T\delta(\tau) && (9.21) \end{aligned}$$

The quantity $T\delta(\tau)$ is dimensionless, and in a discrete version of the imaginary time leads to $\det T\delta(\tau) = 1$. In this basis, the partition function is explicitly given by

$$\begin{aligned} Z &= \exp\left[\mathrm{Tr} \log(-ik_n + \varepsilon)\right] = \exp\left[\sum_n e^{-ik_n 0} \log(-ik_n + \varepsilon) \right] && (9.22) \\ &= \exp\left[\sum_n e^{-ik_n 0} \log\left(-\mathcal{G}^{-1}(ik_n)\right) \right]. && (9.23) \end{aligned}$$

The factor $e^{-ik_n 0^-}$ is made necessary to have a unique result. Read the important remark below to understand the difficulties of interpretation of the above formula.

The derivatives of this formula give correct results if we proceed without asking questions. To verify this, look at the expression for the occupation number

$$\begin{aligned} n &= \frac{\mathrm{Tr}\left(\exp(-\beta H) c^\dagger c\right)}{\mathrm{Tr}\left(\exp(-\beta H)\right)} = -\frac{\partial \ln Z}{\partial(\beta\varepsilon)} \\ &= -\frac{\partial \sum_n \log(-ik_n + \varepsilon) e^{-ik_n 0^-}}{\partial(\beta\varepsilon)} = T \sum_n \frac{e^{-ik_n 0^-}}{(ik_n - \varepsilon)} = \frac{1}{1 + e^{\beta\epsilon}}. \quad (9.24) \end{aligned}$$

In this expression, we have *assumed* that the sum converged to invert the sum and the derivative.

Remark 35 *You will see this formula very often*

$$\exp\left[\sum_n e^{-ik_n 0} \log\left(-\mathcal{G}^{-1}(ik_n)\right) \right] \quad (9.25)$$

in the literature, but as the time-independent case shows, the validity of the standard trick to sum over Matsubara frequencies by deforming a contour is not obvious because it is not even clear whether the sum

$$\sum_n e^{-ik_n 0} \log(-ik_n + \varepsilon) \quad (9.26)$$

converges. This deserves a more detailed discussion that I will not do here.

9.3 Wick's theorem

To find the Green function, we can first assume again that we work in the diagonal basis. Then, in this diagonal basis, we expand the exponential to find

$$\begin{aligned}\frac{-\int \mathcal{D}\eta^\dagger \int \mathcal{D}\eta e^{-\boldsymbol{\eta}^\dagger(-\mathcal{G}^{-1})\boldsymbol{\eta}}\eta_1\eta_1^\dagger}{\int \mathcal{D}\eta^\dagger \int \mathcal{D}\eta e^{-\boldsymbol{\eta}^\dagger(-\mathcal{G}^{-1})\boldsymbol{\eta}}} &= \frac{-\int d\eta_1^\dagger \int d\eta_1 \left(1+\mathcal{G}_{11}^{-1}\eta_1^\dagger\eta_1\right)\eta_1\eta_1^\dagger}{\int d\eta_1^\dagger \int d\eta_1 \left(1+\mathcal{G}_{11}^{-1}\eta_1^\dagger\eta_1\right)} \\ &= -\frac{\int d\eta_1^\dagger \int d\eta_1 \eta_1\eta_1^\dagger}{\int d\eta_1^\dagger \int d\eta_1 \left(1+\mathcal{G}_{11}^{-1}\eta_1^\dagger\eta_1\right)} \\ &= \mathcal{G}_{11} \end{aligned} \tag{9.27}$$

To compute higher order correlation functions, notice that

$$\begin{aligned}\frac{\int \mathcal{D}\eta^\dagger \int \mathcal{D}\eta e^{-\boldsymbol{\eta}^\dagger(-\mathcal{G}^{-1})\boldsymbol{\eta}}\eta_1\eta_1^\dagger\eta_2\eta_2^\dagger}{\int \mathcal{D}\eta^\dagger \int \mathcal{D}\eta e^{-\boldsymbol{\eta}^\dagger(-\mathcal{G}^{-1})\boldsymbol{\eta}}} &= \frac{-\int d\eta_1^\dagger \int d\eta_1 e^{-\eta_1^\dagger(-\mathcal{G}_{11}^{-1})\eta_1}\eta_1\eta_1^\dagger \int d\eta_2^\dagger \int d\eta_2 e^{-\eta_2^\dagger(-\mathcal{G}_{22}^{-1})\eta_2}\eta_2\eta_2^\dagger}{\int d\eta_1^\dagger \int d\eta_1 e^{-\eta_1^\dagger(-\mathcal{G}_{11}^{-1})\eta_1}\int d\eta_2^\dagger \int d\eta_2 e^{-\eta_2^\dagger(-\mathcal{G}_{22}^{-1})\eta_2}} \\ &= -\frac{1}{\int d\eta_1^\dagger \int d\eta_1 e^{-\eta_1^\dagger(-\mathcal{G}_{11}^{-1})\eta_1}\int d\eta_2^\dagger \int d\eta_2 e^{-\eta_2^\dagger(-\mathcal{G}_{22}^{-1})\eta_2}} \\ &= \mathcal{G}_{11}\mathcal{G}_{22}. \end{aligned} \tag{9.28}$$

In this diagonal basis, this is the determinant of the $\mathcal{G}$ matrix. This result thus clearly generalizes, for imaginary time labels, to

$$(-1)^n \left\langle T_\tau c\left(\tau_n\right) c^\dagger\left(\tau_n'\right)\cdots c\left(\tau_2\right) c^\dagger\left(\tau_2'\right) c\left(\tau_1\right) c^\dagger\left(\tau_1'\right)\right\rangle \tag{9.29}$$

$$\begin{aligned} &= (-1)^n \frac{1}{Z}\int \mathcal{D}\eta^\dagger \int \mathcal{D}\eta e^{-\boldsymbol{\eta}^\dagger(-\mathcal{G}^{-1})\boldsymbol{\eta}}\eta\left(\tau_n\right)\eta^\dagger\left(\tau_n'\right)\cdots\eta\left(\tau_2\right)\eta^\dagger\left(\tau_2'\right)\eta\left(\tau_1\right)\eta^\dagger\left(\tau_1'\right) \\ &= \det\begin{bmatrix} \mathcal{G}\left(\tau_1,\tau_1'\right) & \mathcal{G}\left(\tau_1,\tau_2'\right) & \cdots & \mathcal{G}\left(\tau_1,\tau_n'\right) \\ \mathcal{G}\left(\tau_2,\tau_1'\right) & \mathcal{G}\left(\tau_2,\tau_2'\right) & \cdots & \mathcal{G}\left(\tau_2,\tau_n'\right) \\ \cdots & \cdots & \cdots & \cdots \\ \mathcal{G}\left(\tau_n,\tau_1'\right) & \mathcal{G}\left(\tau_n,\tau_2'\right) & \cdots & \mathcal{G}\left(\tau_n,\tau_n'\right) \end{bmatrix}. \end{aligned} \tag{9.30}$$

This is Wick's theorem. We have the product of all contractions with appropriate sign for the permutations.

Part V

Lecture 5 (90 minutes) Many-body perturbation theory

10. SOURCE FIELDS FOR MANY-BODY GREEN'S FUNCTIONS

After introducing the concept of source fields in the familiar context of classical statistical physics, I will generalize this to the case of functional integrals for fermions. The derivation of the Luttinger-Ward functional will not be too complicated after that.

10.1 A simple example in classical statistical mechanics

In elementary statistical mechanics, we can obtain the magnetization by differentiating the free energy with respect to the magnetic field and we can also obtain the magnetic susceptibility, related to the magnetization fluctuations, by differentiating once more.

Consider directly the more general problem of computing $\langle M(\mathbf{x}_1) M(\mathbf{x}_2)\rangle - \langle M(\mathbf{x}_1)\rangle \langle M(\mathbf{x}_2)\rangle$ in classical statistical mechanics. That can still be achieved if we impose a position dependent-external field:

$$Z[h] = \mathrm{Tr}\left[e^{-\beta\left(K - \int d^3\mathbf{x} h(\mathbf{x}) M(\mathbf{x})\right)}\right]. \tag{10.1}$$

It is as if at each position $\mathbf{x}$, there were an independent variable $h(\mathbf{x})$. The position is now just a label. The notation $Z[h]$ means that Z is a functional of $h(\mathbf{x})$.It takes a function and maps it into a scalar. To obtain the magnetization at a single point, we introduce the notion of functional derivative, which is just a simple generalization to the continuum of the idea of partial derivative. To be more specific,

$$\frac{\delta}{\delta h(\mathbf{x}_1)} \int d^3\mathbf{x} h(\mathbf{x}) M(\mathbf{x}) = \int d^3\mathbf{x} \frac{\delta h(\mathbf{x})}{\delta h(\mathbf{x}_1)} M(\mathbf{x}) \tag{10.2}$$

$$= \int d^3\mathbf{x} \delta(\mathbf{x}_1 - \mathbf{x}) M(\mathbf{x}) = M(\mathbf{x}_1). \tag{10.3}$$

In other words, the partial derivative $\partial y_1/\partial y_2 = \delta_{1,2}$ for two independent variables y_1 and y_2 is replaced by

$$\frac{\delta h(\mathbf{x})}{\delta h(\mathbf{x}_1)} = \delta(\mathbf{x}_1 - \mathbf{x}). \tag{10.4}$$

Very simple.

Armed with this notion of functional derivative, one finds that

$$\frac{\delta \ln Z[h]}{\beta \delta h(\mathbf{x}_1)} = \langle M(\mathbf{x}_1)\rangle_h \tag{10.5}$$

and the quantity we want is obtained from one more functional derivative

$$\frac{\delta^2 \ln Z[h]}{\beta^2 \delta h(\mathbf{x}_1)\, \delta h(\mathbf{x}_2)} = \langle M(\mathbf{x}_1) M(\mathbf{x}_2)\rangle_h - \langle M(\mathbf{x}_1)\rangle_h \langle M(\mathbf{x}_2)\rangle_h. \tag{10.6}$$

The $[h]$ near Z reminds us that Z is a functional of the function $h(\mathbf{x})$, i.e. it maps this function to a scalar, namely Z. We can then evaluate everything at $h(\mathbf{x}) = 0$ is that corresponds to the physical situation. The following generalization to Green functions is essentially a faithful copy of the one appearing in the main text.

10.2 c-number source fields in functional integrals to generate fermion bilinears

We have defined Grassmann source fields. Since we are generally interested in response functions that are quadratic in fermion operators, it is also useful to define source fields that are ordinary complex numbers that couple to two Grassmann numbers. More specifically, introduce in the partition function some source fields $\phi(1,2)$:

$$Z[\phi] = \int \mathcal{D}\psi^\dagger \int \mathcal{D}\psi \exp\left(-S - \psi^\dagger\left(\overline{1}\right)\phi\left(\overline{1},\overline{2}\right)\psi\left(\overline{2}\right)\right) \tag{10.7}$$

where we used the short-hand

$$(1) = (\mathbf{x}_1, \tau_1; \sigma_1) \tag{10.8}$$

with the overbar indicating integrals over space-time coordinates and spin sums. More specifically,

$$\psi^\dagger\left(\overline{1}\right)\phi\left(\overline{1},\overline{2}\right)\psi\left(\overline{2}\right) =$$

$$\sum_{\sigma_1,\sigma_2}\int d^3\mathbf{x}_1 \int_0^\beta d\tau_1 \int d^3\mathbf{x}_2 \int_0^\beta d\tau_2 \psi^\dagger_{\sigma_1}(\mathbf{x}_1,\tau_1)\,\phi_{\sigma_1,\sigma_2}(\mathbf{x}_1,\tau_1,\mathbf{x}_2,\tau_2)\,\psi_{\sigma_2}(\mathbf{x}_2,\tau_2).$$

We can think of $\psi^\dagger\left(\overline{1}\right)\phi\left(\overline{1},\overline{2}\right)\psi\left(\overline{2}\right)$ as vector-matrix-vector multiplication. Some of the matrix or vector indices are continuous, but that should not confuse you I think.

The functional derivative with respect to ϕ is defined by

$$\frac{\delta\phi\left(\overline{1},\overline{2}\right)}{\delta\phi(1,2)} = \delta\left(\overline{1}-1\right)\delta\left(\overline{2}-2\right) \tag{10.9}$$

where the delta function is a mixture of Dirac and Kronecker delta functions

$$\delta\left(\overline{1}-1\right) = \delta^3\left(\mathbf{x}_{\overline{1}} - \mathbf{x}_1\right)\delta\left(\tau_{\overline{1}} - \tau_1\right)\delta_{\sigma_{\overline{1}},\sigma_1}. \tag{10.10}$$

We can write the Matsubara Green's function as a functional derivative of the generating function $\ln Z[\phi]$,

$$\begin{aligned}\frac{\delta \ln Z[\phi]}{\delta\phi(1,2)} &= -\frac{1}{Z[\phi]}\int\mathcal{D}\psi^\dagger\int\mathcal{D}\psi\left(\psi^\dagger(1)\psi(2)\right)\exp\left(-S-\psi^\dagger\left(\overline{1}\right)\phi\left(\overline{1},\overline{2}\right)\psi\left(\overline{2}\right)\right)\\ &\equiv \left\langle T_\tau\psi(2)\psi^\dagger(1)\right\rangle_\phi = -\mathcal{G}(2,1)_\phi.\end{aligned} \tag{10.11}$$

where for short-hand, we defined averages $\langle O\rangle_\phi$ of operators O with a ϕ subscript by

$$\langle O\rangle_\phi = \frac{1}{Z[\phi]}\int\mathcal{D}\psi^\dagger\int\mathcal{D}\psi\; O\;\exp\left(-S-\psi^\dagger\left(\overline{1}\right)\phi\left(\overline{1},\overline{2}\right)\psi\left(\overline{2}\right)\right) \tag{10.12}$$

which is nothing but a time-ordered product. To obtain this result, we used the fact that the functional derivative with respect to ϕ does not influence at all the time order, so one can differentiate the exponential inside the Grassmann functional integral that serves as a time-ordered product. Note the reversal in the order of indices in $\mathcal{G}$ and in ϕ. We have also used the fact that in a time ordered product we can displace operators as we wish, as long as we keep track of fermionic minus signs.

Remark 36 *You should keep your mathematician friend as far as possible from you when looking at this notation, because in this notation, the equality* $1 = 2$ *is allowed. What it means is that two different sets of coordinates are equal, so that it is rather innocuous. It is nevertheless a bit disturbing if you are not aware of the context.*

Higher order correlation functions can be obtained by taking further functional derivatives. For a compact notation, define

$$S[\phi] = S + \psi^{\dagger}\left(\overline{1}\right)\phi\left(\overline{1},\overline{2}\right)\psi\left(\overline{2}\right). \tag{10.13}$$

Then,

$$\begin{aligned}
\frac{\delta\mathcal{G}\left(1,2\right)_{\phi}}{\delta\phi\left(3,4\right)} &= -\frac{\delta}{\delta\phi\left(3,4\right)}\frac{1}{Z\left[\phi\right]}\int\mathcal{D}\psi^{\dagger}\int\mathcal{D}\psi\exp\left(-S[\phi]\right)\ \psi\left(1\right)\psi^{\dagger}\left(2\right) \\
&= \frac{1}{Z\left[\phi\right]}\int\mathcal{D}\psi^{\dagger}\int\mathcal{D}\psi\exp\left(-S[\phi]\right)\ \psi\left(1\right)\psi^{\dagger}\left(2\right)\psi^{\dagger}\left(3\right)\psi\left(4\right) \\
&\quad -\frac{1}{Z\left[\phi\right]^{2}}\int\mathcal{D}\psi^{\dagger}\int\mathcal{D}\psi\exp\left(-S[\phi]\right)\ \psi\left(1\right)\psi^{\dagger}\left(2\right) \qquad (10.14) \\
&\quad \times\int\mathcal{D}\psi^{\dagger}\int\mathcal{D}\psi\exp\left(-S[\phi]\right)\ \psi^{\dagger}\left(3\right)\psi\left(4\right) \qquad (10.15) \\
&= \left\langle\psi\left(1\right)\psi^{\dagger}\left(2\right)\psi^{\dagger}\left(3\right)\psi\left(4\right)\right\rangle_{\phi} + \mathcal{G}\left(1,2\right)_{\phi}\mathcal{G}\left(4,3\right)_{\phi}. \qquad (10.16)
\end{aligned}$$

The first term on the right-hand side of the equation for the above functional derivative is called a four-point correlation function. The last term comes from differentiating $Z\left[\phi\right]$ in the denominator. To figure out the minus signs in that last term note that there is one from $-1/Z\left[\phi\right]^{2}$, one from the derivative of the argument of the exponential and one from ordering the field operators in the order corresponding to the definition of $\mathcal{G}_{\sigma}$. The latter is absorbed in the definition of $\mathcal{G}_{\sigma}$.

Remark 37 *The results of this section are independent of the explicit form of the action.*

Remark 38 *Translational invariance: It is very important to understand that even when the system is translationally invariant, you should not assume that it is when using this formalism in the presence of the source term* $\phi\left(1,2\right)$*. This is because* $\phi\left(1,2\right)$ *has to break translational invariance to generate the correlation functions that are needed. Translational invariance is recovered at the end, when you have all the equations that you need. Only then can you set* $\phi = 0$ *and recover all the symmetries of the Hamiltonian.*

10.3 Dyson-Schwinger equation of motion

We need the equation of motion for the Green's function. Let us start with a general interaction

$$\begin{aligned}\hat{V} &= \frac{1}{2}\sum_{\sigma_1,\sigma_2}\int d\mathbf{x}_1\int d\mathbf{x}_2 v\left(\mathbf{x}_1-\mathbf{x}_2\right)\psi^{\dagger}_{\sigma_1}\left(\mathbf{x}_1\right)\psi^{\dagger}_{\sigma_2}\left(\mathbf{x}_2\right)\psi_{\sigma_2}\left(\mathbf{x}_2\right)\psi_{\sigma_1}\left(\mathbf{x}_1\right)\\ \hat{V}_n &= -\sum_{\sigma_1}\int d\mathbf{x}_1\int d\mathbf{x}_2 v\left(\mathbf{x}_1-\mathbf{x}_2\right)\psi^{\dagger}_{\sigma_1}\left(\mathbf{x}_2\right)\psi_{\sigma_1}\left(\mathbf{x}_2\right)n. \qquad (10.17)\end{aligned}$$

The last piece, V_n represents the interaction between a "neutralizing background" of the same uniform density n as the electrons. You can think of the potential as the Coulomb potential $v\left(\mathbf{x}_1-\mathbf{x}_2\right)=\frac{e^2}{4\pi\varepsilon_0|\mathbf{x}_1-\mathbf{x}_2|}$ or as the Hubbard interaction. A more compact notation can be obtained by defining

$$V\left(1,2\right)=V_{\sigma_1,\sigma_2}\left(\mathbf{x}_1,\tau_1;\mathbf{x}_2,\tau_2\right)\equiv\frac{e^2}{4\pi\varepsilon_0\left|\mathbf{x}_1-\mathbf{x}_2\right|}\delta\left(\tau_1-\tau_2\right) \qquad (10.18)$$

and by including the effect of the one-body interaction into $\mathcal{G}_0^{-1}\left(1,2\right)$.

The partition function with both Grassmann and complex-number source fields can then be written as

$$Z[\phi,J^{\dagger},J]=\int\mathcal{D}\psi^{\dagger}\int\mathcal{D}\psi\exp[-S[\phi]-\psi^{\dagger}\left(\overline{1}\right)J\left(\overline{1}\right)-J^{\dagger}\left(\overline{1}\right)\psi\left(\overline{1}\right)] \qquad (10.19)$$

where the action $S[\phi]$ is

$$S[\phi]=\psi^{\dagger}\left(\overline{1}\right)\left[-\mathcal{G}_0^{-1}\left(\overline{1},\overline{2}\right)+\phi\left(\overline{1},\overline{2}\right)\right]\psi\left(\overline{2}\right)+\frac{1}{2}V\left(\overline{1},\overline{2}\right)\psi^{\dagger}\left(\overline{1}\right)\psi^{\dagger}\left(\overline{2}\right)\psi\left(\overline{2}\right)\psi\left(\overline{1}\right). \qquad (10.20)$$

Given that the Grassmann integral of a derivative vanishes, we have that

$$\int\mathcal{D}\psi^{\dagger}\int\mathcal{D}\psi\frac{\partial}{\partial\psi^{\dagger}\left(1\right)}\exp[-S[\phi,J^{\dagger},J]]=0, \qquad (10.21)$$

with

$$S[\phi,J^{\dagger},J]=S[\phi]+\psi^{\dagger}\left(\overline{1}\right)J\left(\overline{1}\right)+J^{\dagger}\left(\overline{1}\right)\psi\left(\overline{1}\right). \qquad (10.22)$$

We thus have

$$-\int\mathcal{D}\psi^{\dagger}\int\mathcal{D}\psi\left[\frac{\partial S[\phi,J^{\dagger},J]}{\partial\psi^{\dagger}\left(1\right)}\right]\exp[-S[\phi,J^{\dagger},J]]=0 \qquad (10.23)$$

and, acting with a Grassmann derivative with respect to a Grassmann source field,

$$-\frac{\partial}{\partial J\left(2\right)}\int\mathcal{D}\psi^{\dagger}\int\mathcal{D}\psi\left[\frac{\partial S[\phi]}{\partial\psi^{\dagger}\left(1\right)}+J\left(1\right)\right]\exp[-S[\phi,J^{\dagger},J]]=0. \qquad (10.24)$$

Dividing by $Z[\phi,J^{\dagger},J]$, using $\partial J\left(1\right)/\partial J\left(2\right)=\delta\left(1-2\right)$, dropping the terms odd in fermion number and evaluating at zero Grassman source fields, we have (note $\frac{\partial}{\partial J(2)}\frac{\partial S[\phi]}{\partial\psi^{\dagger}(1)}=-\frac{\partial S[\phi]}{\partial\psi^{\dagger}(1)}\frac{\partial}{\partial J(2)}$)

$$\frac{1}{Z[\phi]}\int\mathcal{D}\psi^{\dagger}\int\mathcal{D}\psi\left[\frac{\partial S[\phi]}{\partial\psi^{\dagger}\left(1\right)}\psi^{\dagger}\left(2\right)\right]\exp[-S[\phi]]=\delta\left(1-2\right). \qquad (10.25)$$

$$\left[-\mathcal{G}_0^{-1}\left(1,\overline{2}\right)+\phi\left(1,\overline{2}\right)\right]\left\langle\psi\left(\overline{2}\right)\psi^{\dagger}\left(2\right)\right\rangle_{\phi}+V\left(1,\overline{2}\right)\left\langle\psi^{\dagger}\left(\overline{2}\right)\psi\left(\overline{2}\right)\psi\left(1\right)\psi^{\dagger}\left(2\right)\right\rangle_{\phi}=\delta\left(1-2\right) \tag{10.26}$$

$$\left[\mathcal{G}_0^{-1}\left(1,\overline{2}\right)-\phi\left(1,\overline{2}\right)\right]\mathcal{G}\left(\overline{2},2\right)_{\phi}=\delta\left(1-2\right)-V\left(1,\overline{2}\right)\left\langle\psi^{\dagger}\left(\overline{2}\right)\psi\left(\overline{2}\right)\psi\left(1\right)\psi^{\dagger}\left(2\right)\right\rangle_{\phi} \tag{10.27}$$

Given the definition of the self-energy,

$$\left[\mathcal{G}_0^{-1}\left(1,\overline{2}\right)-\phi\left(1,\overline{2}\right)-\Sigma\left(1,\overline{2}\right)_{\phi}\right]\mathcal{G}\left(\overline{2},2\right)_{\phi}=\delta\left(1-2\right) \tag{10.28}$$

we thus have

$$\boxed{\Sigma\left(1,\overline{2}\right)_{\phi}\mathcal{G}\left(\overline{2},2\right)_{\phi}=-V\left(1-\overline{2}\right)\left\langle\psi^{\dagger}\left(\overline{2^{+}}\right)\psi\left(\overline{2}\right)\psi\left(1\right)\psi^{\dagger}\left(2\right)\right\rangle_{\phi},} \tag{10.29}$$

which is known as the Dyson-Schwinger equation for the self-energy. The notation $\overline{2^{+}}$ is to remind ourselves that in the time-ordered product $\psi^{\dagger}\left(\overline{2^{+}}\right)$ is to the left of $\psi\left(\overline{2}\right)$, a notation that is superfluous in the Grassmann functional integral formulation.

We can combine the two previous equations in the form

$$\left[\mathcal{G}_0^{-1}\left(1,\overline{2}\right)-\phi\left(1,\overline{2}\right)-\Sigma\left(1,\overline{2}\right)_{\phi}\right]\mathcal{G}\left(\overline{2},2\right)_{\phi}=\delta\left(1-2\right) \tag{10.30}$$

leading to the useful equation

$$\boxed{\mathcal{G}^{-1}\left(1,\overline{2}\right)_{\phi}=\mathcal{G}_0^{-1}\left(1,\overline{2}\right)-\phi\left(1,\overline{2}\right)-\Sigma\left(1,\overline{2}\right)_{\phi}} \tag{10.31}$$

10.4 Four-point function from functional derivatives

Since we need a four-point function to compute the self-energy and we know $\mathcal{G}_{\phi}$ if we know the self-energy, let us find an equation for the four-point function in terms of functional derivatives as we saw at length in Eq.(10.16)

$$\boxed{\frac{\delta\mathcal{G}(1,2)_{\phi}}{\delta\phi(3,4)}=\left\langle T_{\tau}\psi\left(1\right)\psi^{\dagger}\left(2\right)\psi^{\dagger}\left(3\right)\psi\left(4\right)\right\rangle_{\phi}+\mathcal{G}\left(1,2\right)_{\phi}\mathcal{G}\left(4,3\right)_{\phi}.} \tag{10.32}$$

The equation for the functional derivative is then easy to find using $\mathcal{G}\mathcal{G}^{-1}=1$ and our matrix notation,

$$\frac{\delta\left(\mathcal{G}\mathcal{G}^{-1}\right)}{\delta\phi} = 0 \tag{10.33}$$

$$\frac{\delta\mathcal{G}}{\delta\phi}\mathcal{G}^{-1}+\mathcal{G}\frac{\delta\mathcal{G}^{-1}}{\delta\phi} = 0 \tag{10.34}$$

$$\frac{\delta\mathcal{G}}{\delta\phi} = -\mathcal{G}\frac{\delta\mathcal{G}^{-1}}{\delta\phi}\mathcal{G}. \tag{10.35}$$

With Dyson's equation Eq. (10.30) for $\mathcal{G}^{-1}$ we find the right-hand side of that equation

$$\frac{\delta\mathcal{G}}{\delta\phi}=\mathcal{G}\frac{\delta\phi}{\delta\phi}\mathcal{G}+\mathcal{G}\frac{\delta\Sigma}{\delta\phi}\mathcal{G}. \tag{10.36}$$

Just to make sure what we mean, let us restore indices. This then takes the form

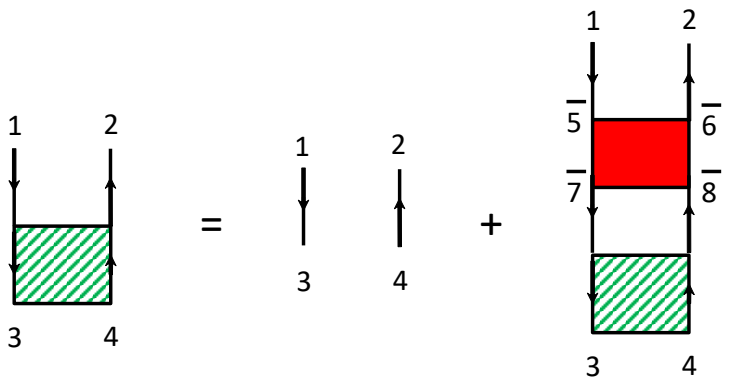

Figure 10-1 Diagrammatic representation of the integral equation for the four point function represented on the left of the equation. The two lines on the right of the equal sign and on top of the last block are Green's function. The filled box is the functional derivative of the self-energy. It is called the particle-hole irreducible vertex. It plays, for the four-point function the role of the self-energy for the Green's function.

$$\begin{aligned}\frac{\delta\mathcal{G}\left(1,2\right)_{\phi}}{\delta\phi\left(3,4\right)} &= \mathcal{G}\left(1,\overline{1}\right)_{\phi}\frac{\delta\phi\left(\overline{1},\overline{2}\right)}{\delta\phi\left(3,4\right)}\mathcal{G}\left(\overline{2},2\right)_{\phi}+\mathcal{G}\left(1,\overline{5}\right)_{\phi}\frac{\delta\Sigma\left(\overline{5},\overline{6}\right)_{\phi}}{\delta\phi\left(3,4\right)}\mathcal{G}\left(\overline{6},2\right)_{\phi}\\ &= \mathcal{G}\left(1,3\right)_{\phi}\mathcal{G}\left(4,2\right)_{\phi}+\mathcal{G}\left(1,\overline{5}\right)_{\phi}\frac{\delta\Sigma\left(\overline{5},\overline{6}\right)_{\phi}}{\delta\phi\left(3,4\right)}\mathcal{G}\left(\overline{6},2\right)_{\phi}. \qquad (10.37)\end{aligned}$$

If you take the convention that $\mathcal{G}\left(1,2\right)$ is represented by an arrow going from 1 to 2 from left to right, then we can represent $\frac{\delta\mathcal{G}(1,2)_{\phi}}{\delta\phi(3,4)}$ as $\mathcal{G}\left(1,2\right)$ being pinched by $\phi\left(3,4\right)$, i.e. having an arrow starting at 1 and ending at 2 with $3,4$ at the bottom.

This last equation shows that Σ has no explicit dependence on ϕ. It depends on ϕ only through its dependence on $\mathcal{G}$. We will see this is a self-consistent assumption. Taking that into account, and using the chain rule, this last equation can also be written in the form

$$\begin{aligned}\frac{\delta\mathcal{G}\left(1,2\right)_{\phi}}{\delta\phi\left(3,4\right)} &= \mathcal{G}\left(1,3\right)_{\phi}\mathcal{G}\left(4,2\right)_{\phi}\\ &\quad+\mathcal{G}\left(1,\overline{5}\right)_{\phi}\left(\frac{\delta\Sigma\left(\overline{5},\overline{6}\right)_{\phi}}{\delta\mathcal{G}\left(\overline{7},\overline{8}\right)_{\phi}}\frac{\delta\mathcal{G}\left(\overline{7},\overline{8}\right)_{\phi}}{\delta\phi\left(3,4\right)}\right)\mathcal{G}\left(\overline{6},2\right)_{\phi}. \qquad (10.38)\end{aligned}$$

This general equation can also be written in short-hand notation

$$\frac{\delta\mathcal{G}}{\delta\phi}=\mathcal{G}\hat{\cdot}\mathcal{G}+\mathcal{G}\quad\frac{\frac{\delta\Sigma}{\delta\mathcal{G}}}{\frac{\delta\mathcal{G}}{\delta\phi}}\quad\mathcal{G}\ , \qquad (10.39)$$

where the caret $\hat{\cdot}$ reminds us that the indices adjacent to it are the same as those of ϕ and where the two terms on top of one another are matrix multiplied top down as well. In the top down multiplication, it is pairs of indices of $\mathcal{G}$ that are considered as a single matrix index. Fig. 10-1 illustrates the equation with the indices. The diagrams go from top to bottom to remind ourselves of where the indices are in the algebraic equation, but we may rotate the diagrams in any direction we want.

Definition 3 *In the jargon,* $\frac{\delta\Sigma}{\delta\mathcal{G}}$ *is the vertex function which is irreducible in a particle-hole channel. (There are two particle-hole channels). This means that*

if we iterate the equation for $\frac{\delta \mathcal{G}}{\delta \phi}$, we generate all the diagrams that have Green's function lines going in opposite direction. Those diagrams for $\frac{\delta \mathcal{G}}{\delta \phi}$ can thus be cut in two by cutting these two lines. They are reducible. $\frac{\delta \Sigma}{\delta \mathcal{G}}$ contains the diagrams that cannot be cut in two in this way. It sort of plays the role of a self-energy for response functions.

Remark 39 *Connection between labels (that we also call indices) in the Green's function and the direction of the arrow in the diagram: We take the convention that for $\mathcal{G}(1,2)_\phi$ the arrow begins at the annihilation operator 1 and ends at the creation operator 2. It might have been natural to begin at the creation operator instead. In fact it does not matter, as long as one is consistent. Both conventions can be found in the literature.*

Remark 40 $\frac{\delta \mathcal{G}\left(1,1^+\right)_\phi}{\delta \phi\left(2^+,2\right)}$ *in Eq. (10.32) is related to minus the density-density correlation function:*

$$-\left[\left\langle \psi^\dagger\left(1^+\right)\psi(1)\,\psi^\dagger\left(2^+\right)\psi(2)\right\rangle_\phi - \left\langle \psi^\dagger\left(1^+\right)\psi(1)\right\rangle_\phi \left\langle \psi^\dagger\left(2^+\right)\psi(2)\right\rangle_\phi\right]. \tag{10.40}$$

Using the exact result for this quantity, namely Eq. (10.38), we see that even when there are no interactions, this quantity is $\mathcal{G}(1,2)_\phi \mathcal{G}(2,1)_\phi$. We thus see the necessity to know Green's functions to compute observables, even in the non-interacting case. Physically, this term is a so-called exchange term. It makes sure that two electrons with the same spin are not on top of exach other. This comes from the Pauli exclusion principle.

10.5 Self-energy from functional derivatives

To compute the self-energy, according to Eq.(10.29), what we need is

$$\boxed{\Sigma(1,3)_\phi = -V\left(1-\overline{2}\right)\left\langle T_\tau\left[\psi^\dagger\left(\overline{2^+}\right)\psi\left(\overline{2}\right)\psi(1)\,\psi^\dagger\left(\overline{4}\right)\right]\right\rangle_\phi \mathcal{G}_\phi^{-1}\left(\overline{4},3\right).} \tag{10.41}$$

We write the four-point function with the help of the functional derivative Eq.(10.32) by replacing in the latter equation $3 \to \overline{2^+}$, $4 \to \overline{2}$, $1 \to 1$, $2 \to \overline{4}$ so that

$$\Sigma(1,3)_\phi = -V\left(1-\overline{2}\right)\left[\frac{\delta \mathcal{G}\left(1,\overline{4}\right)_\phi}{\delta \phi\left(\overline{2^+},\overline{2}\right)} - \mathcal{G}\left(\overline{2},\overline{2^+}\right)_\phi \mathcal{G}\left(1,\overline{4}\right)_\phi\right]\mathcal{G}^{-1}\left(\overline{4},3\right)_\phi \tag{10.42}$$

Remark 41 *Mnemotechnic: The first label of the $V\left(1-\overline{2}\right)$ is the same as the first label of $\mathcal{G}\left(1,\overline{4}\right)_\phi$ on the numerator and the same as the first label on the left-hand side of the equation. The second label is summed over and is the same as the label on the denominator of $\frac{\delta \mathcal{G}\left(1,\overline{4}\right)_\phi}{\delta \phi\left(\overline{2^+},\overline{2}\right)}$. The two Green's function in $\mathcal{G}\left(\overline{2},\overline{2^+}\right)_\phi \mathcal{G}\left(1,\overline{4}\right)_\phi$ can be arranged on top of one another so that this rule is preserved.*

The final expression is easy to obtain if we change the labels of the exact four-point function Eq.(10.38) so that they correspond to those above. Namely, we

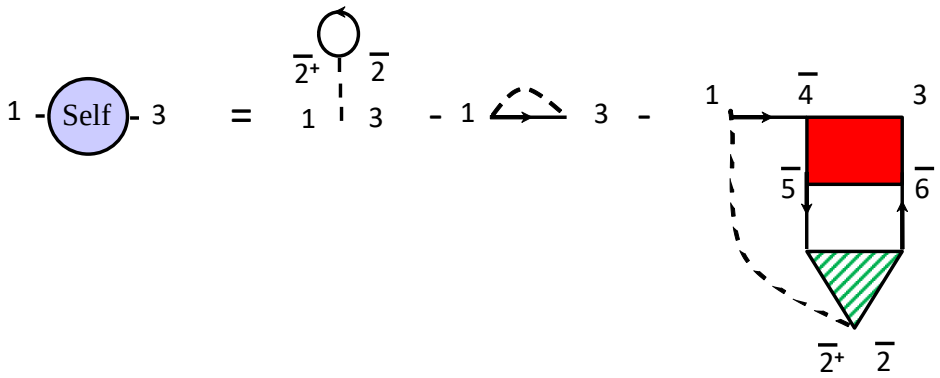

Figure 10-2 Diagrams for the self-energy. The dashed line represent the interaction. The first two terms are, respectively, the Hatree and the Fock contributions. The textured square appearing in the previous figure for the four-point function has been squeezed to a triangle to illustrate the fact that two of the indices (coordinates) are identical.

write

$$\frac{\delta \mathcal{G}\left(1,\overline{4}\right)_{\phi}}{\delta\phi\left(\overline{2^{+}},\overline{2}\right)} = \mathcal{G}\left(1,\overline{2^{+}}\right)_{\phi}\mathcal{G}\left(\overline{2},\overline{4}\right)_{\phi} + \mathcal{G}\left(1,\overline{7}\right)_{\phi}\left(\frac{\delta\Sigma\left(\overline{7},\overline{8}\right)_{\phi}}{\delta\mathcal{G}\left(\overline{5},\overline{6}\right)_{\phi}}\frac{\delta\mathcal{G}\left(\overline{5},\overline{6}\right)_{\phi}}{\delta\phi\left(\overline{2^{+}},\overline{2}\right)}\right)\mathcal{G}\left(\overline{8},\overline{4}\right)_{\phi}. \quad (10.43)$$

Substituting in the expression for the self-energy Eq.(10.42) using $\mathcal{G}\left(1,\overline{4}\right)_{\phi}\mathcal{G}^{-1}\left(\overline{4},3\right)_{\phi} = \delta\left(1-3\right)$ (and changing the dummy label $\overline{7}\rightarrow\overline{4}$) this yields,

$$\Sigma\left(1,3\right)_{\phi} = -V\left(1-3\right)\mathcal{G}\left(1,3^{+}\right)_{\phi} - V\left(1-\overline{2}\right)\mathcal{G}\left(1,\overline{4}\right)_{\phi}\frac{\delta\Sigma\left(\overline{4},3\right)_{\phi}}{\delta\mathcal{G}\left(\overline{5},\overline{6}\right)_{\phi}}\frac{\delta\mathcal{G}\left(\overline{5},\overline{6}\right)_{\phi}}{\delta\phi\left(\overline{2^{+}},\overline{2}\right)} + V\left(1-\overline{2}\right)\mathcal{G}\left(\overline{2},\overline{2^{+}}\right)_{\phi}\delta\left(1-3\right). \quad (10.44)$$

The second term is the only one that will give a frequency dependence, and hence an imaginary part, to the self-energy. The other two terms in the above equation are the Hartree-Fock contribution that we will discuss at length later on. Note that $V\left(1-\overline{2}\right)$ is instantaneous, i.e. there is a delta function $\delta\left(\tau_1-\tau_{\overline{2}}\right)$, and whether we have $V\left(1-3\right)$ or $V\left(1-3^{+}\right)$ is irrelevant. In the Green's functions however, it is important to keep track of the $+$. Indeed, that reflects the fact that in the Hamiltonian, the creation operators are always to the left of the annihilation operators. That is the way to preserve that property in a time-ordered product.

The equation for the self-energy is represented schematically in Fig. 10-2. Note that the diagrams are one-particle irreducible, i.e. they cannot be cut in two seperate pieces by cutting a single propagator.

Remark 42 *Historically, the expressions "self-energy" is inspired by the fact that it is the electromagnetic field of the electron itself that leads to modifications of the properties of the electron even when it is moving in a vacuum. In the latter case, the electromagnetic field of the electron contains virtual photons that can in turn create virtual electron-positron pairs, the analog of electron-hole excitations.*

10.6 The self-energy, one-particle irreducibility and Green's function

It is clear from the diagrammatic illustration of the self-energy in Fig. 10-2 that all internal indices are integrated over, as the Feynman rules would specify. In addition, the diagrams are connected and none of them can be cut into two distinct pieces by cutting one Green's function line. We say that the self-energy contains all the diagrams that are one-particle irreducible. The Feynman rules tell us that the self-energy contains all the topologically distinct connected diagrams that end and begin with an interaction and a Green's function at the same point. There are rules for their sign as well: One minus sign for each order in perturbation theory and one minus sign for every closed loop. The Feynman rules are generally formulated in terms of bare Green's functions. Here, the dressed Green's functions appear but, as you will check in an exercise, it is also possible to recover the perturbation theory in terms of bare Green's functions.

Finally notice that if we iterate the Dyson equation,

$$\begin{aligned} \mathcal{G} &= \mathcal{G}_0 + \mathcal{G}_0\Sigma\mathcal{G} && (10.45)\\ &= \mathcal{G}_0 + \mathcal{G}_0\Sigma\mathcal{G}_0 + \mathcal{G}_0\Sigma\mathcal{G}_0\Sigma\mathcal{G}_0 + \mathcal{G}_0\Sigma\mathcal{G}_0\Sigma\mathcal{G}_0\Sigma\mathcal{G}_0 + \dots && (10.46)\end{aligned}$$

it becomes clear that the Green's function is given by the sum of all diagrams that end at the destruction operator and begin at the annihilation operator and contains all possible topologically distinct diagrams. The Green's function diagrams are, however, one-particle reducible.

11. LUTTINGER-WARD FUNCTIONAL

There is a very elegant formulation of the Many-Body problem that focuses on a functional of the interacting Green function instead of on a functional of source fields. The two approaches are related by a Legendre transform. This is where one encounters the so-called Luttinger-Ward functional [46][73], that plays a prominent role in defining approximations that satisfy conservation laws, thermodynamic consistency and in deriving Dynamical Mean-Field Theory. But first, a short digression to argue that the self-energy can be written as a functional derivative with respect to the Green's function.

11.1 The self-energy can be expressed as a functional derivative with respect to the Green's function

In this section, I follow Baym [9] to show that the functional derivative of the self-energy obeys a curl condition that proves that the self-energy itself is a functional derivative with respect to $\mathcal{G}$ of an appropriately defined Luttinger-Ward functional that we find in the following sections.

We have seen in Eq. (10.36) that the four-point function can be written as

$$\frac{\delta \mathcal{G}}{\delta \phi} = \mathcal{G}\frac{\delta \phi}{\delta \phi}\mathcal{G} + \mathcal{G}\frac{\delta \Sigma}{\delta \phi}\mathcal{G}. \tag{11.1}$$

This suggests that the functional dependence of Σ on ϕ comes only from the dependence of $\mathcal{G}$ on ϕ. Hence, the above equation may be rewritten as follows

$$\boxed{\frac{\delta \mathcal{G}}{\delta \phi} = \mathcal{G}\frac{\delta \phi}{\delta \phi}\mathcal{G} + \mathcal{G}\left(\frac{\delta \Sigma}{\delta \mathcal{G}}\frac{\delta \mathcal{G}}{\delta \phi}\right)\mathcal{G}.} \tag{11.2}$$

Multiplying by $\mathcal{G}^{-1}$ on both sides, we are left with the following

$$\mathcal{G}^{-1}\frac{\delta \mathcal{G}}{\delta \phi}\mathcal{G}^{-1} = \frac{\delta \phi}{\delta \phi} + \left(\frac{\delta \Sigma}{\delta \mathcal{G}}\frac{\delta \mathcal{G}}{\delta \phi}\right). \tag{11.3}$$

To avoid confusion, let us rewrite all the indices. Then, the above can be rewritten as follows

$$\left[\mathcal{G}^{-1}\left(1', \overline{1}\right)\mathcal{G}^{-1}\left(\overline{2}, 2'\right) - \frac{\delta \Sigma\left(1', 2'\right)}{\delta \mathcal{G}\left(\overline{1}, \overline{2}\right)}\right]\frac{\delta \mathcal{G}\left(\overline{1}, \overline{2}\right)}{\delta \phi\left(3, 4\right)} = \delta\left(1' - 3\right)\delta\left(2' - 4\right). \tag{11.4}$$

This equation means that the quantity in brackets is the inverse of $\delta \mathcal{G}\left(1, 2\right)/\delta \phi\left(3, 4\right)$. But since $\mathcal{G}\left(1, 2\right) = -\delta \ln Z[\phi]/\delta \phi\left(2, 1\right)$, the matrix $\delta \mathcal{G}\left(1, 2\right)/\delta \phi\left(3, 4\right)$ is symmetric under the interchange $2, 1 \rightarrow 3, 4$, in other words,

$$\frac{\delta \mathcal{G}\left(1, 2\right)}{\delta \phi\left(3, 4\right)} = \frac{\delta \mathcal{G}\left(4, 3\right)}{\delta \phi\left(2, 1\right)} \tag{11.5}$$

Note that the symmetry here means interchanging indices of the numerator with those of the denominator, and then permuting the indices of the numerator and of the denominator separately. So for example, $\mathcal{G}^{-1}\left(1',\overline{1}\right)\mathcal{G}^{-1}\left(\overline{2},2'\right)$ has this symmetry taking $1'$ and $2'$ as indices in the numerator and $\overline{1},\overline{2}$ as indices of the denominator.

The inverse of as symmetric matrix is also symmetric. This will be true if and only if

$$\frac{\delta\Sigma\left(1',2'\right)}{\delta\mathcal{G}\left(1,2\right)}=\frac{\delta\Sigma\left(2,1\right)}{\delta\mathcal{G}\left(2',1'\right)}. \tag{11.6}$$

This is a curl condition that will be satisfied if and only if the self-energy is itself a functional derivative with respect to $\mathcal{G}$, in other words if

$$\frac{1}{T}\frac{\delta\Phi\left[\mathcal{G}\right]}{\delta\mathcal{G}\left(2',1'\right)}=\Sigma\left(1',2'\right). \tag{11.7}$$

The quantity $\Phi\left[\mathcal{G}\right]$ will be the Luttinger-Ward functional. We will see that it also has a diagrammatic expansion that is related to the potential energy.

11.2 The Luttinger-Ward functional and the Legendre transform of $-T\ln Z\left[\phi\right]$

The first two equations of the previous section can be used to define a Legendre transform of the generating function, where $\mathcal{G}$ is the natural variable:

$$\Omega[\mathcal{G}]=F\left[\phi\right]-\mathrm{Tr}\left[\phi\mathcal{G}\right]. \tag{11.8}$$

The physical free energy is $F\left[\phi=0\right]$.

Remark 43 *Legendre transforms are usually defined between convex functions. We cannot prove continuity in our case. The best we can hope is that the Legendre transform is defined locally and check that the results make sense. Recent results show that indeed there may be problems with the assumption that the Legendre transform is always well defined [37]. In the latter reference, it is shown that perturbation in the dressed $\mathcal{G}$ at large interaction can lead to an unphysical branch of the self-energy when the interaction is large. This does not happen with the expansion is in terms of $\mathcal{G}_0$.*

The functional $\Omega[\mathcal{G}]$ is the so-called Kadanoff-Baym functional. As expected for Legendre transforms

$$\frac{1}{T}\frac{\delta\Omega\left[\mathcal{G}\right]}{\delta\mathcal{G}\left(1,2\right)}=-\phi\left(2,1\right). \tag{11.9}$$

Proof:

$$\begin{aligned}\frac{1}{T}\frac{\delta\Omega\left[\mathcal{G}\right]}{\delta\mathcal{G}\left(1,2\right)} &= \frac{1}{T}\frac{\delta F\left[\phi\right]}{\delta\phi\left(\overline{3},\overline{4}\right)}\frac{\delta\phi\left(\overline{3},\overline{4}\right)}{\delta\mathcal{G}\left(1,2\right)}-\frac{\delta}{\delta\mathcal{G}\left(1,2\right)}\left[\phi\left(\overline{3},\overline{4}\right)\mathcal{G}\left(\overline{4},\overline{3}\right)\right] &(11.10)\\ &= \mathcal{G}\left(\overline{4},\overline{3}\right)\frac{\delta\phi\left(\overline{3},\overline{4}\right)}{\delta\mathcal{G}\left(1,2\right)}-\frac{\delta\phi\left(\overline{3},\overline{4}\right)}{\delta\mathcal{G}\left(1,2\right)}\mathcal{G}\left(\overline{4},\overline{3}\right)-\phi\left(2,1\right). &(11.11)\end{aligned}$$

Using the Dyson-Schwinger equations of motion, we have that the relation between ϕ and $\mathcal{G}$ is given by

$$\mathcal{G}^{-1}(1,2)_{\phi} = \mathcal{G}_0^{-1}(1,2) - \phi(1,2) - \Sigma(1,2)_{\phi} \tag{11.12}$$

which means that

$$\frac{1}{T}\frac{\delta\Omega[\mathcal{G}]}{\delta\mathcal{G}(1,2)} = -\phi(2,1) = \mathcal{G}^{-1}(2,1)_{\phi} - \mathcal{G}_0^{-1}(2,1) + \Sigma(2,1)_{\phi} \tag{11.13}$$

and Dyson's equation in its usual form is satisfied only for $\phi = 0$ where the extremum principle

$$\frac{1}{T}\frac{\delta\Omega[\mathcal{G}]}{\delta\mathcal{G}(1,2)} = 0 \tag{11.14}$$

is satisfied and where the functional $\Omega[\mathcal{G}]$ is simply equal to the free energy as follows from the definition Eq.(11.8) with $\phi = 0$.

We can guess an explicit expression for $\Omega[\mathcal{G}]$ in the general case ($\phi \neq 0$) by starting from its derivative Eq.(11.13). We obtain the so-called Baym-Kadanoff functional,

$$\Omega[\mathcal{G}] = \Phi[\mathcal{G}] - \mathrm{Tr}\left[\left(\mathcal{G}_0^{-1} - \mathcal{G}^{-1}\right)\mathcal{G}\right] + \mathrm{Tr}\left[\ln\left(\frac{-\mathcal{G}}{-\mathcal{G}_{\infty}}\right)\right] \tag{11.15}$$

which gives the correct result in the non-interacting case and in the general case ($\mathcal{G}_{\infty}$ is included for convergence reasons. See the full lecture notes) and reduces to Eq.(11.13) when functionally differentiated, as long as

$$\frac{1}{T}\frac{\delta\Phi[\mathcal{G}]}{\delta\mathcal{G}(1,2)} = \Sigma(2,1). \tag{11.16}$$

That this functional exists was discussed in section (11.1) above. We also need to prove that $\frac{1}{T}\frac{\delta}{\delta\mathcal{G}(1,2)}\mathrm{Tr}\left[\ln\left(\frac{-\mathcal{G}}{-\mathcal{G}_{\infty}}\right)\right] = \mathcal{G}^{-1}(2,1)$. The proof follows the same steps as those in the previous section. Also, note that

$$\frac{1}{T}\mathrm{Tr}\left[\ln\left(\frac{-\mathcal{G}}{-\mathcal{G}_{\infty}}\right)\right] = -\frac{1}{T}\mathrm{Tr}\left[\ln\left(\frac{-\mathcal{G}^{-1}}{-\mathcal{G}_{\infty}^{-1}}\right)\right]. \tag{11.17}$$

The latter form is more common.

The functional $\Phi[\mathcal{G}]$ is the so-called Luttinger-Ward functional. We can obtain an explicit form for it by using the basic property of Legendre transforms exemplified by our example with pressure in ordinary statistical mechanics. More specifically, multiply the potential energy term in the Hamiltonian by λ, then the physical case corresponds to $\lambda = 1$ and the general properties of Legendre transforms tell us that

$$\left.\frac{\partial\Omega_{\lambda}[\mathcal{G}]}{\partial\lambda}\right|_{\mathcal{G}} = \left.\frac{\partial F_{\lambda}[\phi]}{\partial\lambda}\right|_{\phi}. \tag{11.18}$$

But the explicit form of the Baym-Kadanoff functional Eq.(11.15) tells us that

$$\left.\frac{\partial\Omega_{\lambda}[\mathcal{G}]}{\partial\lambda}\right|_{\mathcal{G}} = \left.\frac{\partial\Phi_{\lambda}[\mathcal{G}]}{\partial\lambda}\right|_{\mathcal{G}} \tag{11.19}$$

while the derivative of the free energy is

$$\left.\frac{\partial F_{\lambda}[\phi]}{\partial\lambda}\right|_{\phi} = \frac{1}{\lambda}\left\langle\lambda\hat{V}\right\rangle_{\lambda}. \tag{11.20}$$

The average $\langle\rangle_\lambda$ means that the potential energy is averaged with the Hamiltonian where the coupling constant is multiplied by λ so that $\hat{V} \to \lambda\hat{V}$. Hence, knowing that $\Phi_{\lambda=0} = 0$, I can obtain the Luttinger-Ward functional by a coupling constant integration

$$\Phi_{\lambda=1}[\mathcal{G}] = \int_0^1 d\lambda \frac{1}{\lambda} \left\langle \lambda\hat{V} \right\rangle_\lambda . \tag{11.21}$$

Note that since the equality of the two potentials with respect to λ, Eq.(11.18), is valid for any $\mathcal{G}$ and the corresponding ϕ, the coupling constant integration for the Luttinger-Ward functional may be evaluated for $\phi = 0$ and for $\mathcal{G}$ that satisfies the usual Dyson equation or for any $\mathcal{G}$ we wish. The average of the potential energy in the last equation is related to the density-density correlation function. The resulting integral over coupling constant gives for $\Phi_\lambda[\mathcal{G}]$ the same result that we would have obtained from the linked cluster theorem. There is a $1/n$ factor for a term of order n.

Remark 44 *$\Phi[\mathcal{G}]$ is the sum of two-particle irreducible skeleton diagrams hence $\frac{1}{T}\frac{\delta\Phi[\mathcal{G}]}{\delta\mathcal{G}(1,2)} = \Sigma(2,1)$ is the sum of all one-particle irreducible skeleton diagrams. This is proven in Section (11.3). A skeleton diagram is a diagram that has no self-energy insertions.*

11.3 Another derivation of the Baym-Kadanoff functional

Instead of "guessing" the correct form of the Baym-Kadanoff functional Eq. (11.15), as we did above, we can start from the differential equation (11.18) for the coupling-constant dependence of the Baym-Kadanoff functional $\Omega_\lambda[\mathcal{G}]$. We find that

$$\Omega_{\lambda=1}[\mathcal{G}] = \Omega_{\lambda=0}[\mathcal{G}] + \int_0^1 d\lambda \frac{1}{\lambda} \left\langle \lambda\hat{V} \right\rangle_\lambda \tag{11.22}$$

$$= \Omega_{\lambda=0}[\mathcal{G}] + \Phi_{\lambda=1}[\mathcal{G}] \tag{11.23}$$

But we know $\Omega_{\lambda=0}[\mathcal{G}]$ since $\mathcal{G}$ is given and $\lambda = 0$ means that we are considering a case when there is no interaction but where $\mathcal{G}$ takes the value it should have for the full problem. So, using the Legendre transform formula Eq.(11.8), we have

$$\Omega_{\lambda=0}[\mathcal{G}] = F_{\lambda=0}[\phi_0] - \mathrm{Tr}[\phi_0\mathcal{G}] \tag{11.24}$$

where the "constraining field" ϕ_0 is the value of the source field that is necessary for $\mathcal{G}$ to take the correct value for the Green's function. When $\lambda = 0$ we know that

$$F_{\lambda=0}[\phi_0] = \mathrm{Tr}\left[\ln\left(\frac{-\mathcal{G}}{-\mathcal{G}_\infty}\right)\right] \tag{11.25}$$

because this is the result for the non-interacting case when we know $\mathcal{G}$, the actual value of $\mathcal{G}$ as enforced by our choice of ϕ_0. Substituting the equation for $F_{\lambda=0}[\phi_0]$ in our expression for $\Omega_{\lambda=0}[\mathcal{G}]$ and then in our expression for $\Omega_\lambda[\mathcal{G}]$ in Eq.(11.23), we are left with

$$\Omega_{\lambda=1}[\mathcal{G}] = \mathrm{Tr}\left[\ln\left(\frac{-\mathcal{G}}{-\mathcal{G}_\infty}\right)\right] - \mathrm{Tr}[\phi_0\mathcal{G}] + \Phi_{\lambda=1}[\mathcal{G}] \tag{11.26}$$

All that we need to know is $\phi_0(1,2)$ .But by definition of $\phi_0(1,2)$ as the source field that allows the non-interacting problem to have the same Green's function as the interacting one, we have that

$$\mathcal{G}^{-1}(1,2)_\phi = \mathcal{G}_0^{-1}(1,2) - \phi_0(1,2). \tag{11.27}$$

This gives us the expression for $\phi_0(1,2)$ (basically the self-energy when $\phi = 0$) so that, finally, $\Omega_{\lambda=1}[\mathcal{G}]$ in the next to last equation takes the form

$$\Omega_{\lambda=1}[\mathcal{G}] = \mathrm{Tr}\left[\ln\left(\frac{-\mathcal{G}}{-\mathcal{G}_\infty}\right)\right] - \mathrm{Tr}\left[(\mathcal{G}_0^{-1} - \mathcal{G}^{-1})\mathcal{G}\right] + \Phi_{\lambda=1}[\mathcal{G}], \tag{11.28}$$

which is what we were looking for.

Part VI

Lecture 6 (90 minutes) Lindhard function, TPSC and other approaches

12. FIRST STEPS WITH FUNCTIONAL DERIVATIVES: HARTREE-FOCK AND RPA

These are the two most famous approximations: Hartree-Fock for the self-energy and RPA for the density-density correlation function. We will see later on why these come out naturally from simple considerations, including the variational principle.

12.1 Hartree-fock and RPA in space-time

The expression for the self-energy and an iterative procedure can be used to compute $\frac{\delta\Sigma}{\delta\mathcal{G}}$ that appears both in the exact expression for the self-energy Eq.(10.44) and in the exact expression for the four-point function Eq.(10.38), four-point function that also appears in the self-energy. A look at the last two figures that we drew is helpful.

Refering to the exact expression for the four-point function Eq.(10.38), what we need to obtain the so-called Random Phase Approximation (RPA) is $\frac{\delta\Sigma(5,6)_\phi}{\delta\mathcal{G}(7,8)_\phi}$ evaluated from the the Hartree-Fock approximation, namely the first two terms in Fig. (10-2).

$$\begin{aligned}\frac{\delta\Sigma\left(5,6\right)_\phi}{\delta\mathcal{G}\left(7,8\right)_\phi} &= V\left(5-\overline{9}\right)\delta\left(\overline{9}-7\right)\delta\left(\overline{9}-8\right)\delta\left(5-6\right)-V\left(5-6\right)\delta\left(7-5\right)\delta\left(8-6\right)\\ &= V\left(5-7\right)\delta\left(7-8\right)\delta\left(5-6\right)-V\left(5-6\right)\delta\left(7-5\right)\delta\left(8-6\right).\end{aligned}$$

It is easier to imagine the result by looking back at the illustration of the Hartree-Fock term in Fig. 10-1. The result of the functional derivative is illustrated in Fig. 12-1. When two coordinates are written on one end of the interaction line, it is because there is a delta function. For example, there is a $\delta\left(5-6\right)$ for the vertical line.

Substituting back in the equation for the exact found-point function $\frac{\delta\mathcal{G}}{\delta\phi}$ Eq.(10.38), we find

$$\begin{aligned}\frac{\delta\mathcal{G}\left(1,2\right)_\phi}{\delta\phi\left(3,4\right)} &= \mathcal{G}\left(1,3\right)_\phi\mathcal{G}\left(4,2\right)_\phi\\ &\quad+\mathcal{G}\left(1,\overline{5}\right)_\phi\left(V\left(\overline{5}-\overline{7}\right)\frac{\delta\mathcal{G}\left(\overline{7},\overline{7}\right)_\phi}{\delta\phi\left(3,4\right)}\right)\mathcal{G}\left(\overline{5},2\right)_\phi \qquad (12.1)\\ &\quad-\mathcal{G}\left(1,\overline{5}\right)_\phi\left(V\left(\overline{5}-\overline{6}\right)\frac{\delta\mathcal{G}\left(\overline{5},\overline{6}\right)_\phi}{\delta\phi\left(3,4\right)}\right)\mathcal{G}\left(\overline{6},2\right)_\phi. \qquad (12.2)\end{aligned}$$

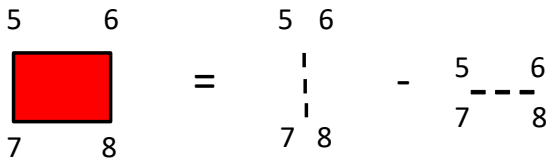

Figure 12-1 Expression for the irreducible vertex in the Hartree-Fock approximation. The labels on either side of the bare interaction represented by a dashed line are at the same point, in other words there is a delta function.

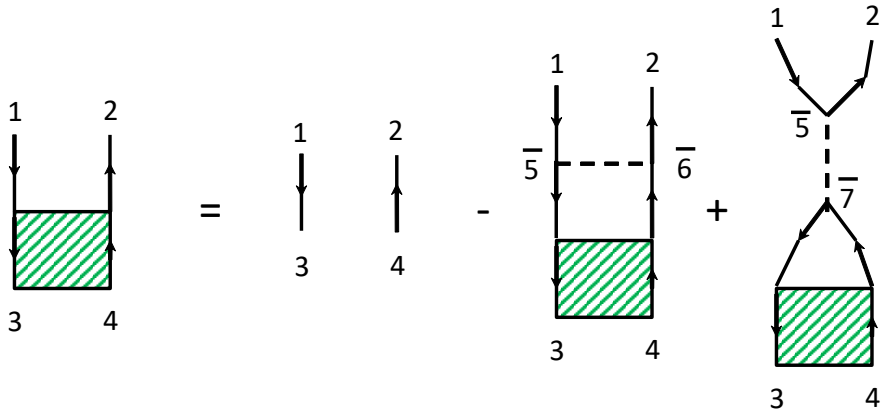

Figure 12-2 Integral equation for $\delta\mathcal{G}/\delta\phi$ in the Hartree-Fock approximation.

This expression is easy to deduce from the general diagrammatic representation of the general integral equation Fig. 10-1 by replacing the irreducible vertex by that in Fig. 12-1 that follows from the Hartree-Fock approximation. This is illustrated in Fig. 12-2.

To compute a better approximation for the self-energy we will need $\delta\phi\left(2^{+},2\right)$ instead of $\delta\phi\left(3,4\right)$, as can be seen from our exact result Eq.(10.44). Although one might guess it from symmetry, we will also see that all that we will need is, $\delta\mathcal{G}\left(1,1^{+}\right)$, although it is not obvious at this point. It is quite natural however that the density-density correlation function plays an important role since it is related to the dielectric constant. From the previous equation, that special case can be written

$$\frac{\delta\mathcal{G}\left(1,1^{+}\right)_{\phi}}{\delta\phi\left(2^{+},2\right)} = \mathcal{G}\left(1,2\right)_{\phi}\mathcal{G}\left(2,1\right)_{\phi} \tag{12.3}$$

$$+\mathcal{G}\left(1,\overline{5}\right)_{\phi}\left(V\left(\overline{5}-\overline{7}\right)\frac{\delta\mathcal{G}\left(\overline{7},\overline{7}\right)_{\phi}}{\delta\phi\left(2^{+},2\right)}\right)\mathcal{G}\left(\overline{5},1\right)_{\phi} \tag{12.4}$$

$$-\mathcal{G}\left(1,\overline{5}\right)_{\phi}\left(V\left(\overline{5}-\overline{6}\right)\frac{\delta\mathcal{G}\left(\overline{5},\overline{6}\right)_{\phi}}{\delta\phi\left(2^{+},2\right)}\right)\mathcal{G}\left(\overline{6},1\right)_{\phi}. \tag{12.5}$$

This equation is refered to as the generalized RPA. When the last term is neglected, this is the RPA. We will discuss this in more details later.

Remark 45 *Clearly, external points, such as* $1,2,3,4$ *are fixed, but the coordinates that appear inside diagrams must be integrated over. This is a simple rule*

for interpreting diagrams. There are analogous rules in momentum-Matsubara space when there is translational invariance, as we proceed to show.

12.2 Hartree-Fock and RPA in Matsubara and momentum space with $\phi = 0$

We are ready to set $\phi = 0$. As we have discussed, it is important not to do that too soon. Once this is done, we can use translational invariance so that $\Sigma(1,2) = \Sigma(1-2)$ and $\mathcal{G}(1,2) = \mathcal{G}(1-2)$. In addition, spin rotational invariance implies that these objects are diagonal in spin space. We then Fourier transform to take advantage of the translational invariance. In that case, restoring spin indices we can define

$$\mathcal{G}_\sigma(k) = \int d(\mathbf{x}_1 - \mathbf{x}_2) \int_0^\beta d(\tau_1 - \tau_2)\, e^{-i\mathbf{k}\cdot(\mathbf{x}_1-\mathbf{x}_2)} e^{ik_n(\tau_1-\tau_2)} \mathcal{G}_\sigma(1-2) \quad (12.6)$$

In this expression, k_n is a fermionic Matsubara frequency and the Green's function is diagonal in spin indices σ_1 and σ_2. For clarity then, we have explicitly written a single spin label. We thus make the following rule:

- When in position space there is an arrow representing $\mathcal{G}(1-2)$ in the translationally invariant case, in momentum space, you can think of this arrow as carrying a momentum $\mathbf{k}$.

For the potential we define

$$V_{\sigma,\sigma'}(q) = \int d(\mathbf{x}_1 - \mathbf{x}_2) \int_0^\beta d(\tau_1 - \tau_2)\, e^{-i\mathbf{q}\cdot(\mathbf{x}_1-\mathbf{x}_2)} e^{iq_n(\tau_1-\tau_2)} V_{\sigma,\sigma'}(1-2) \quad (12.7)$$

where q_n is, this time, a bosonic Matsubara frequency, in other words

$$q_n = 2n\pi T \quad (12.8)$$

with n an integer. Again we have explicitly written the spin indices even if $V_{\sigma,\sigma'}(1-2)$ is independent of spin.

- An interaction in a diagram is represented by a dotted line. Note that because $V(1-2) = V(2-1)$, in momentum space we are free to choose the direction of $\mathbf{q}$ on the dotted line at will. Once a convention is chosen, we stick with it.

Remark 46 *General spin-dependent interaction: In more general theories, there are four spin labels attached to interaction vertices. These labels correspond to those of the four fermion fields. Here the situation is simpler because the interaction not only conserves spin at each vertex but is also spin independent.*

Whether we compute $\mathcal{G}(1-2)$ or a susceptibility $\chi(1-2)$, when we go to momentum space, it is as if we were injecting a momentum (frequency) in the diagram. It is convenient to work completely in momentum space by starting from the above position space expressions, and their diagrammatic equivalent, and now

write every $\mathcal{G}(1-2)$ and $V(1-2)$ entering the internal lines of a diagram also in terms of their Fourier-Matsubara transforms, namely

$$\mathcal{G}_\sigma(1-2) = \int \frac{d^3\mathbf{k}}{(2\pi)^3} T \sum_{n=-\infty}^{\infty} e^{i\mathbf{k}\cdot(\mathbf{x}_1-\mathbf{x}_2)} e^{-ik_n(\tau_1-\tau_2)} \mathcal{G}_\sigma(k) \tag{12.9}$$

$$V_{\sigma,\sigma'}(1-2) = \int \frac{d^3\mathbf{q}}{(2\pi)^3} T \sum_{n=-\infty}^{\infty} e^{i\mathbf{q}\cdot(\mathbf{x}_1-\mathbf{x}_2)} e^{-iq_n(\tau_1-\tau_2)} V_{\sigma,\sigma'}(q) \tag{12.10}$$

or in the discrete version of momentum

$$\mathcal{G}_\sigma(1-2) = \frac{1}{V}\sum_{\mathbf{k}} T \sum_{n=-\infty}^{\infty} e^{i\mathbf{k}\cdot(\mathbf{x}_1-\mathbf{x}_2)} e^{-ik_n(\tau_1-\tau_2)} \mathcal{G}_\sigma(k) \tag{12.11}$$

$$V_{\sigma,\sigma'}(1-2) = \frac{1}{V}\sum_{\mathbf{q}} T \sum_{n=-\infty}^{\infty} e^{i\mathbf{q}\cdot(\mathbf{x}_1-\mathbf{x}_2)} e^{-iq_n(\tau_1-\tau_2)} V_{\sigma,\sigma'}(q) \tag{12.12}$$

I hope the change of notation does not confuse you. I have taken out the spin index explicitly, so that now, $1 = (\mathbf{x}_1, \tau_1)$.

Then, consider an internal vertex, as illustrated in Fig.(12-3), where one has

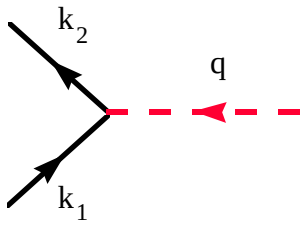

Figure 12-3 A typical interaction vertex and momentum conservation at the vertex.

to do the integral over the space-time position of the vertex, say 2 (in addition to the spin sum). Leaving aside the spin coordinates, that behave just as in position space, the integral to perform is

$$\int d\mathbf{x}_2 \int_0^\beta d\tau_2 e^{-i(\mathbf{k}_1-\mathbf{k}_2+\mathbf{q})\cdot\mathbf{x}_2} e^{i(k_{1,n}-k_{2,n}+q_n)\tau_2} \tag{12.13}$$

$$= (2\pi)^3 \delta(\mathbf{k}_1-\mathbf{k}_2+\mathbf{q}) \beta\delta_{(k_{2,n}-k_{1,n}),q_n} \tag{12.14}$$

$$= V\delta_{\mathbf{k}_1-\mathbf{k}_2,\mathbf{q}}\beta\delta_{(k_{2,n}-k_{1,n}),q_n} \tag{12.15}$$

$\delta_{\mathbf{k}_1-\mathbf{k}_2,\mathbf{q}}\delta_{(k_{2,n}-k_{1,n}),q_n}$ are Kronecker delta functions. The last line is for the discrete version of momentum. Note that the sum of two fermionic Matsubara frequencies is a bosonic Matsubara frequency since the sum of two odd numbers is necessarily even. This means that the integral over τ_1' is equal to β if $k_{1,n} - k_{2,n} + q_n = 0$ while it is equal to zero otherwise because $\exp(i(k_{1,n} - k_{2,n} + q_n)\tau_1')$is periodic in the interval 0 to β. The conclusion of this is that momentum and Matsubara frequencies are conserved at each interaction vertex. In other words, we obtain the following rule:

- *The sum of all wave vectors entering an interaction vertex vanishes. And similarly for Matsubara frequencies.*

This means that a lot of the momentum integrals and Matsubara frequency sums can be done by simply using conservation of momentum and of Matsubara frequencies at each vertex. We are left with the following rules:

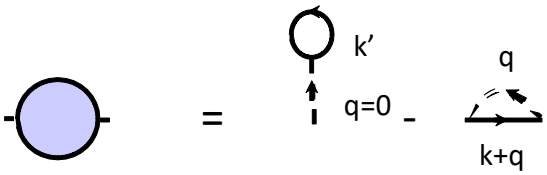

Figure 12-4 Diagram for the self-energy in momentum space in the Hartree-Fock approximation. There is an integral over all momenta and spins not determined by spin and momentum conservation.

- *One must integrate over the momenta and sum over Matsubara frequencies that are not determined by momentum conservation.* In general, there are as many integrals to perform as there are closed loops in a diagram.

- *We must also sum over spins that appear in internal indices, conserving spin at each interaction vertex when the interaction has this property.* The propagator $\mathcal{G}_\sigma$will then be diagonal in spin index.

Suppose we have $\mathcal{G}_\sigma(1-2)$ in terms of products of various $\mathcal{G}_\sigma$ and interactions. We want to write the corresponding expression in momentum space. This means that we take the Fourier-Matsubara transform of $\mathcal{G}_\sigma(1-2)$ to obtain $\mathcal{G}_\sigma(k)$. As mentioned above, a momentum k must flow in and out.

Example 4 *Writing*

$$k=(\mathbf{k},ik_n), \tag{12.16}$$

the Hartree-Fock approximation for the self-energy is

$$\Sigma(k)=-\frac{1}{\mathrm{V}}\sum_{\mathbf{q}}T\sum_{n=-\infty}^{\infty}V(q)\,\mathcal{G}(k+q)\,e^{-ik_n0^-}+V(q=0)\,\frac{1}{\mathrm{V}}\sum_{\mathbf{k}}T\sum_{n=-\infty}^{\infty}e^{-ik_n0^-}\mathcal{G}(k). \tag{12.17}$$

The sign of the wave vector q, or direction of the arrow in the diagram, must be decided once for each diagram but this choice is arbitrary since the potential is invariant under the interchange of coordinates, as mentioned above. This is illustrated in Fig. 12-4Note that here the $q=0$ contribution in the Hartree (so-called tadpole diagram) is cancelled by the positive ion background since $\mathcal{G}\left(\overline{2},\overline{2^+}\right)$ is just the electron density, which is the same as the ion density. You can convince yourself that $\mathcal{G}\left(\overline{2},\overline{2^+}\right)=\frac{1}{\mathrm{V}}\sum_{\mathbf{k}}T\sum_{n=-\infty}^{\infty}e^{ik_n0^+}\mathcal{G}(k)$.

Example 5 *For the four-point function, there are four outside coordinates so we would need three independent outside momenta. However, all that we will need, as we shall see, are the density-density fluctuations. In other words, as we can see from the general expression for the self-energy in Fig. 10-2, we can identify two of the space-time points at the bottom of the graph. We have already written the expression in coordinates in Eq.(12.3). Writing the diagrams for that expression and using our rules for momentum conservation with a four-momentum q flowing top down, the four-point function in Fig. 12-2 becomes as illustrated in Fig. 12-5. You can skip the next chapter if you are satisfied with the functional derivative (source, or Schwinger) approach.*

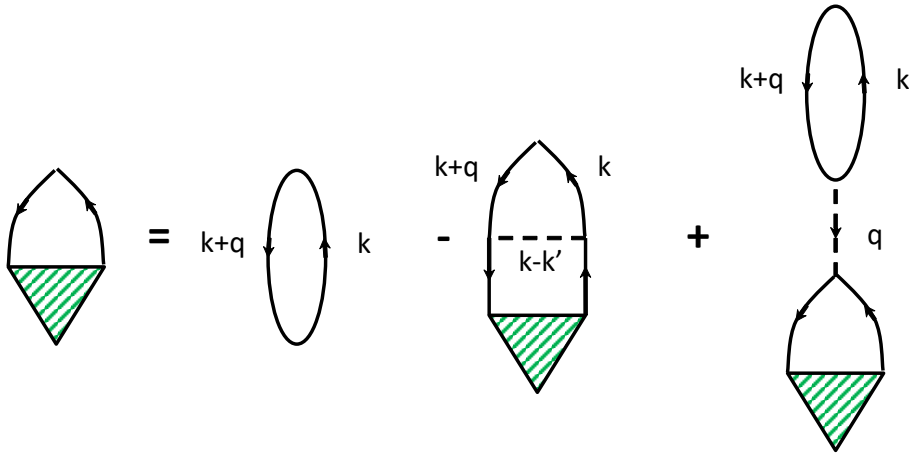

Figure 12-5 Diagrams for $\delta\mathcal{G}/\delta\phi$, which is minus the density-density correlation function. We imagine a momentum q flowing from the top of the diagram and conserve momentum at every vertex.

12.3 Density response in the non-interacting limit in terms of $\mathcal{G}^0_\sigma$

The density response can be expressed in terms of Green's function starting either from the Feynman or from the functional derivative approach. In this section we focus on the Schwinger way.

12.3.1 The Schwinger way (source fields)

Start from the expression for the four-point function Eq.(10.32) for $\phi = 0$ and point $2 = 1^+$ and $3 = 2^+$, and $4 = 2$. Then we find

$$\frac{\delta\mathcal{G}\left(1,1^+\right)}{\delta\phi\left(2^+,2\right)} = -\left\langle T_\tau\psi^\dagger\left(1^+\right)\psi\left(1\right)\psi^\dagger\left(2^+\right)\psi\left(2\right)\right\rangle + \mathcal{G}\left(1,1^+\right)\mathcal{G}\left(2,2^+\right). \quad (12.18)$$

If we sum over the spins associated with point 1 and the spins associated with point 2 and recall that once we sum over spins, we have $\mathcal{G}\left(1,1^+\right) = \mathcal{G}\left(2,2^+\right) = n$ where n is the average density, then

$$\begin{aligned} -\sum_{\sigma_1,\sigma_2}\frac{\delta\mathcal{G}\left(1,1^+\right)}{\delta\phi\left(2^+,2\right)} &= \sum_{\sigma_1,\sigma_2}\left\langle T_\tau\psi^\dagger\left(1^+\right)\psi\left(1\right)\psi^\dagger\left(2^+\right)\psi\left(2\right)\right\rangle - n^2 & (12.19)\\ &= \left\langle T_\tau n\left(1\right)n\left(2\right)\right\rangle - n^2 & (12.20)\\ &= \left\langle T_\tau\left(n\left(1\right)-n\right)\left(n\left(2\right)-n\right)\right\rangle \\ &= \chi_{nn}(1-2). & (12.21)\end{aligned}$$

The last expression is from the definition of the density-density correlation function.

The non-interacting contribution is given by the first term in Fig. 12-5 (taking into account the minus sign above) or, if you want, from the first term in Eq.(12.3)

for the functional derivative. It takes the form

$$\chi_{nn}(1-2) = -\sum_{\sigma} \mathcal{G}^0_\sigma(1-2)\,\mathcal{G}^0_\sigma(2-1)\,. \tag{12.22}$$

Only one spin sum is left because the spins corresponding the label 1 are identical in $\frac{\delta \mathcal{G}(1,1^+)}{\delta\phi(2^+,2)}$, as are the spin labels for label 2. Furthermore, spin is conserved, so the spin cannot flip in going from 1 to 2 in $\mathcal{G}^0_\sigma(1-2)$. Taking the Fourier transform and using the convolution theorem, one obtains,

$$\chi^0_{nn}(\mathbf{q}, iq_n) = -\frac{1}{\mathcal{V}}\sum_{\sigma}\sum_{\mathbf{k}} T\sum_{ik_n} \mathcal{G}^0_\sigma(\mathbf{k}+\mathbf{q}, ik_n+iq_n)\,\mathcal{G}^0_\sigma(\mathbf{k}, ik_n)\,. \tag{12.23}$$

One of the sums over spins has disappeared because we should think of $\mathcal{G}^0_\sigma$ as a matrix that is diagonal in spin indices. This is the so-called Lindhard function. It is also known as the bubble diagram .

Remark 47 *To obtain the above result from the first term in Fig. 12-5, note that it is as if we were injecting a momentum (Matsubara-frequency)* $\mathbf{q}$ *on one side of the diagram and using our rules for momentum conservation at each vertex.*

12.4 Density response in the non-interacting limit: Lindhard function

To compute

$$\chi^0_{nn}(\mathbf{q}, iq_n) = -\frac{1}{\mathcal{V}}\sum_{\sigma}\sum_{\mathbf{k}} T\sum_{ik_n} \mathcal{G}^0_\sigma(\mathbf{k}+\mathbf{q}, ik_n+iq_n)\,\mathcal{G}^0_\sigma(\mathbf{k}, ik_n) \tag{12.24}$$

the sums over Matsubara frequency should be performed first and they are easy to do. The technique is standard. First introduce the notation

$$\boxed{\zeta_{\mathbf{k}} \equiv \varepsilon_{\mathbf{k}} - \mu} \tag{12.25}$$

and note that

$$T\sum_{ik_n} \mathcal{G}^0_\sigma(\mathbf{k}+\mathbf{q}, ik_n+iq_n)\,\mathcal{G}^0_\sigma(\mathbf{k}, ik_n) = T\sum_{ik_n} \frac{1}{ik_n+iq_n-\zeta_{\mathbf{k}+\mathbf{q}}}\frac{1}{ik_n-\zeta_{\mathbf{k}}}. \tag{12.26}$$

Substituting in the expression for the susceptibility and decomposing in partial fractions, we find.

$$\chi^0_{nn}(\mathbf{q}, iq_n) = -2\int \frac{d^3\mathbf{k}}{(2\pi)^3} T\sum_{ik_n}\left[\frac{1}{ik_n-\zeta_{\mathbf{k}}} - \frac{1}{ik_n+iq_n-\zeta_{\mathbf{k}+\mathbf{q}}}\right]\frac{1}{iq_n-\zeta_{\mathbf{k}+\mathbf{q}}+\zeta_{\mathbf{k}}}. \tag{12.27}$$

The factor of two comes from the sum over spin σ. After the decomposition in partial fractions, it seems that now we need a convergence factor to do each sum individually. Using the general results of the preceding chapter for Matsubara sums, Eqs.(4.5) and (4.6), it is clear that as long as we take the same convergence factor for both terms, the result is

$$\chi^0_{nn}(\mathbf{q}, iq_n) = -2\int \frac{d^3\mathbf{k}}{(2\pi)^3}\frac{f(\zeta_{\mathbf{k}}) - f(\zeta_{\mathbf{k}+\mathbf{q}})}{iq_n+\zeta_{\mathbf{k}}-\zeta_{\mathbf{k}+\mathbf{q}}} \tag{12.28}$$

independently of the choice of convergence factor. Before the partial fractions, the terms in the ik_n series decreased like $(ik_n)^{-2}$ so, in fact, no convergence factor is needed.

The retarded function is easy to obtain by analytic continuation. It is the so-called Lindhard function

$$\boxed{\chi^{0R}_{nn}(\mathbf{q},\omega) = -2\int \frac{d^3\mathbf{k}}{(2\pi)^3}\frac{f(\zeta_{\mathbf{k}})-f\left(\zeta_{\mathbf{k}+\mathbf{q}}\right)}{\omega+i\eta+\zeta_{\mathbf{k}}-\zeta_{\mathbf{k}+\mathbf{q}}}} \tag{12.29}$$

This form is very close to the Lehmann representation for this response function. Clearly *at zero temperature* poles will be located at $\omega = \zeta_{\mathbf{k}+\mathbf{q}} - \zeta_{\mathbf{k}}$ as long as the states $\mathbf{k}$ and $\mathbf{k}+\mathbf{q}$ are not on the same side of the Fermi surface. These poles are particle-hole excitations instead of single-particle excitations as in the case of the Green's function. The sign difference between $\zeta_{\mathbf{k}+\mathbf{q}}$ and $\zeta_{\mathbf{k}}$ comes from the fact that one of them plays the role of a particle while the other plays the role of a hole.

Remark 48 *Summing over ik_n first: Note that the iq_n in the denominator of $\frac{1}{ik_n+iq_n-\zeta_{\mathbf{k}+\mathbf{q}}}$ did not influence the result for the sum over Matsubara frequencies ik_n because iq_n is bosonic, which means that ik_n+iq_n is a fermionic frequency: an odd number plus an even number is an odd number and the sum is from minus to plus infinity. The sums over Matsubara freuencies must be performed first, before analytic continuation (unless the sums and integrals are uniformly convergent, and that is rare).*

Remark 49 *Diagrammatic form of particle-hole excitations: If we return to the diagrams, we should notice the following general feature. If we cut the diagram in two by a vertical line, we see that it is crossed by lines that go in opposite directions. Hence, we have a particle-hole excitation. In particle-particle or hole-hole excitations, the lines go in the same direction and the two single-particle energies $\zeta_{\mathbf{k}+\mathbf{q}}$ and $\zeta_{\mathbf{k}}$ add up instead of subtract.*

Remark 50 *Absorptive vs reactive part of the response, real vs virtual excitations: There is a contribution to the imaginary part, in other words absorption, if for a given $\mathbf{k}$ and $\mathbf{q}$ energy is conserved in the intermediate state, i.e. if the condition $\omega = \zeta_{\mathbf{k}+\mathbf{q}} - \zeta_{\mathbf{k}}$ is realized. If this condition is not realized, the corresponding contribution is reactive, not dissipative, and it goes to the real part of the response only. The intermediate state then is only virtual. To understand the type of excitations involved in the imaginary part, rewrite $f(\zeta_{\mathbf{k}}) - f\left(\zeta_{\mathbf{k}+\mathbf{q}}\right) = \left(1-f\left(\zeta_{\mathbf{k}+\mathbf{q}}\right)\right)f(\zeta_{\mathbf{k}}) - (1-f(\zeta_{\mathbf{k}}))f\left(\zeta_{\mathbf{k}+\mathbf{q}}\right)$. We see that either $\zeta_{\mathbf{k}}$ can correspond to a hole and $\zeta_{\mathbf{k}+\mathbf{q}}$ to a particle or the other way around. In other words a single Green function line contains both the hole and the particle propagation, as we expect from its definition that allows either a creation operator or a destruction operator to act first.*

Remark 51 *When there are many Green's functions, partial fractions are always an option, but it can be much more efficient to use the Fermi function and contour integration as in Fig. (4-1) and to deform it around the poles using Cauchy's theorem.*

12.5 Density-density correlations, RPA

We keep following our first step approach that gave us the Hartree-Fock approximation and corresponding susceptibility. Returning to our expression for the

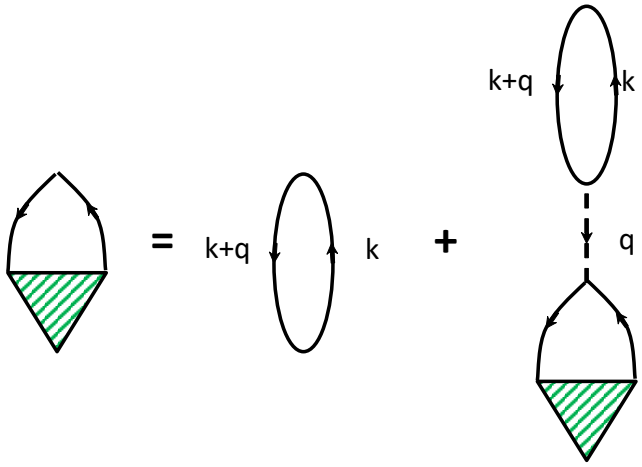

Figure 12-6 Fourier transform of $\frac{\delta \mathcal{G}\left(1,1^{+}\right)}{\delta \phi\left(2^{+},2\right)}$ with a momentum q flowing top to bottom that is used to compute the density-density correlation function in the RPA approximation.

susceptibility in terms a functional derivative Eq.(12.19), namely

$$-\sum_{\sigma_1,\sigma_2} \frac{\delta \mathcal{G}\left(1,1^{+}\right)}{\delta \phi\left(2^{+},2\right)} = \chi_{nn}\left(1-2\right) \tag{12.30}$$

and Fourier transforming, we obtain in the case where the irreducible vertex is obtained from functional derivatives of the Hartree-Fock self-energy the set of diagrams in Fig. 12-5. In the middle diagram on the right-hand side of the equality, there is a sum over wave vectors k' because three of the original coordinates of the functional derivative at the bottom of the diagram were different. This means there are two independent momenta, contrary to the last diagram in the figure. One of the independent momenta can be taken as q by momentum conservation while the other one, k', must be integrated over. The contribution from that middle diagram is not singular at small wave vector because the Coulomb potential is integrated over. By contrast, the last diagram has a $1/q^2$ from the interaction potential, which is divergent. We thus keep only that last term. The integral equation then takes an algebraic form

$$\chi_{nn}(q) = \chi^0_{nn}(q) - \chi^0_{nn}(q) V_{\mathbf{q}} \chi_{nn}(q). \tag{12.31}$$

To figure out the sign from the figure, recall that the green triangle stands for $\frac{\delta \mathcal{G}\left(1,1^{+}\right)}{\delta \phi\left(2^{+},2\right)}$, while there is a minus sign in the equation for the susceptibility. Since the integral equation for $\chi_{nn}(q)$ has become an algebraic equation in Fourier-Matsubara space, it is easy to solve. We find,

$$\chi_{nn}(q) = \frac{\chi^0_{nn}(q)}{1 + V_{\mathbf{q}} \chi^0_{nn}(q)} = \frac{1}{\chi^0_{nn}(q)^{-1} + V_{\mathbf{q}}}. \tag{12.32}$$

This is the so-called Random Phase Approximation, or RPA. The last form of the equality highlights the fact that the irreducible vertex, here $V_{\mathbf{q}}$, plays the role of an irreducible self-energy in the particle-hole channel. The analytical continuation will be trivial.

Note that we have written $\chi^0_{nn}(q)$ for the bubble diagram, i.e. the first term on the right-hand side of the equation in Fig. 12-5 even though everything we have up to now in the Schwinger formalism are dressed Green's functions. The

reason is that neglecting the middle diagram on the right-hand side of the equality is like neglecting the contribution from the Fock, or exchange self-energy in Fig. 12-4. The only term left then is is the Hartree term that we argued should vanish because of the neutralizing background. Hence, the Green's functions are bare ones and the corresponding susceptibility is the Linhard function.

Remark 52 *The integral equation (12.31) for χ_{nn} shows very well that the irreducible vertex $V_{\mathbf{q}}$ here plays the role of a self-energy for the particle-hole response function. Compare that equation with $\mathcal{G} = \mathcal{G}^0 + \mathcal{G}^0\Sigma\mathcal{G}$. Alternatively, compare $\mathcal{G}^{-1} = \mathcal{G}^{0-1} - \Sigma$ and the equation for the RPA susceptibility Eq. (12.32) $\chi_{nn}^{-1} = \chi_{nn}^{0-1} - V_{\mathbf{q}}$.*

Remark 53 *Equivalence to an infinite set of bubble diagrams: The integral equation for the susceptibility has turned into an algebraic equation in (12.31). By recursively replacing $\chi_{nn}(q)$ on the right-hand side of that equation by higher and higher order approximations in powers of $V_{\mathbf{q}}$ we obtain*

$$\begin{aligned} \chi_{nn}^{(1)}(q) &= \chi_{nn}^0(q) - \chi_{nn}^0(q)V_{\mathbf{q}}\chi_{nn}^0(q) \\ \chi_{nn}^{(2)}(q) &= \chi_{nn}^0(q) - \chi_{nn}^0(q)V_{\mathbf{q}}\chi_{nn}^0(q) && (12.33) \\ &\quad +\chi_{nn}^0(q)V_{\mathbf{q}}\chi_{nn}^0(q)V_{\mathbf{q}}\chi_{nn}^0(q) + \dots && (12.34) \end{aligned}$$

*etc. By solving the algebraic equation then, it is as if we had summed an infinite series which diagrammatically would look, if we turn it sideways, like Fig. **??**. The analogy with the self-energy in the case of the Green's function is again clear.*

Remark 54 *A direct expansion in powers of $V_{\mathbf{q}}$ without resumming would have been disatrous. Already the first term $\chi_{nn}^0(q)V_{\mathbf{q}}\chi_{nn}^0(q)$ diverges as $1/\mathbf{q}^2$ as $\mathbf{q}$ vanishes, and the following term as $1/\mathbf{q}^4$ etc. Doing perturbation theory with the Feynman formalism immediately leads to the questions of why are there divergences and why should we do infinite resummation to get rid of them. The reason why is clearer in the Schwinger formalism. Self-consistency is built in naturally in the formalism.*

13. SECOND STEP OF THE APPROXIMATION: GW CURING HARTREE-FOCK THEORY

In this Section, we present the solution to the failure of Hartree-Fock that was found by Gell-Man and Brueckner[**?**]. In brief, in the first step of the calculation we obtained collective modes with bare Green's functions. We saw that just trying to do Hartree-Fock at the single-particle level was a disaster. Now we want to improve our calculation of the single-particle properties. The Physics is that the interaction appearing in Hartree-Fock theory should be screened. Or equivalently, the self-energy that we find should be consistent with the density fluctuations found earlier since $\Sigma\mathcal{G}$ is simply related to density fluctuations. The resulting expresssion that we will find is also known as the GW approximation. We will come back on this nomenclature.

The first subsection should be read if you follow the Feynman way. Otherwise, skip to the next subsection.

13.1 Self-energy and screening, GW the Schwinger way

We have derived an expression for the product $\Sigma\mathcal{G}$. When $\phi = 0$ and $2 = 1^+$, this equation reduces to

$$\boxed{\Sigma\left(1,\overline{2}\right)_\phi \mathcal{G}\left(\overline{2},1^+\right)_\phi = V\left(1-\overline{2}\right)\left\langle T_\tau\left[\psi^\dagger\left(\overline{2^+}\right)\psi\left(\overline{2}\right)\psi^\dagger\left(1^+\right)\psi\left(1\right)\right]\right\rangle.} \tag{13.1}$$

It shows that we should have an approximation for the self-energy that, when multiplied by $\mathcal{G}$, gives the density-density correlation function. That is a very general result, or sum-rule, is a sort of consistency relation between one- and two-particle properties. This is a very important property that we will use also later in the context of non-perturbative treatments of the Hubbard model.

To obtain an approximation for the self-energy Σ that is consistent with the density-density correlation function that we just evaluated in the RPA approximation, we return to the general expression for the self-energy Eq.(10.44) and the corresponding pictorial representation Eq.(10-2). We replace the irreducible vertex $\delta\Sigma/\delta\mathcal{G}$ by the that we used to compute the density-density correlation function illustrated in Fig. 12-5. Note however that, as we did before, we keep only the terms where $V_{\mathbf{q}}$ carries a momentum $\mathbf{q}$. We neglect the next to last diagram in Fig.12-5. The other way to justify why we keep only these terms is that they are the most divergent diagrams. Their sum to infinity is however finite. We also know that by summing all diagrams to infinity, we are calculating the two-particle equivalent of a self-energy, shifting poles of the non-interacting density-density correlation function, as we should.

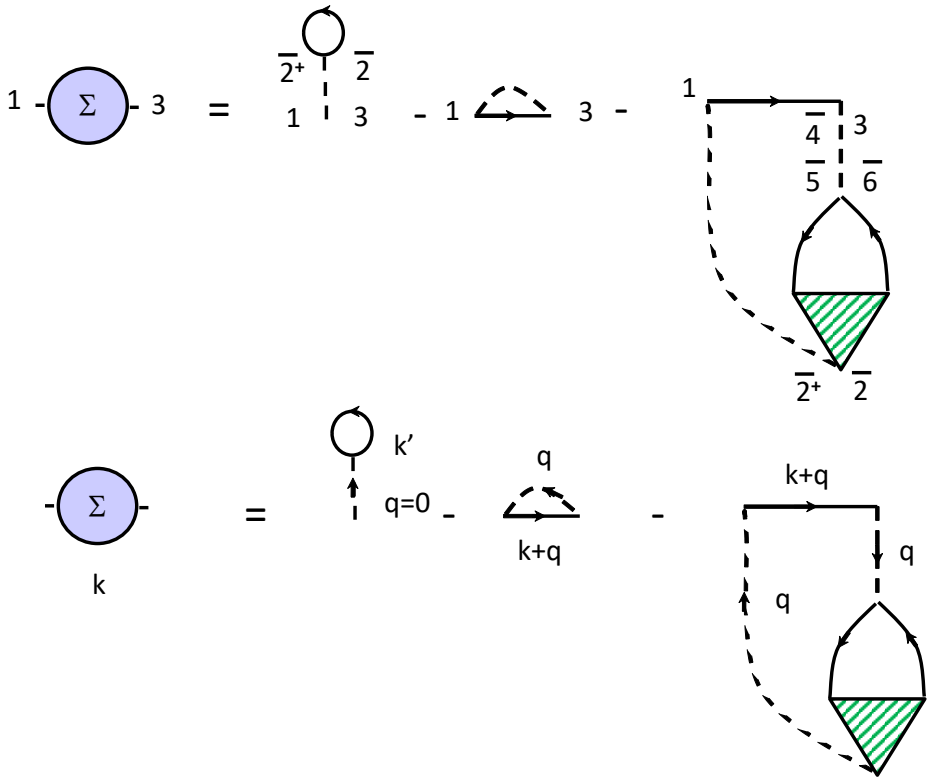

Figure 13-1 Coordinate (top) and momentum space (bottom) expressions for the self-energy at the second step of the approximation. The result, when multiplied by $\mathcal{G}$, is compatible with the density-density correlation function calculated in the RPA approximation.

The final result is illustrated in Fig. 13-1. We just need to replace the functional derivative of the Green function appearing at the bottom right by the RPA series. Recalling that the Hartree term vanishes, the final result is equivalent, when looked at sideways, to the series of bubble diagrams

The algebraic expression for this second level of approximation for the self-energy can be read off the figure. It takes the explicit form

$$\begin{aligned}\Sigma_{RPA}\left(\mathbf{k},ik_n\right) &= \Sigma^{(2)}\left(\mathbf{k},ik_n\right) \\ &= -\int\frac{d^3\mathbf{q}}{\left(2\pi\right)^3}T\sum_{iq_n}V_{\mathbf{q}}\left[1-\frac{V_{\mathbf{q}}\chi^0_{nn}\left(\mathbf{q},iq_n\right)}{1+V_{\mathbf{q}}\chi^0_{nn}\left(\mathbf{q},iq_n\right)}\right]\mathcal{G}^0\left(\mathbf{k}+\mathbf{q},ik_n+iq_n\right)\end{aligned} \tag{13.2}$$

where the first term comes from the Fock contribution. The minus sign in the second term comes from the fact that the bubble with vertex is related to $\delta\mathcal{G}/\delta\phi$ that is minus the charge susceptibility. The two terms can be combined into the single expression

$$\Sigma^{(2)}\left(\mathbf{k},ik_n\right)=-\int\frac{d^3\mathbf{q}}{\left(2\pi\right)^3}T\sum_{iq_n}\frac{V_{\mathbf{q}}}{1+V_{\mathbf{q}}\chi^0_{nn}\left(\mathbf{q},iq_n\right)}\mathcal{G}^0\left(\mathbf{k}+\mathbf{q},ik_n+iq_n\right). \tag{13.3}$$

Using our result for the longitudinal dielectric constant that follows from the density fluctuations in the RPA approximation, the last result can be written as

$$\Sigma^{(2)}\left(\mathbf{k},ik_n\right)=-\int\frac{d^3\mathbf{q}}{\left(2\pi\right)^3}T\sum_{iq_n}\frac{V_{\mathbf{q}}}{\varepsilon_L\left(\mathbf{q},iq_n\right)/\varepsilon_0}\mathcal{G}^0\left(\mathbf{k}+\mathbf{q},ik_n+iq_n\right) \tag{13.4}$$

which has the very interesting interpretation that the effective interaction entering the Fock term should be the screened one instead of the bare one. The two are equal only at very high frequency. The screened potential

$$\frac{V_{\mathbf{q}}}{\varepsilon_L\left(\mathbf{q},iq_n\right)/\varepsilon_0}=\frac{e^2}{\varepsilon_L\left(\mathbf{q},iq_n\right)q^2}$$

is often denoted W which means that the integrand is $W\mathcal{G}^0$, hence the name GW approximation.

Remark 55 *We can check that the relation between $\Sigma\mathcal{G}$ Eq.(13.1) and density fluctuations is satisfied by noticing that when we integrate this equation over* 1*, it is equivalent to computing a trace. That trace can be computed in any basis, in particular in the* $\mathbf{k}$ *basis. Diagrammatically, from Fig. 13-1, it is clear that multiplying by $\mathcal{G}^0$ and summing over* $\mathbf{k}$ *(i.e. taking the trace), we obtain the series of bubble diagrams for the density fluctuations, multiplied by the potential. That corresponds to the total potential energy. Hence, one recovers the sum-rule relating single and two-particle properties. Algebraically, we start from Eq.(13.3) just above and compute*

$$\int\frac{d^3\mathbf{k}}{\left(2\pi\right)^3}T\sum_{ik_n}\Sigma^{(2)}\left(\mathbf{k},ik_n\right)\mathcal{G}^0\left(\mathbf{k},ik_n\right)e^{-ik_n0^-}=$$

$$-\int\frac{d^3\mathbf{q}}{\left(2\pi\right)^3}T\sum_{iq_n}\frac{V_{\mathbf{q}}}{1+V_{\mathbf{q}}\chi^0_{nn}\left(\mathbf{q},iq_n\right)}\int\frac{d^3\mathbf{k}}{\left(2\pi\right)^3}T\sum_{ik_n}\mathcal{G}^0\left(\mathbf{k}+\mathbf{q},ik_n+iq_n\right)\mathcal{G}^0\left(\mathbf{k},ik_n\right)e^{-ik_n0^-}$$

The convergence factor $e^{-ik_n0^-}$ is necessary to enforce $\Sigma\left(1,\overline{2}\right)G\left(\overline{2},1^+\right)$ and obtain the potential energy to the right. It is not obvious from the right-hand side that we need the convergence factor until one realizes that there is a sum over k_n and q_n and only two Green's functions $\mathcal{G}^0\left(\mathbf{k}+\mathbf{q},ik_n+iq_n\right)\mathcal{G}^0\left(\mathbf{k},ik_n\right)$ that survive at very large frequency, giving a result that is formally divergent. Hence we should not invert the order of summation over k_n and q_n as we did.

14. THE HUBBARD MODEL IN THE FOOTSTEPS OF THE ELECTRON GAS

In this Chapter, we follow the same steps as the electron gas and derive RPA equations for the response functions. While spin fluctuations did not play a prominent role in the electron gas, they will be dominant in the Hubbard model and we will see why. The one-band Hubbard model (I do not justify it here) is given by

$$\widehat{H} = -\sum_{i,j}\sum_{\sigma} t_{i,j}\left(c^{\dagger}_{i,\sigma}c_{j,\sigma}\right) + U\sum_{i} n_{i,\uparrow}n_{i,\downarrow}. \tag{14.1}$$

There is one orbital per lattice site. The interaction is screened by the dielectric constant and is as short-range as it can be, namely local. The interaction is diagonal in position space while the kinetic energy, represented by the hopping parameters $t_{i,j}$ is diagonal in momentum space. So, when the potential and kinetic energy are comparable, the problem is extremely difficult. We can start with Hartree-Fock and RPA. RPA for the Hubbard model however has major deficiencies: It does not satisfy the Mermin-Wagner theorem, nor the Pauli exclusion principle, as we will see. This had no major consequence for the eletron gas, but in the case of the Hubbard model this is crucial. We will see how to cure this problem and others using the Two-Particle Self-Consistent Approach in the next Chapter.

14.1 Response functions for spin and charge

Response (four-point) functions for spin and charge excitations can be obtained from functional derivatives $(\delta\mathcal{G}/\delta\phi)$ of the source-dependent propagator. We will see that a linear combination of these response functions is related to $\delta\mathcal{G}_{\sigma}\left(1,2\right)_{\phi}/\delta\phi_{-\sigma}\left(1^{+},1\right)$ above. Following the standard approach and using matrix notation to abbreviate the summations and integrations we have,

$$\mathcal{G}\mathcal{G}^{-1} = 1 \tag{14.2}$$

$$\frac{\delta\mathcal{G}}{\delta\phi}\mathcal{G}^{-1} + \mathcal{G}\frac{\delta\mathcal{G}^{-1}}{\delta\phi} = 0. \tag{14.3}$$

Using the Dyson equation $\mathcal{G}^{-1} = \mathcal{G}_0^{-1} - \phi - \Sigma$ this may be rewritten

$$\frac{\delta\mathcal{G}}{\delta\phi} = -\mathcal{G}\frac{\delta\mathcal{G}^{-1}}{\delta\phi}\mathcal{G} = \mathcal{G}\circ\mathcal{G} + \mathcal{G}\frac{\delta\Sigma}{\delta\phi}\mathcal{G}, \tag{14.4}$$

where the symbol $\circ$ reminds us that the neighboring labels of the propagators have to be the same as those of the ϕ in the functional derivative. If perturbation theory converges, we may write the self-energy as a functional of the propagator. From the chain rule, one then obtains an integral equation for the response function in

the particle-hole channel that is the analog of the *Bethe-Salpeter equation* in the particle-particle channel

$$\frac{\delta \mathcal{G}}{\delta \phi} = \mathcal{G} \cdot \mathcal{G} + \mathcal{G} \left[\frac{\delta \Sigma}{\delta \mathcal{G}} \frac{\delta \mathcal{G}}{\delta \phi} \right] \mathcal{G}. \tag{14.5}$$

The labels of the propagators in the last term are attached to the self energy, as in Eq.(14.4) [1].

In the Coulomb-gas case, we have solved this equation in the RPA approximation, where only charge fluctuations are involved. Here let us drop any special assumption, other than spin-rotation invariance, concerning the form of the irreducible vertices. We will see that in general, both spin and charge fluctuations influence the self-energy, contrary to the Coulomb gas where only charge fluctuations were involved.

Remark 56 *In the RPA approximation for the Coulomb gas, the spin fluctuations are given by a single bubble. The diagrams that are reducible with respect to the Coulomb interaction all vanish. See the exercises.*

To obtain spin and charge fluctuations from the above formula, we restore spin indices explicitly and represent coordinates with numbers (in our previous convention, numbers included spin labels, but not here). When the external field is diagonal in spin indices we need only one spin label on $\mathcal{G}$ and ϕ. The response function that can be used then to build both spin and charge fluctuations is

$$\begin{aligned} -\frac{\delta \mathcal{G}_\sigma (1,1^+)}{\delta \phi_{\sigma'} (2^+,2)} &= \left\langle T_\tau \psi^\dagger_\sigma (1^+) \psi_\sigma (1) \psi^\dagger_{\sigma'} (2^+) \psi_{\sigma'} (2) \right\rangle_\phi - \mathcal{G}_\sigma (1,1^+)_\phi \mathcal{G}_{\sigma'} (2,2^+)_\phi \\ &= \langle T_\tau n_\sigma (1) n_{\sigma'} (2) \rangle_\phi - \langle n_\sigma (1) \rangle_\phi \langle n_{\sigma'} (2) \rangle_\phi . \end{aligned} \tag{14.6}$$

The charge and spin given by

$$n_i \equiv n_{i\uparrow} + n_{i\downarrow} \tag{14.7}$$

$$S^z_i \equiv n_{i\uparrow} (\tau) - n_{i\downarrow} (\tau) . \tag{14.8}$$

Hence, the charge fluctuations are obtained from

$$\chi_{ch} (1,2) = -\sum_{\sigma,\sigma'} \frac{\delta \mathcal{G}_\sigma (1,1^+)}{\delta \phi_{\sigma'} (2^+,2)} \tag{14.9}$$

and the spin fluctuations from

$$\chi_{sp} (1,2) = -\sum_{\sigma,\sigma'} \sigma \frac{\delta \mathcal{G}_\sigma (1,1^+)}{\delta \phi_{\sigma'} (2^+,2)} \sigma'. \tag{14.10}$$

We want to write separate equations for the spin and charge fluctuations. It is useful to proceed as follows. Define the matrix

$$\chi_{\sigma,\sigma'} = -\frac{\delta \mathcal{G}_\sigma}{\delta \phi_{\sigma'}}. \tag{14.11}$$

The spin and charge susceptibilities are then given by

$$\chi_{ch} = \sum_{\sigma,\sigma'} \chi_{\sigma,\sigma'} \; ; \; \chi_{sp} = \sum_{\sigma,\sigma'} \sigma \chi_{\sigma,\sigma'} \sigma' \tag{14.12}$$

[1] To remind ourselves of this, we may also adopt an additional "vertical matrix notation" convention and write Eq.(7) as $\frac{\delta G}{\delta \phi} = G \cdot G + G \left[\frac{\delta \Sigma}{\delta G} \frac{\delta G}{\delta \phi} \right] G$.

With the 2×2 matrix

$$\boldsymbol{\chi} = \begin{pmatrix} \boldsymbol{\chi}_{\uparrow\uparrow} & \boldsymbol{\chi}_{\uparrow\downarrow} \\ \chi_{\downarrow\uparrow} & \boldsymbol{\chi}_{\downarrow\downarrow} \end{pmatrix} \tag{14.13}$$

and vectors

$$\mathbf{s} = \begin{pmatrix} 1 \\ 1 \end{pmatrix} \; ; \; \mathbf{a} = \begin{pmatrix} 1 \\ -1 \end{pmatrix}. \tag{14.14}$$

we can rewrite in matrix rotation

$$\chi_{ch} = \mathbf{s^T} \boldsymbol{\chi}\, \mathbf{s} \; ; \; \chi_{sp} = \mathbf{a^T} \boldsymbol{\chi}\, \mathbf{a}. \tag{14.15}$$

Because we have spin rotational invariance, the following relations hold $\chi_{\uparrow\uparrow} = \chi_{\downarrow\downarrow}$ et $\chi_{\uparrow\downarrow} = \chi_{\downarrow\uparrow}$ so that the following holds

$$0 = \mathbf{s^T} \boldsymbol{\chi}\, \mathbf{a} \; ; \; 0 = \mathbf{a^T} \boldsymbol{\chi}\, \mathbf{s} \tag{14.16}$$

It is convenient to have a similar definition of the vertex

$$\Gamma_{\sigma,\sigma'} = \frac{\delta \Sigma_\sigma}{\delta \mathcal{G}_{\sigma'}} \tag{14.17}$$

and of the corresponding matrix

$$\boldsymbol{\Gamma} = \begin{pmatrix} \boldsymbol{\Gamma}_{\uparrow\uparrow} & \boldsymbol{\Gamma}_{\uparrow\downarrow} \\ \Gamma_{\downarrow\uparrow} & \boldsymbol{\Gamma}_{\downarrow\downarrow} \end{pmatrix} \tag{14.18}$$

that has the same properties as $\boldsymbol{\chi}$ under spin rotation (This is related to the fact that Σ_σ itself is a functional derivative oa the Luttinger Ward with respect to $\mathcal{G}_\sigma$). Defining

$$P^a_{ij} = a_i a_j \; ; \; P^s_{ij} = s_i s_j \tag{14.19}$$

that we write as

$$\mathbf{P}^a = \mathbf{a} \otimes \mathbf{a^T} = \begin{pmatrix} \mathbf{1} & \mathbf{-1} \\ -1 & \mathbf{1} \end{pmatrix} \; ; \; \mathbf{P}^s = \mathbf{s} \otimes \mathbf{s^T} = \begin{pmatrix} \mathbf{1} & \mathbf{1} \\ 1 & \mathbf{1} \end{pmatrix} \tag{14.20}$$

so that

$$P^a_{ij} + P^s_{ij} = 2\delta_{i,j}. \tag{14.21}$$

This allows us to easily project the general equation

$$\frac{\delta \mathcal{G}_\sigma}{\delta \phi_{\sigma'}} = \mathcal{G}_\sigma \mathcal{G} \delta_{\sigma,\sigma'} + \mathcal{G}_\sigma \left[\frac{\delta \Sigma_\sigma}{\delta \mathcal{G}_{\bar{\sigma}}} \frac{\delta \mathcal{G}_{\bar{\sigma}}}{\delta \phi_{\sigma'}} \right] \mathcal{G}_\sigma. \tag{14.22}$$

into the spin and charge chanels:

$$-\mathbf{s^T} \boldsymbol{\chi}\, \mathbf{s} = \mathbf{2}\, \mathcal{G}_\sigma \mathcal{G} + \mathcal{G}\, \mathbf{s^T} \boldsymbol{\Gamma} \left(\frac{\mathbf{a} \otimes \mathbf{a^T} + \mathbf{s} \otimes \mathbf{s^T}}{2} \right) (-\boldsymbol{\chi}\, \mathbf{s})\, \mathcal{G} \tag{14.23}$$

which, given $\mathbf{s^T \Gamma a} = \mathbf{0}$ leads to

$$\boxed{\chi_{ch} = -2\mathcal{G}_\sigma \mathcal{G} + \mathcal{G} \left[\left(\frac{\delta \Sigma_\uparrow}{\delta \mathcal{G}_\uparrow} + \frac{\delta \Sigma_\downarrow}{\delta \mathcal{G}_\uparrow} \right) \chi_{ch} \right] \mathcal{G}} \tag{14.24}$$

Similarly for spin, form

$$-\mathbf{a^T} \boldsymbol{\chi}\, \mathbf{a} = \mathbf{2}\, \mathcal{G}_\sigma \mathcal{G} + \mathcal{G}\, \mathbf{a^T} \boldsymbol{\Gamma} \left(\frac{\mathbf{a} \otimes \mathbf{a^T} + \mathbf{s} \otimes \mathbf{s^T}}{2} \right) (-\boldsymbol{\chi}\, \mathbf{a})\, \mathcal{G} \tag{14.25}$$

we find, given $\mathbf{a^T \Gamma s} = \mathbf{0}$

$$\boxed{\chi_{sp} = -2\mathcal{G}_\sigma \mathcal{G} - \mathcal{G} \left[\left(\frac{\delta \Sigma_\uparrow}{\delta \mathcal{G}_\downarrow} - \frac{\delta \Sigma_\uparrow}{\delta \mathcal{G}_\uparrow} \right) \chi_{sp} \right] \mathcal{G}} \tag{14.26}$$

In summary, we define irreducible vertices appropriate for spin and charge responses as follows,

$$\begin{array}{|l|}\hline U_{sp}=\frac{\delta\Sigma_{\uparrow}}{\delta\mathcal{G}_{\downarrow}}-\frac{\delta\Sigma_{\uparrow}}{\delta\mathcal{G}_{\uparrow}}\\ \hline U_{ch}=\frac{\delta\Sigma_{\uparrow}}{\delta\mathcal{G}_{\downarrow}}+\frac{\delta\Sigma_{\uparrow}}{\delta\mathcal{G}_{\uparrow}}\\ \hline\end{array}. \tag{14.27}$$

14.2 Hartree-Fock and RPA

As an example of calculation of response functions, consider the Hartree-Fock approximation which corresponds to factoring the four-point function in the definition of the self-energy as if there were no interactions, in which case it is easy to see that $\frac{\delta\mathcal{G}_{\sigma}(1,2)_{\phi}}{\delta\phi_{-\sigma}(1^{+},1)}=0$. To be more specific, starting from

$$\Sigma_{\sigma}\left(1,\overline{1}\right)_{\phi}\mathcal{G}_{\sigma}\left(\overline{1},2\right)_{\phi} = -U\left\langle T_{\tau}\psi_{-\sigma}^{\dagger}\left(1^{+}\right)\psi_{-\sigma}\left(1\right)\psi_{\sigma}\left(1\right)\psi_{\sigma}^{\dagger}\left(2\right)\right\rangle_{\phi} \tag{14.28}$$

$$= -U\left[\frac{\delta\mathcal{G}_{\sigma}\left(1,2\right)_{\phi}}{\delta\phi_{-\sigma}\left(1^{+},1\right)}-\mathcal{G}_{-\sigma}\left(1,1^{+}\right)_{\phi}\mathcal{G}_{\sigma}\left(1,2\right)_{\phi}\right] \tag{14.29}$$

the Hartree-Fock approximation is

$$\Sigma_{\sigma}^{H}\left(1,\overline{1}\right)_{\phi}\mathcal{G}_{\sigma}^{H}\left(\overline{1},2\right)_{\phi}=U\mathcal{G}_{-\sigma}^{H}\left(1,1^{+}\right)_{\phi}\mathcal{G}_{\sigma}^{H}\left(1,2\right)_{\phi}.$$

Multiplying the above equation by $\left(G_{\sigma}^{H}\right)^{-1}$, we are left with

$$\Sigma_{\sigma}^{H}\left(1,2\right)_{\phi}=U\mathcal{G}_{-\sigma}^{H}\left(1,1^{+}\right)_{\phi}\delta\left(1-2\right), \tag{14.30}$$

so that

$$\left.\frac{\delta\Sigma_{\uparrow}^{H}\left(1,2\right)_{\phi}}{\delta\mathcal{G}_{\downarrow}^{H}\left(3,4\right)_{\phi}}\right|_{\phi=0}=U\delta\left(1-2\right)\delta\left(3-1\right)\delta\left(4-2\right), \tag{14.31}$$

and

$$\left.\frac{\delta\Sigma_{\uparrow}^{H}\left(1,2\right)_{\phi}}{\delta\mathcal{G}_{\uparrow}^{H}\left(3,4\right)_{\phi}}\right|_{\phi=0}=0.$$

which, when substituted in the integral equation (14.5) for the response function, tells us that we have generated the random phase approximation (RPA) with, from Eq.(14.27), $U_{sp}=U_{ch}=U$. Indeed, when the irreducible vertex comes from the Hartree term, the same structure as the one found before for the electron gas results. The charge susceptibility that follows from the result of the previous section Eq.(14.24) for χ_{ch} and the definition U_{ch} for the corresponding irreducible vertex Eq.(14.27) is

$$\chi_{ch}\left(1,2\right)=\chi^{(0)}\left(1,2\right)-\frac{1}{2}\chi^{(0)}\left(1,\overline{3}\right)U_{ch}\chi_{ch}\left(\overline{3},2\right) \tag{14.32}$$

with $\chi^{(0)}\left(1,2\right)=-2\mathcal{G}\left(1,2\right)\mathcal{G}\left(2,1\right)$. The Fourier transform is

$$\chi_{ch}\left(q\right)=\chi^{(0)}\left(q\right)-\frac{U_{ch}}{2}\chi^{(0)}\left(q\right)\chi_{ch}\left(q\right). \tag{14.33}$$

Since at this point the self-energy is a constant, we take for $\mathcal{G}$ the non-interacting Green's function. In Fourier-Matsubara space, $\chi_0(q)$ then is the Lindhard function that, in analytically continued retarded form is, for a discrete lattice of N sites,

$$\chi^{0R}(\mathbf{q},\omega) = -\frac{2}{N}\sum_{\mathbf{k}} \frac{f\left(\zeta_{\mathbf{k}}\right) - f\left(\zeta_{\mathbf{k}+\mathbf{q}}\right)}{\omega + i\eta + \zeta_{\mathbf{k}} - \zeta_{\mathbf{k}+\mathbf{q}}}. \tag{14.34}$$

Similarly, for the spin susceptibility, using the integral equation Eq.(14.26) and the definition U_{sp} for the corresponding irreducible vertex Eq.(14.27), we obtain

$$\chi_{sp}\left(q\right) = \chi^{(0)}\left(q\right) + \frac{U_{sp}}{2}\chi^{(0)}\left(q\right)\chi_{sp}\left(q\right). \tag{14.35}$$

The equations for the spin and charge fluctuations can easily be solved and yield, respectively

$$\chi_{sp}(q) = \frac{\chi_0(q)}{1 - \frac{1}{2}U\chi_0(q)} \tag{14.36}$$

$$\chi_{ch}(q) = \frac{\chi_0(q)}{1 + \frac{1}{2}U\chi_0(q)} \tag{14.37}$$

It is known on general grounds [9] that RPA satisfies conservation laws. We will describe the general methods that lead to approximations that are consistent with conservation laws in a later chapter. But it is easy to check that for a special case. Since spin and charge are conserved, then the equalities $\chi^R_{sp}(\mathbf{q}=\mathbf{0},\omega) = 0$ and $\chi^R_{ch}(\mathbf{q}=\mathbf{0},\omega) = 0$ for $\omega \neq 0$ follow from the corresponding equality for the non-interacting Lindhard function $\chi^{0R}(\mathbf{q}=\mathbf{0},\omega) = 0$.

Remark 57 *If we had used dressed Green's function to compute the Lindhard susceptibility, the conservation law $\chi_{sp,ch}\left(\mathbf{q}=\mathbf{0},i\omega_n\right) = 0$ for $i\omega_n \neq 0$ would have been violated, as shown in Appendix A of Ref.[97]. In general, irreducible vertices and self-energy (and corresponding Green's functions) must be taken at the same level of approximation.*

14.3 RPA and violation of the Pauli exclusion principle

RPA has a drawback that is particularly important for the Hubbard model. It violates the Pauli exclusion principle that is assumed to be satisfied exactly in its definition where up spins interact only with down spins. To see this requires a bit more thinking. We derive a sum rule that rests on the use of the Pauli exclusion principle and check that it is violated by RPA to second order in U.

First note that if we sum the spin and charge susceptibilities over all wave vectors $\mathbf{q}$ and all Matsubara frequencies iq_n, we obtain local, equal-time correlation functions, namely

$$\frac{T}{N}\sum_{\mathbf{q}}\sum_{iq_n}\chi_{sp}(\mathbf{q},iq_n) = \left\langle\left(n_\uparrow - n_\downarrow\right)^2\right\rangle = \langle n_\uparrow\rangle + \langle n_\downarrow\rangle - 2\left\langle n_\uparrow n_\downarrow\right\rangle \tag{14.38}$$

and

$$\frac{T}{N}\sum_{\mathbf{q}}\sum_{iq_n}\chi_{ch}(\mathbf{q},iq_n) = \left\langle\left(n_\uparrow + n_\downarrow\right)^2\right\rangle - \langle n_\uparrow + n_\downarrow\rangle^2 = \langle n_\uparrow\rangle + \langle n_\downarrow\rangle + 2\left\langle n_\uparrow n_\downarrow\right\rangle - n^2 \tag{14.39}$$

where on the right-hand side, we used the Pauli exclusion principle $n_\sigma^2 = \left(c_\sigma^\dagger c_\sigma\right)\left(c_\sigma^\dagger c_\sigma\right) = c_\sigma^\dagger c_\sigma - c_\sigma^\dagger c_\sigma^\dagger c_\sigma c_\sigma = c_\sigma^\dagger c_\sigma = n_\sigma$ that follows from $c_\sigma^\dagger c_\sigma^\dagger = c_\sigma c_\sigma = 0$. This is the simplest version of the Pauli exclusion principle. Full antisymmetry is another matter [13, 33]. We call the first of the above displayed equations the local spin sum-rule and the second one the local charge sum-rule. For RPA, adding the two sum rules yields

$$\frac{T}{N}\sum_{\mathbf{q}}\sum_{iq_n}\left(\chi_{sp}(\mathbf{q},iq_n)+\chi_{ch}(\mathbf{q},iq_n)\right) = \tag{14.40}$$

$$\frac{T}{N}\sum_{q}\left(\frac{\chi_0(q)}{1-\frac{1}{2}U\chi_0(q)}+\frac{\chi_0(q)}{1+\frac{1}{2}U\chi_0(q)}\right) = 2n-n^2. \tag{14.41}$$

Since the non-interacting susceptibility $\chi_0(q)$ satisfies the sum rule, we see by expanding the denominators that in the interacting case it is violated already to second order in U because $\chi_0(q)$ being real and positive,, the quantity $\sum_q \chi_0(q)^3$ cannot vanish.

14.4 RPA, phase transitions and the Mermin-Wagner theorem

The RPA predicts that the normal state is sometimes unstable, namely that if we decrease the temperature, spin fluctuations at zero frequency start, in certain cases, to diverge. Below the temperature where that occurs, the spin susceptibility is negative, which is prohibited by thermodynamic stability. This indicates that a paramagnetic ground state is an unstable state. This happens even in two-dimensions with RPA because

$$\chi_0(q) = \int \frac{d\omega'}{\pi}\frac{\chi''_{sp}(\mathbf{q},\omega')\omega'}{\omega'^2+q_n^2}$$

is positive so that the expression for the spin susceptibility

$$\chi_{sp}(q) = \frac{\chi_0(q)}{1-\frac{1}{2}U\chi_0(q)} \tag{14.42}$$

is quite likely to become negative for a U sufficiently large.

By the way, why does a negative spin susceptibility at $q_n = 0$ signal an instability? Because there is a thermodynamic inequality that says that susceptibilities of the form dA/da, where A and a are thermodynamically conjugate variables, are positive since entropy is a maximum at equilibrium. But there is another way to look at this from the thermodynamic sum rule

$$\chi_{sp}(\mathbf{Q},0) = \int \frac{d\omega}{\pi}\frac{\chi''_{sp}(\mathbf{Q},\omega)}{\omega}. \tag{14.43}$$

Indeed, if the left-hand side is negative, this means that the imaginary part of the spin susceptibility for positive frequencies has to be negative.[2] This violates the positivity criterion imposed by stability, namely $\chi''_{sp}(\mathbf{Q},\omega)\omega > 0$. Hence, the system is unstable.

[2] It is positive at negative frequencies since it must be odd.

Such an instability in two dimensions at finite temperature is prohibited by the Mermin-Wagner theorem that says that a continuous symmetry cannot be broken in two dimensions at finite temperature. We will come back on this theorem in a later chapter, but for now the theorem may intuitively be understood as follows. If there is long-range order in the presence of a continuous symmetry, there will be a term in the free energy that will be proportional to $|\nabla\phi|^2$, where ϕ is the angle representing the deviation of the spins say, from their equilibrium position. The equipartition theorem then says that

$$\mathbf{q}^2 \left\langle \phi_{\mathbf{q}} \phi_{-\mathbf{q}} \right\rangle = \frac{T}{2}. \tag{14.44}$$

Thus, in two dimensions, the thermal fluctuations of that angle are infinite, proving the theorem by contradiction:

$$\left\langle \phi^2 \right\rangle = \int_0^\infty \frac{d^2q}{q^2} \frac{T}{2} = \infty.$$

We may think that the instability will occur for U so large that anyway RPA does not apply. This is not the case. Let us illustrate that this happens with a specific example where in fact the instability occurs for infinitesimal U.

We evaluate the Lindhard function Eq.(14.34) at zero frequency in the case where we have only nearest neighbor hopping on a cubic lattice, in other words, $\varepsilon_{\mathbf{k}} = -2t\left(\cos k_x + \cos k_y + \cos k_z\right)$. In $d = 2$ this would be replaced by $\zeta_{\mathbf{k}} = \varepsilon_{\mathbf{k}} = -2t\left(\cos k_x + \cos k_y\right)$. Then, if we take $\mu = 0$, which in this case corresponds to half-filling, and choose the wave vector corresponding to an antiferromagnetic fluctuation, namely $Q = (\pi, \pi, \pi)$ that leads to a phase $+1$ or -1 on alternating sites, we find

$$\chi^{0R}(\mathbf{Q}, 0) = -\frac{2}{N} \sum_{\mathbf{k}} \frac{2f\left(\varepsilon_{\mathbf{k}}\right) - 1}{2\varepsilon_{\mathbf{k}}} \tag{14.45}$$

because of the equality $f(-\varepsilon) = 1 - f(\varepsilon)$ and the co-called nesting property $\varepsilon_{\mathbf{k}} = -\varepsilon_{\mathbf{k}+\mathbf{Q}}$. But $2f\left(\varepsilon_{\mathbf{k}}\right) - 1 = -\tanh\left(\beta\varepsilon_{\mathbf{k}}/2\right)$ which allows one to write by using the definition of the density of states $N(\varepsilon)$

$$\begin{aligned}
\chi^{0R}(\mathbf{Q}, 0) &= \frac{2}{N} \sum_{\mathbf{k}} \frac{\tanh\left(\beta\varepsilon_{\mathbf{k}}/2\right)}{2\varepsilon_{\mathbf{k}}} && (14.46)\\
&\sim 2 \int \frac{d^3\mathbf{k}}{(2\pi)^3} \frac{\tanh\left(\beta\varepsilon_{\mathbf{k}}/2\right)}{2\varepsilon_{\mathbf{k}}} && (14.47)\\
&\sim \int d\varepsilon N(\varepsilon) \frac{\tanh\left(\beta\varepsilon/2\right)}{2\varepsilon}. && (14.48)
\end{aligned}$$

This last result takes the same form in $d = 2$. You just need to replace the density of states by the two-dimensional one. The last integral diverges when $T \to 0$ or $\beta \to \infty$. Indeed, take $N(\varepsilon)$ constant near the Fermi level, up to a cutoff energy $\pm E_F$. Near the Fermi level, $\varepsilon = 0$, when $\varepsilon > T$ we can approximate $\tanh\left(\beta\varepsilon/2\right)/2\varepsilon \sim 1/4T$. So we can extract the logarithmically divergent part of the integral as follows:

$$\begin{aligned}
\int d\varepsilon N(\varepsilon) \frac{\tanh\left(\beta\varepsilon/2\right)}{2\varepsilon} &\sim \int_T^{E_F} d\varepsilon N(0) \frac{1}{\varepsilon}\\
&\sim N(0) \ln\left(\frac{E_F}{T}\right). && (14.49)
\end{aligned}$$

For T sufficiently small, $\chi^{0R}(\mathbf{Q}, 0)$ diverges, which means that at a certain temperature, the denominator of the spin susceptibility Eq.(14.36) goes through zero,

even with infinitesimal U. At that temperature, the spin susceptibility diverges. Below that it is negative, signaling an instability.

This instability signals a second-order phase transition that it physical. In two dimensions, $N(\varepsilon)$ has a logarithmic divergence at $\varepsilon = 0$ so the above result must be modified. We would obtain a $\ln^2(E_F/T)$ instead of $\ln(E_F/T)$. Nevertheless, the qualitative result would be the same. There is an instability even in the presence of an infinitesimal U. However, in two-dimensions, one cannot have a phase transition that breaks a continuous symmetry at finite temperature in two dimensions. That is the content of the Mermin Wagner theorem.[59, 31] Hence, RPA fails miserably on many grounds in two dimensions: It violates the Pauli exclusion principle and the Mermin-Wagner theorem. The approach in the next section fixes these two problems and more.

15. THE TWO-PARTICLE-SELF-CONSISTENT APPROACH

The two-particle-self-consistent approach (TPSC) is designed to remedy the deficiencies found above in the study of the the one-band Hubbard model. It is also possible to generalize to cases where near-neighbor interactions are included.

TPSC is valid from weak to intermediate coupling. Hence, on the negative side, it does not describe the Mott transition. Nevertheless, there is a large number of physical phenomena that it allows to study. An important one is antiferromagnetic fluctuations. It is extremely important physically that in two dimensions there is a wide range of temperatures where there are huge antiferromagnetic fluctuations in the paramagnetic state, without long-range order, as imposed by the Mermin-Wagner theorem. The standard way to treat fluctuations in many-body theory, the Random Phase Approximation (RPA) misses this and also, as we saw, the RPA also violates the Pauli exclusion principle in an important way. The composite operator method (COM), by F. Mancini, is another approach that satisfies the Mermin-Wagner theorem and the Pauli exclusion principle. [52, 53, 51] The Fluctuation Exchange Approximation (FLEX) [11, 12], and the self-consistent renormalized theory of Moriya-Lonzarich [62, 45, 63] are other approaches that satisfy the Mermin-Wagner theorem at weak coupling. Each has its strengths and weaknesses, as discussed in Refs. [97, 4]. Weak coupling renormalization group approaches become uncontrolled when the antiferromagnetic fluctuations begin to diverge [23, 77, 42, 32]. Other approaches include the effective spin-Hamiltonian approach [89].

In summary, the advantages and disadvantages of TPSC are as follows. Advantages:

- There are no adjustable parameters.
- Several exact results are satisfied: Conservation laws for spin and charge, the Mermin-Wagner theorem, the Pauli exclusion principle in the form $\left\langle n_{\uparrow}^{2}\right\rangle = \langle n_{\uparrow}\rangle$, the local moment and local-charge sum rules and the f sum-rule.
- Consistency between one and two-particle properties serves as a guide to the domain of validity of the approach. (Double occupancy obtained from sum rules on spin and charge equals that obtained from the self-energy and the Green function).
- Up to intermediate coupling, TPSC agrees within a few percent with Quantum Monte Carlo (QMC) calculations. Note that QMC calculations can serve as benchmarks since they are exact within statistical accuracy, but they are limited in the range of physical parameter accessible.
- We do not need to assume that Migdal's theorem applies to be able to obtain the self-energy.

The main successes of TPSC include

- Understanding the physics of the pseudogap induced by precursors of a long-range ordered phase in two dimensions. For this understanding, one needs

a method that satisfies the Mermin-Wagner theorem to create a broad temperature range where the antiferromagnetic correlation length is larger than the thermal de Broglie wavelength. That method must also allow one to compute the self-energy reliably. Only TPSC does both.

- Explaining the pseudogap in electron-doped cuprate superconductors over a wide range of dopings.
- Finding estimates of the transition temperature for d-wave superconductivity that were found later in agreement with quantum cluster approaches such as the Dynamical Cluster Approximation.
- Giving quantitative estimates of the range of temperature where quantum critical behavior can affect the physics.

The drawbacks of this approach, that I explain as we go along, are that

- It works well in two or more dimensions, not in one dimension [1] [66].
- It is not valid at strong coupling, except at very high temperature and large U where it recovers the atomic limit [20].
- It is not valid deep in the renormalized classical regime [93].
- For models other than the one-band Hubbard model, one usually runs out of sum rules and it is in general not possible to find all parameters self-consistently. With nearest-neighbor repulsion, it has been possible to find a way out [21].

For detailed comparisons with QMC calculations, discussions of the physics and detailed comparisons with other approaches, you can refer to Ref.[97, 4]. You can read Ref.[88] for a review of the work related to the pseudogap and superconductivity up to 2005 including detailed comparisons with Quantum Cluster approaches in the regime of validity that overlaps with TPSC (intermediate coupling). A more recent review appeared in Ref. [87].

15.1 TPSC First step: two-particle self-consistency for $\mathcal{G}^{(1)}$, $\Sigma^{(1)}$, $\Gamma^{(1)}_{sp} = U_{sp}$ and $\Gamma^{(1)}_{ch} = U_{ch}$

Details of the more formal derivation may be also be found in Ref. [3]. In conserving approximations, the self-energy is obtained from a functional derivative $\Sigma[\mathcal{G}] = \delta\Phi[\mathcal{G}]/\delta\mathcal{G}$ of Φ the Luttinger-Ward functional, which is itself computed from a set of diagrams. We will see this approach later in the course. To liberate ourselves from diagrams and find results that are valid beyond perturbation theory, we start instead from the exact expression for the self-energy

$$\Sigma_\sigma(1,\overline{1})_\phi \mathcal{G}_\sigma(\overline{1},2)_\phi = -U\left\langle T_\tau \psi^\dagger_{-\sigma}(1^+)\psi_{-\sigma}(1)\psi_\sigma(1)\psi^\dagger_\sigma(2)\right\rangle_\phi$$

and notice that when label 2 equals 1^+, the right-hand side of this equation is equal to double-occupancy $\langle n_\uparrow n_\downarrow\rangle$. Factoring as in Hartree-Fock amounts to assuming

[1] Modifications have been proposed in zero dimension to use as impurity solver for DMFT [26]

no correlations. Instead, we should insist that $\langle n_\uparrow n_\downarrow \rangle$ should be obtained self-consistently. After all, in the Hubbard model, there are only two local four point functions: $\langle n_\uparrow n_\downarrow \rangle$ and $\left\langle n_\uparrow^2 \right\rangle = \left\langle n_\downarrow^2 \right\rangle$. The latter is given exactly, through the Pauli exclusion principle, by $\left\langle n_\uparrow^2 \right\rangle = \left\langle n_\downarrow^2 \right\rangle = \langle n_\uparrow \rangle = \langle n_\downarrow \rangle = n/2$, when the filling n is known. In a way, $\langle n_\uparrow n_\downarrow \rangle$ in the self-energy equation can be considered as an initial condition for the four point function when one of the points, 2, separates from all the others which are at 1. When that label 2 does not coincide with 1, it becomes more reasonable to factor *à la* Hartree-Fock. These physical ideas are implemented by postulating

$$\Sigma_\sigma^{(1)}\left(1,\overline{1}\right)_\phi \mathcal{G}_\sigma^{(1)}\left(\overline{1},2\right)_\phi = A_\phi \mathcal{G}_{-\sigma}^{(1)}\left(1,1^+\right)_\phi \mathcal{G}_\sigma^{(1)}\left(1,2\right)_\phi \tag{15.1a}$$

where A_ϕ depends on external field and is chosen such that the exact result [2]

$$\Sigma_\sigma\left(1,\overline{1}\right)_\phi \mathcal{G}_\sigma\left(\overline{1},1^+\right)_\phi = U\left\langle n_\uparrow\left(1\right) n_\downarrow\left(1\right)\right\rangle_\phi \tag{15.2}$$

is satisfied. It is easy to see that the solution is

$$A_\phi = U\frac{\left\langle n_\uparrow\left(1\right) n_\downarrow\left(1\right)\right\rangle_\phi}{\left\langle n_\uparrow\left(1\right)\right\rangle_\phi \left\langle n_\downarrow\left(1\right)\right\rangle_\phi}. \tag{15.3}$$

Substituting A_ϕ back into our *ansatz,* we obtain our first approximation for the self-energy by right-multiplying by $\left(\mathcal{G}_\sigma^{(1)}\right)^{-1}$:

$$\Sigma_\sigma^{(1)}\left(1,2\right)_\phi = A_\phi \mathcal{G}_{-\sigma}^{(1)}\left(1,1^+\right)_\phi \delta\left(1-2\right). \tag{15.4}$$

We are now ready to obtain irreducible vertices using the prescription of section 14.1, Eq.(14.27), namely through functional derivatives of Σ with respect to $\mathcal{G}$. In the calculation of U_{sp}, the functional derivative of $\langle n_\uparrow n_\downarrow \rangle / \left(\langle n_\uparrow \rangle \langle n_\downarrow \rangle\right)$ drops out, so we are left with [3],

$$\begin{aligned}\left.\frac{\delta\Sigma_\uparrow^{(1)}\left(1,2\right)_\phi}{\delta\mathcal{G}_\downarrow^{(1)}\left(3,4\right)_\phi}\right|_{\phi=0} - \left.\frac{\delta\Sigma_\uparrow^{(1)}\left(1,2\right)_\phi}{\delta\mathcal{G}_\uparrow^{(1)}\left(3,4\right)_\phi}\right|_{\phi=0} &= U_{sp}\delta\left(1-2\right)\delta\left(3-1\right)\delta\left(4-2\right) \\ U_{sp} &= A_{\phi=0} = U\frac{\langle n_\uparrow n_\downarrow \rangle}{\langle n_\uparrow \rangle \langle n_\downarrow \rangle}.\end{aligned} \tag{15.5}$$

The renormalization of this irreducible vertex may be physically understood as coming from the physics described by Kanamori and Brueckner [97] (in the latter case in the context of nuclear physics): The value of the bare interaction is renormalized down by the fact that the two-particle wave function will want to be smaller where U is larger. In the language of perturbation theory, one must sum the Born series to compute how two particles scatter off each other and not work in the first Born approximation. This completes the derivation of the *ansatz* that is central to TPSC.

The functional-derivative procedure generates an expression for the charge vertex U_{ch} which involves the functional derivative of $\langle n_\uparrow n_\downarrow \rangle / \left(\langle n_\uparrow \rangle \langle n_\downarrow \rangle\right)$ which contains six point functions that one does not really know how to evaluate. But, if we again assume that the vertex U_{ch} is a constant, it is simply determined by the requirement that charge fluctuations also satisfy the fluctuation-dissipation

[2] See footnote (14) of Ref. [4] for a discussion of the choice of limit 1^+ vs 1^-.

[3] For $n > 1$, all particle occupation numbers must be replaced by hole occupation numbers.

theorem and the Pauli exclusion principle, as in Eq.(14.39). In summary, spin and charge fluctuations are obtained from

$$\chi_{sp}(q) = \frac{\chi^{(1)}(q)}{1-\frac{1}{2}U_{sp}\chi^{(1)}(q)} \tag{15.6}$$

$$\chi_{ch}(q) = \frac{\chi^{(1)}(q)}{1+\frac{1}{2}U_{ch}\chi^{(1)}(q)}. \tag{15.7}$$

with the irreducible vertices determined from the sum rules

$$\frac{T}{N}\sum_{\mathbf{q}}\sum_{iq_n}\frac{\chi^{(1)}(q)}{1-\frac{1}{2}U_{sp}\chi^{(1)}(q)} = n - 2\langle n_\uparrow n_\downarrow\rangle \tag{15.8}$$

and

$$\frac{T}{N}\sum_{\mathbf{q}}\sum_{iq_n}\frac{\chi^{(1)}(q)}{1+\frac{1}{2}U_{ch}\chi^{(1)}(q)} = n + 2\langle n_\uparrow n_\downarrow\rangle - n^2. \tag{15.9}$$

along with the relations that relates U_{sp} to double occupancy, Eq.(15.5).

Remark 58 *Note that, in principle, $\Sigma^{(1)}$ also depends on double-occupancy, but since $\Sigma^{(1)}$ is a constant, it is absorbed in the definition of the chemical potential and we do not need to worry about it in this case. That is why the non-interacting irreducible susceptibility $\chi^{(1)}(q) = \chi_0(q)$ appears in the expressions for the susceptibility, even though it should be evaluated with $\mathcal{G}^{(1)}$ that contains $\Sigma^{(1)}$. A rough estimate of the renormalized chemical potential (or equivalently of $\Sigma^{(1)}$), is given in the appendix of Ref. ([4]). One can check that spin and charge conservation are satisfied by the TPSC susceptibilities.*

Remark 59 *$U_{sp}\langle n_\uparrow\rangle\langle n_\downarrow\rangle = U\langle n_\uparrow n_\downarrow\rangle$ can be understood as correcting the Hatree-Fock factorization so that the correct double occupancy be obtained. Expressing the irreducible vertex in terms of an equal-time correlation function is inspired by the approach of Singwi [82] to the electron gas. But TPSC is different since it also enforces the Pauli exclusion principle and connects to a local correlation function, namely $\langle n_\uparrow n_\downarrow\rangle$.*

15.2 TPSC Second step: an improved self-energy $\sum^{(2)}$

Collective charge and spin excitations can be obtained accurately from Green's functions that contain a simple self-energy, as we have just seen. Such modes are emergent objects that are less influenced by details of the single-particle properties than the other way around, especially at finite temperature where the lowest fermionic Matsubara frequency is not zero. The self-energy on the other hand is much more sensitive to collective modes since these are important at low frequency. The second step of TPSC is thus to find a better approximation for the self-energy. This is similar in spirit to what is done in the electron gas [48] where plasmons are found with non-interacting particles and then used to compute an improved approximation for the self-energy. This two step process is also analogous to renormalization group calculations where renormalized interactions are evaluated to one-loop order and quasiparticle renormalization appears only to two-loop order [58, 16, 99].

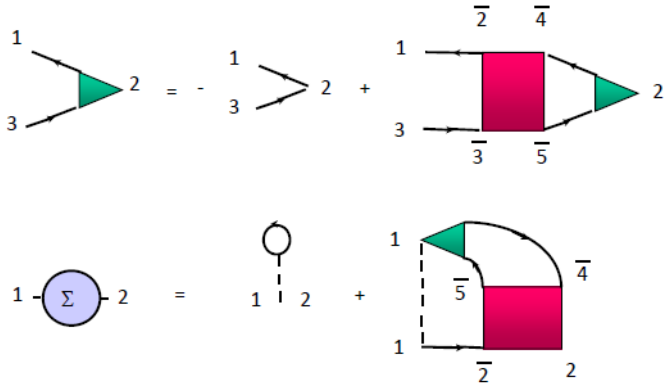

Figure 15-1 Exact expression for the three point vertex (green triangle) in the first line and for the self-energy in the second line. Irreducible vertices are the red boxes and Green's functions solid black lines. The numbers refer to spin, space and imaginary time coordinates. Symbols with an over-bard are summed/integrated over. The self-energy is the blue circle and the bare interaction U the dashed line.

The procedure will be the same as for the electron gas. But before we move to the algebra, we can understand physically the result by looking at Fig. 15-1 that shows the exact diagrammatic expressions for the three-point vertex (green triangle) and self-energy (blue circle) in terms of Green's functions (solid black lines) and irreducible vertices (red boxes). The bare interaction U is the dashed line. One should keep in mind that we are not using perturbation theory despite the fact that we draw diagrams. Even within an exact approach, the quantities defined in the figure have well defined meanings. The numbers on the figure refer to spin, space and imaginary time coordinates. When there is an over-bar, there is a sum over spin and spatial indices and an integral over imaginary time.

In TPSC, the irreducible vertices in the first line of Fig. 15-1 are local, i.e. completely momentum and frequency independent. They are given by U_{sp} and U_{ch}. If we set point 3 to be the same as point 1, then we can obtain directly the TPSC spin and charge susceptibilities from that first line. In the second line of the figure, the exact expression for the self-energy is displayed[4]. The first term on the right-hand side is the Hartree-Fock contribution. In the second term, one recognizes the bare interaction U at one vertex that excites a collective mode represented by the green triangle and the two Green's functions. The other vertex is dressed, as expected. In the electron gas, the collective mode would be the plasmon. If we replace the irreducible vertex using U_{sp} and U_{ch} found for the collective modes, we find that here, both types of modes, spin and charge, contribute to the self-energy [95].

Moving now to the algebra, let us repeat our procedure for the electron gas to show how to obtain an improved approximation for the self-energy that takes advantage of the fact that we have found accurate approximations for the low-frequency spin and charge fluctuations. We begin from the general definition of the self-energy obtained from Dyson-Schwinger's equation (10.29). The right-hand side of that equation can be obtained either from a functional derivative with respect to an external field that is diagonal in spin, as in our generating function Eq.(10.11), or by a functional derivative of $\left\langle \psi_{-\sigma}(1)\,\psi^{\dagger}_{\sigma}(2)\right\rangle_{\phi_t}$ with respect to a

[4] In the Hubbard model the Fock term cancels with the same-spin Hartree term

transverse external field ϕ_t, namely an external field that is not diagonal in spin indices.

Working first in the longitudinal channel, the right-hand side of the general definition of the self-energy Eq.(10.29) may be written as

$$\Sigma_\sigma\left(1,\overline{1}\right)\mathcal{G}_\sigma\left(\overline{1},2\right)=-U\left[\left.\frac{\delta\mathcal{G}_\sigma\left(1,2\right)_\phi}{\delta\phi_{-\sigma}\left(1^+,1\right)}\right|_{\phi=0}-\mathcal{G}_{-\sigma}\left(1,1^+\right)_\phi\mathcal{G}_\sigma\left(1,2\right)_\phi\right]. \quad (15.10)$$

The last term is the Hartree-Fock contribution. It gives the exact result for the self-energy in the limit $\omega\to\infty$.[97] The $\delta\mathcal{G}_\sigma/\delta\phi_{-\sigma}$ term is thus a contribution to lower frequencies and it comes from the spin and charge fluctuations. Right-multiplying the last equation by $\mathcal{G}^{-1}$ and replacing the lower energy part $\delta\mathcal{G}_\sigma/\delta\phi_{-\sigma}$ by its general expression in terms of irreducible vertices, Eq.(14.5) (recalling that for $\delta\mathcal{G}_\sigma/\delta\phi_{-\sigma}$ the first term vanishes) we find

$$\begin{aligned}\Sigma_\sigma^{(2)}\left(1,2\right) &= U\mathcal{G}_{-\sigma}^{(1)}\left(1,1^+\right)\delta\left(1-2\right) \quad (15.11)\\ &\quad -U\mathcal{G}_\sigma^{(1)}\left(1,\overline{3}\right)\left[\left.\frac{\delta\Sigma_\sigma^{(1)}\left(\overline{3},2\right)_\phi}{\delta\mathcal{G}_{\overline{\sigma}}^{(1)}\left(\overline{4},\overline{5}\right)_\phi}\right|_{\phi=0}\left.\frac{\delta\mathcal{G}_{\overline{\sigma}}^{(1)}\left(\overline{4},\overline{5}\right)_\phi}{\delta\phi_{-\sigma}\left(1^+,1\right)_\phi}\right|_{\phi=0}\right].\end{aligned}$$

Every quantity appearing on the right-hand side of that equation has to be taken from the TPSC results. This means in particular that the irreducible vertices $\delta\Sigma_\sigma^{(1)}/\delta\mathcal{G}_{\sigma'}^{(1)}$ are at the same level of approximation as the Green functions $\mathcal{G}_\sigma^{(1)}$ and self-energies $\Sigma_\sigma^{(1)}$. In other approaches one often sees renormalized Green functions $\mathcal{G}^{(2)}$ appearing on the right-hand side along with unrenormalized vertices, $\delta\Sigma_\sigma/\delta\mathcal{G}_{\sigma'}\to U$. We will see later in the context of electron-phonon interactions that this is equivalent to assuming, without justification, that the so-called Migdal's theorem applies to spin and charge fluctuations.

In terms of U_{sp} and U_{ch} in Fourier space, the above formula[95] reads,

$$\Sigma_\sigma^{(2)}(k)_{long}=Un_{-\sigma}+\frac{U}{4}\frac{T}{N}\sum_q\left[U_{sp}\chi_{sp}^{(1)}(q)+U_{ch}\chi_{ch}^{(1)}(q)\right]\mathcal{G}_\sigma^{(1)}(k+q). \quad (15.12)$$

This can be seen simply by noting in Eq.(15.11) that

$$\begin{aligned}\frac{\delta\Sigma_\sigma^{(1)}}{\delta\mathcal{G}_\sigma^{(1)}}\frac{\delta\mathcal{G}_\sigma^{(1)}}{\delta\phi_{-\sigma}} &= \frac{1}{2}\left(U_{ch}-U_{sp}\right)\frac{1}{4}\left(\chi_{ch}-\chi_{sp}\right) \quad (15.13)\\ \frac{\delta\Sigma_\sigma^{(1)}}{\delta\mathcal{G}_{-\sigma}^{(1)}}\frac{\delta\mathcal{G}_{-\sigma}^{(1)}}{\delta\phi_{-\sigma}} &= \frac{1}{2}\left(U_{ch}+U_{sp}\right)\frac{1}{4}\left(\chi_{ch}+\chi_{sp}\right). \quad (15.14)\end{aligned}$$

The approach to obtain a self-energy formula that takes into account both longitudinal and transverse fluctuations is detailed in Ref.([4]). Crossing symmetry, rotational symmetry and sum rules and comparisons with QMC dictate the final formula for the improved self-energy $\Sigma^{(2)}$ as we now sketch.

There is an ambiguity in obtaining the self-energy formula [65]. Within the assumption that only U_{sp} and U_{ch} enter as irreducible particle-hole vertices, the self-energy expression in the transverse spin fluctuation channel is different. What do we mean by that? Consider the exact formula for the self-energy represented symbolically by the diagram of Fig. 15-2. This is the so-called Schwinger-Dyson equation. It can be understood from the fact that $\Sigma\mathcal{G}$ is a four-point function, which means two Green's functions in, and two out that scatter in the middle. One of the Green's functions has disappeared because to obtain Σ, we need to

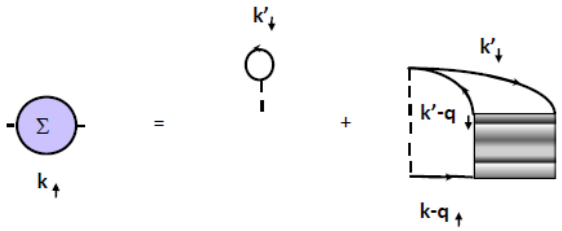

Figure 15-2 Exact self-energy in terms of the Hartree-Fock contribution and of the fully reducible vertex Γ represented by a textured box.

multiply by $\mathcal{G}^{-1}$. In the figure, the textured box is the fully reducible vertex $\Gamma\left(q, k-k', k+k'-q\right)$ that depends in general on three momentum-frequency indices. $\Gamma\left(q, k-k', k+k'-q\right)$ comes from the four-point function in the definition of the self-energy $\left.\frac{\delta \mathcal{G}_\sigma\left(1,\overline{2}\right)_\phi}{\delta \phi_{-\sigma}(1^+,1)}\right|_{\phi=0} \mathcal{G}_\sigma^{-1}\left(\overline{2},3\right)_\phi$ with two incoming Green's function and one outgoing one explicitly written down. The other outgoing Green's function is removed by $\mathcal{G}_\sigma^{-1}\left(\overline{2},3\right)_\phi$. The longitudinal version of the self-energy corresponds to expanding the fully reducible vertex $\Gamma\left(q, k-k', k+k'-q\right)$ in terms of diagrams that are irreducible in the longitudinal (parallel spins) channel illustrated in Fig. 15-1. This takes good care of the singularity of Γ when its first argument q is near (π, π). The transverse version [65, 4] does the same for the dependence on the second argument $k-k'$, which corresponds to the other (antiparallel spins) particle-hole channel. But the fully reducible vertex obeys crossing symmetry. In other words, interchanging two fermions just leads to a minus sign. One then expects that averaging the two possibilities gives a better approximation for Γ since it preserves crossing symmetry in the two particle-hole channels [65]. By considering both particle-hole channels only, we neglect the dependence of Γ on $k+k'-q$ because the particle-particle channel is not singular. The final formula that we obtain is [65]

$$\Sigma_\sigma^{(2)}(k) = U n_{-\sigma} + \frac{U}{8}\frac{T}{N}\sum_q \left[3U_{sp}\chi_{sp}(q) + U_{ch}\chi_{ch}(q)\right]\mathcal{G}_\sigma^{(1)}(k+q). \tag{15.15}$$

The superscript (2) reminds us that we are at the second level of approximation. $\mathcal{G}_\sigma^{(1)}$ is the same Green's function as that used to compute the susceptibilities $\chi^{(1)}(q)$. Since the self-energy is constant at that first level of approximation, this means that $\mathcal{G}_\sigma^{(1)}$ is the non-interacting Green's function with the chemical potential that gives the correct filling. That chemical potential $\mu^{(1)}$ is slightly different from the one that we must use in $\left(\mathcal{G}^{(2)}\right)^{-1} = iq_n + \mu^{(2)} - \varepsilon_{\mathbf{k}} - \Sigma^{(2)}$ to obtain the same density [38]. Estimates of $\mu^{(1)}$ may be found in Ref. [4, 38]. Further justifications for the above formula are given below in Sect. (15.3).

Remark 60 *Note that a spin fluctuation has $S = 1$, to that is why, physically, there is a factor of 3 in front of the spin fluctuations.*

15.3 TPSC, internal accuracy checks

How can we make sure that TPSC is accurate? We will show sample comparisons with benchmark Quantum Monte Carlo calculations, but we can check the accuracy in other ways. For example, we have already mentioned that the f-sum rule is exactly satisfied at the first level of approximation (i.e. with $n_{\mathbf{k}}^{(1)}$ on the right-hand side). Suppose that on the right-hand side of that equation, one uses $n_{\mathbf{k}}$ obtained from $\mathcal{G}^{(2)}$ instead of the Fermi function. One should find that the result does not change by more than a few percent. This is what happens when agreement with QMC is good.

When we are in the Fermi liquid regime, another way to verify the accuracy of the approach is to verify if the Fermi surface obtained from $\mathcal{G}^{(2)}$ satisfies Luttinger's theorem very closely. Luttinger's theorem says that even an interacting system, when there is a jump in $n_{\mathbf{k}}$ at the Fermi surface at $T = 0$ (as we have seen in the electron gas) then the particle density is determined by the number of $\mathbf{k}$ points inside the Fermi surface, as in the non-interacting case.

Finally, there is a consistency relation between one- and two-particle quantities (Σ and $\langle n_\uparrow n_\downarrow \rangle$). The relation

$$\Sigma_\sigma\left(1,\bar{1}\right)\mathcal{G}_\sigma\left(\bar{1},1^+\right) \equiv \frac{1}{2}\mathrm{Tr}\left(\Sigma\mathcal{G}\right) = \frac{T}{N}\sum_{\mathbf{k}}\sum_{n}\Sigma(\mathbf{k},iq_n)\mathcal{G}(\mathbf{k},iq_n)e^{-iq_n0^-} = U\left\langle n_\uparrow n_\downarrow\right\rangle \tag{15.16}$$

should be satisfied exactly for the Hubbard model. In standard many-body books [49], it is encountered in the calculation of the free energy through a coupling-constant integration. In TPSC, it is not difficult to show [5] that the following equation

$$\frac{1}{2}\mathrm{Tr}\left(\Sigma^{(2)}\mathcal{G}^{(1)}\right) = U\left\langle n_\uparrow n_\downarrow\right\rangle \tag{15.17}$$

is satisfied exactly with the self-consistent $U\langle n_\uparrow n_\downarrow\rangle$ obtained with the susceptibilities[6]. An internal accuracy check consists in verifying by how much $\frac{1}{2}\mathrm{Tr}\left(\Sigma^{(2)}\mathcal{G}^{(2)}\right)$ differs from $\frac{1}{2}\mathrm{Tr}\left(\Sigma^{(2)}\mathcal{G}^{(1)}\right)$. Again, in regimes where we have agreement with Quantum Monte Carlo calculations, the difference is only a few percent.

The above relation between Σ and $\langle n_\uparrow n_\downarrow\rangle$ gives us another way to justify our expression for $\Sigma^{(2)}$. Suppose one starts from Fig. 15-1 to obtain a self-energy expression that contains only the longitudinal spin fluctuations and the charge fluctuations, as was done in the first papers on TPSC [93]. One finds that each of these separately contributes an amount $U\langle n_\uparrow n_\downarrow\rangle/2$ to the consistency relation Eq.(15.17). Similarly, if we work only in the transverse spin channel [65, 4] we find that each of the two transverse spin components also contributes $U\langle n_\uparrow n_\downarrow\rangle/2$ to $\frac{1}{2}\mathrm{Tr}\left(\Sigma^{(2)}\mathcal{G}^{(1)}\right)$. Hence, averaging the two expressions also preserves rotational invariance. In addition, one verifies numerically that the exact sum rule (Ref. [97] Appendix A)

$$-\int\frac{d\omega'}{\pi}\Sigma''^R_\sigma\left(\mathbf{k},\omega'\right) = U^2 n_{-\sigma}\left(1-n_{-\sigma}\right) \tag{15.18}$$

determining the high-frequency behavior is satisfied to a higher degree of accuracy with the symmetrized self-energy expression Eq. (15.15).

Eq. (15.15) for $\Sigma^{(2)}$ is different from so-called Berk-Schrieffer type expressions [10] that do not satisfy [7] the consistency condition between one- and two-particle properties, $\frac{1}{2}\mathrm{Tr}\left(\Sigma\mathcal{G}\right) = U\left\langle n_\uparrow n_\downarrow\right\rangle$.

[5] Appendix B or Ref. [97]

[6] FLEX does not satisfy this consistency requirement. See Appendix E of [97]. In fact double-occupancy obtained from ΣG can even become negative [6].

[7] [97] Appendix E)

Remark 61 *Schemes, such as the fluctuation exchange approximation (FLEX), that we will discuss later, use on the right-hand side $G^{(2)}$, are thermodynamically consistent and might look better. However, as we just saw FLEX misses some important physics. The reason [97] is that the vertex entering the self-energy in FLEX is not at the same level of approximation as the Green's functions. Indeed, since the latter contain self-energies that are strongly momentum and frequency dependent, the irreducible vertices that can be derived from these self-energies should also be frequency and momentum dependent, but they are not. In fact they are the bare vertices. It is as if the quasi-particles had a lifetime while at the same time interacting with each other with the bare interaction. Using dressed Green's functions in the susceptibilities with momentum and frequency independent vertices leads to problems as well. For example, the conservation law $\chi_{sp,ch}(\mathbf{q}=\mathbf{0},iq_n) = 0$ is violated in that case, as shown in Appendix A of Ref.[97]. Further criticism of conserving approaches appears in Appendix E of Ref.[97] and in Ref.[4].*

15.4 Benchmarking

Quantum Monte Carlo calculations, that we explain in a later Chapter of this book, can be considered exact within statistical sampling. Hence they can be used as benchmarks for any approximation scheme. In this section, we present a few benchmarks on spin and charge fluctuations, and then on self-energy. More comparisons may be found in Refs. [88] and [93, 97, 95, 41] and others quoted in these papers.

15.4.1 Spin and charge fluctuations

The set of TPSC equations for spin and charge fluctuations Eqs.(**??**,**??**,**??**) is rather intuitive and simple. The agreement of calculations with benchmark QMC calculations is rather spectacular, as shown in Fig.(15-3). There, one can see the results of QMC calculations of the structure factors, i.e. the Fourier transform of the equal-time charge and spin correlation functions, compared with the corresponding TPSC results.

This figure allows one to watch the Pauli exclusion principle in action. At $U = 4t$, Fig.(15-3a) shows that the charge structure factor does not have a monotonic dependence on density. This is because, as we approach half-filling, the spin fluctuations are becoming so large that the charge fluctuations have to decrease so that the sum still satisfies the Pauli exclusion principle, as expressed by Eq.(14.41). This kind of agreement is found even at couplings of the order of the bandwidth and when second-neighbor hopping t' is present [90, 91].

Remark 62 *Even though the entry in the renormalized classical regime is well described by TPSC [40], equation (**??**) for U_{sp} fails deep in that regime because $\Sigma^{(1)}$ becomes too different from the true self-energy. At $n = 1$, $t' = 0$, deep in the renormalized classical regime, U_{sp} becomes arbitrarily small, which is clearly unphysical. However, by assuming that $\langle n_\uparrow n_\downarrow \rangle$ is temperature independent below T_X, a property that can be verified from QMC calculations, one obtains a qualitatively correct description of the renormalized-classical regime. One can even drop*

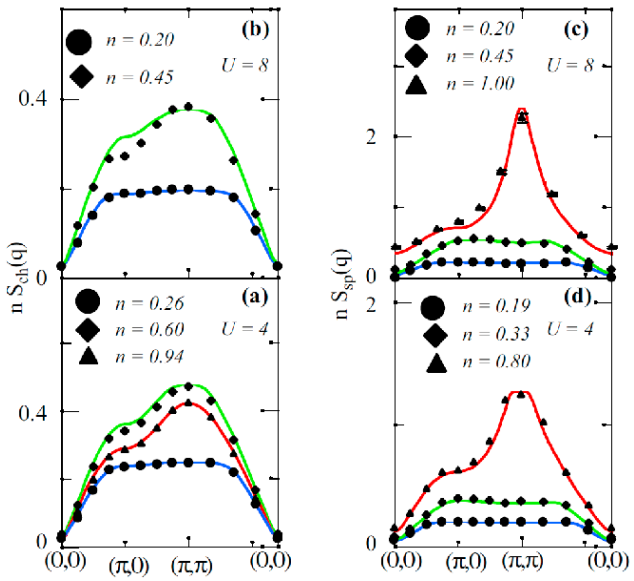

Figure 15-3 Wave vector $(\mathbf{q})$ dependence of the spin and charge structure factors for different sets of parameters. Solid lines are from TPSC and symbols are QMC data. Monte Carlo data for $n = 1$ and $U = 8t$ are for 6×6 clusters and $T = 0.5t$; all other data are for 8×8 clusters and $T = 0.2t$. Error bars are shown only when significant. From Ref. [93].

*the ansatz and take $\langle n_\uparrow n_\downarrow \rangle$ from QMC on the right-hand side of the local moment sum-rule Eq.(**??**) to obtain U_{sp}.*

15.4.2 Self-energy

We check that the formula for the self-energy Eq.(15.15) is accurate by comparing in Fig. 15-4 the spectral weight (imaginary part of the Green's function) obtained from Eq.(15.15) with that obtained from Quantum Monte Carlo calculations. The latter are exact within statistical accuracy and can be considered as benchmarks. The meaning of the curves are detailed in the caption. The comparison is for half-filling in a regime where the simulations can be done at very low temperature and where a non-trivial phenomenon, the pseudogap, appears. This all important phenomenon is discussed further below in subsection 16.1 and in the first case study, Sect. 16.2. In the third panel, we show the results of another popular Many-Body Approach, the FLuctuation Exchange Approximation (FLEX) [11]. It misses [22] the physics of the pseudogap in the single-particle spectral weight because it uses fully dressed Green's functions and assumes that Migdal's theorem applies, i.e. that the vertex does not need to be renormalized consequently Ref.[97, 61]. The same problem exists in the corresponding version of the GW approximation. [30]

Remark 63 *The dressing of one vertex in the second line of Fig. 15-1 means that we do not assume a Migdal theorem. Migdal's theorem arises in the case of electron-phonon interactions [49]. There, the small ratio m/M, where m is the electronic mass and M the ionic mass, allows one to show that the vertex*

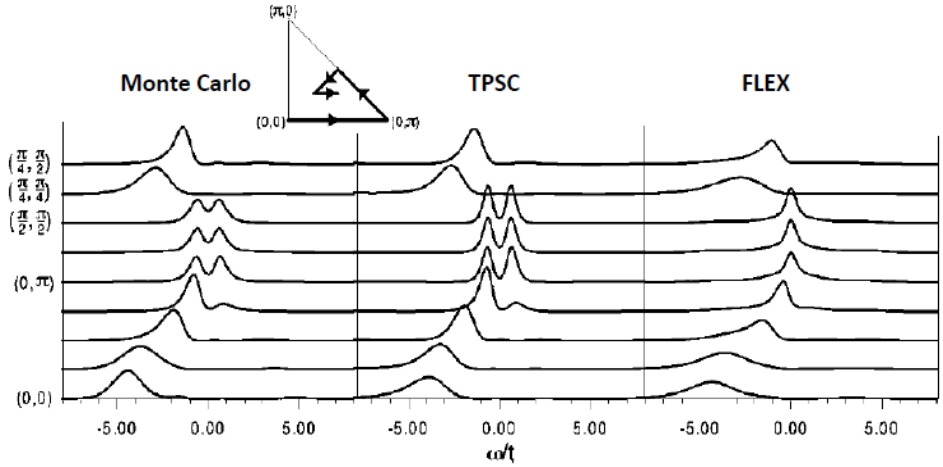

Figure 15-4 Single-particle spectral weight $A(\mathbf{k},\omega)$ for $U=4$, $\beta=5$, $n=1$, and all independent wave vectors $\mathbf{k}$ of an 8×8 lattice. Results obtained from maximum entropy inversion of Quantum Monte Carlo data on the left panel, from TPSC in the middle panel and form the FLEX approximation on the right panel. (Relative error in all cases is about 0.3%). Figure from Ref.[65]

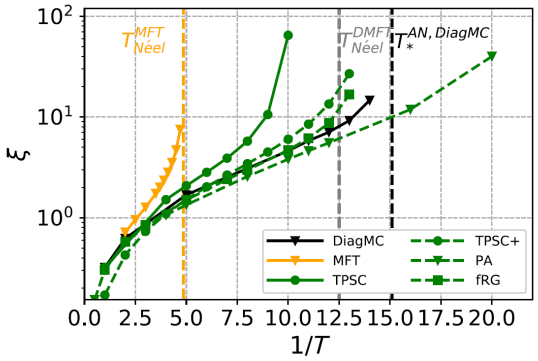

corrections are negligible. This is extremely useful to formulate the Eliashberg theory of superconductivity.

Remark 64 *In Refs. [97, 65] we used the notation $\Sigma^{(1)}$ instead of $\Sigma^{(2)}$. The notation of the present paper is the same as that of Ref. [4]*

15.4.3 TPSC+, Beyond TPSC

TPSC has been compared to a number of other state of the art methods in [75]. Fig. (15.4.3) for the Hubbard model at half-filling at $U=2t$ shows the correlation length as a function of temperature. The DiagMC result can be considered exact. This is one of the cases where TPSC is at its worse. It is expected that it does not work in the renormalized classical regime. An improvement of TPSC, namely TPSC+ [24] gives better results. The combination of TPSC with DMFT also gives some improvements [54] and, more importantly, it will allow TPSC to be

generalized to multi-band cases. It has already been applied to the three-band Emery model for the cuprates [25].

16. *ANTIFERROMAGNETISM CLOSE TO HALF-FILLING AND PSEUDOGAP IN TWO DIMENSIONS

We return to the normal state and look at the dominant instability in the half-filled case $n = 1$. In that case, the Fermi surface of the Hubbard model with nearest-neighbor hopping exhibits the phenomenon of nesting. For example, the Fermi surface in the two-dimensional case is a diamond, as illustrated in Fig. (?). All the points of the flat surfaces are connected by the same wave vector $\mathbf{Q} = (\pi, \pi)$ which leads to a very large susceptibility. Whereas at low filling the maximum susceptibility is at $q = 0$, in the present case it is a local maximum that is smaller than the maximum at $\mathbf{Q}$, as we will see.

Let us compute the spin susceptibility at that nesting wave vector. Nesting in the present case means that

$$\zeta_{\mathbf{p}+\mathbf{Q}} = -2t \left(\cos \left(k_x + \pi \right) + \cos \left(k_y + \pi \right) \right) = -\zeta_{\mathbf{p}}. \tag{16.1}$$

Using this result we find that the zero-frequency susceptibility at that wave vector $\mathbf{Q}$ is

$$\chi_0^R \left(\mathbf{Q}, 0 \right) = -\frac{2}{N} \sum_{\mathbf{p}} \frac{f\left(\zeta_{\mathbf{p}}\right) - f\left(\zeta_{\mathbf{p}+\mathbf{Q}}\right)}{\zeta_{\mathbf{p}} - \zeta_{\mathbf{p}+\mathbf{Q}}} = -\frac{2}{N} \sum_{\mathbf{p}} \frac{f\left(\zeta_{\mathbf{p}}\right) - f\left(-\zeta_{\mathbf{p}}\right)}{2\zeta_{\mathbf{p}}} \tag{16.2}$$

$$= \frac{1}{N} \sum_{\mathbf{p}} \frac{1 - 2f\left(\zeta_{\mathbf{p}}\right)}{\zeta_{\mathbf{p}}} = \int d\varepsilon N\left(\varepsilon\right) \frac{\tanh\left(\frac{\beta\varepsilon}{2}\right)}{\varepsilon}. \tag{16.3}$$

Assume that the density of states is a constant. For $\varepsilon \gg T$, we are integrating $1/\varepsilon$. However, for $\varepsilon < T$ the singularity in the denominator of the integrand is cutoff. In other words, we obtain a contribution that diverges at low temperature like $\ln\left(W/T\right)$ where W is the bandwidth. This means that at sufficiently low temperature, the criterion $1 - \frac{U}{2}\chi_0^R\left(\mathbf{Q}, 0\right) = 0$ will always be satisfied whatever the value of U and there will be a transition to a state characterized by the wave vector $\mathbf{Q}$. This is the antiferromagnetic state where spins alternate in direction from one site to the other. In two dimensions for example, the chemical potential at $n = 1$ sits right at a logarithmic van Hove singularity in $N\left(\varepsilon\right)$ so that in fact $\chi_0^R\left(\mathbf{Q}, 0\right)$ scales like $\ln^2\left(W/T\right)$, which is larger than the single power of ln that one would obtain at $q = 0$.

When there is no nesting, like when the next-nearest neighbor hopping t' contributes, the susceptibility does not diverge at low temperature. In that case, the transition will occur only if U is large enough.

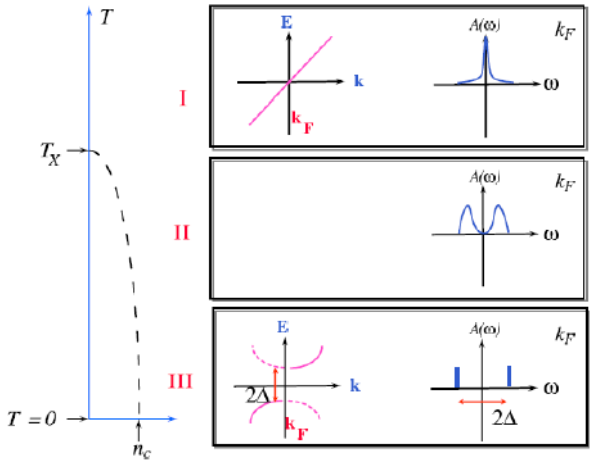

Figure 16-1 Cartoon explanation of the pseudogap due to precursors of long-range order. When the antiferromagnetic correlation length ξ becomes larger than the thermal de Broglie wavelength, there appears precursors of the $T = 0$ Bogoliubov quasi-particles for the long-range ordered antiferromagnet. This can occur only in the renormalized classical regime, below the dashed line on the left of the figure.

16.1 Pseudogap in the renormalized classical regime

When we compared TPSC with Quantum Monte Carlo simulations and with FLEX in Fig. 15-4 above, perhaps you noticed that at the Fermi surface, the frequency dependent spectral weight has two peaks instead of one. In addition, at zero frequency, it has a minimum instead of a maximum. That is called a pseudogap. A cartoon explanation [88] of this pseudogap is given in Fig. 16-1. At high temperature we start from a Fermi liquid, as illustrated in panel I. Now, suppose the ground state has long-range antiferromagnetic order as in panel III, in other words at a filling between half-filling and n_c. In the mean-field approximation we have a gap and the Bogoliubov transformation from fermion creation-annihilation operators to quasi-particles has weight at both positive and negative energies. In two dimensions, because of the Mermin-Wagner theorem, as soon as we raise the temperature above zero, long-range order disappears, but the antiferromagnetic correlation length ξ remains large so we obtain the pseudogap illustrated in panel II. As we will explain analytically below, the pseudogap survives as long as ξ is much larger than the thermal de Broglie wave length $\xi_{th} \equiv v_F/(\pi T)$ in our usual units. At the crossover temperature T_X, the relative size of ξ and ξ_{th} changes and we recover the Fermi liquid.

We now proceed to sketch analytically where these results come from starting from finite T. Details and more complete formulae may be found in Refs. [93, 95, 97, 94][1]. We begin from the TPSC expression (15.15) for the self-energy. Normally one has to do the sum over bosonic Matsubara frequencies first, but the zero Matsubara frequency contribution has the correct asymptotic behavior in fermionic frequencies iq_n so that, as in Sect.??, one can once more isolate on the right-hand side the contribution from the zero Matsubara frequency. In the

[1] Note also the following study from zero temperature [14]

renormalized classical regime then, we have [2]

$$\Sigma(\mathbf{k}_F, ik_n) \propto T \int q^{d-1} dq \frac{1}{q^2 + \xi^{-2}} \frac{1}{ik_n - \varepsilon_{\mathbf{k}_F+\mathbf{Q}+\mathbf{q}}} \tag{16.4}$$

where $\mathbf{Q}$ is the wave vector of the instability. This integral can be done analytically in two dimensions [97, 92]. But it is more useful to analyze limiting cases [95]. Expanding around the points known as hot spots where $\varepsilon_{\mathbf{k}_F+\mathbf{Q}} = 0$, we find after analytical continuation that the imaginary part of the retarded self-energy at zero frequency takes the form

$$\Sigma''^R(\mathbf{k}_F, 0) \propto -\pi T \int d^{d-1} q_\perp dq_{||} \frac{1}{q_\perp^2 + q_{||}^2 + \xi^{-2}} \delta(v'_F q_{||}) \tag{16.5}$$

$$\propto \frac{\pi T}{v'_F} \xi^{3-d}. \tag{16.6}$$

In the last line, we just used dimensional analysis to do the integral.

The importance of dimension comes out clearly [95]. In $d = 4$, $\Sigma''^R(\mathbf{k}_F, 0)$ vanishes as temperature decreases, $d = 3$ is the marginal dimension and in $d = 2$ we have that $\Sigma''^R(\mathbf{k}_F, 0) \propto \xi/\xi_{th}$ that diverges at zero temperature. In a Fermi liquid the quantity $\Sigma''^R(\mathbf{k}_F, 0)$ vanishes at zero temperature, hence in three or four dimensions one recovers the Fermi liquid (or close to one in $d = 3$). But in two dimensions, a diverging $\Sigma''^R(\mathbf{k}_F, 0)$ corresponds to a vanishingly small $A(\mathbf{k}_F, \omega = 0)$ as we can see from

$$A(\mathbf{k}, \omega) = \frac{-2\Sigma''^R(\mathbf{k}_F, \omega)}{(\omega - \varepsilon_{\mathbf{k}} - \Sigma'^R(\mathbf{k}_F, \omega))^2 + \Sigma''^R(\mathbf{k}_F, \omega)^2}. \tag{16.7}$$

Fig. 31 of Ref.[88] illustrates graphically the relationship between the location of the pseudogap and large scattering rates at the Fermi surface. At stronger U the scattering rate is large over a broader region, leading to a depletion of $A(\mathbf{k},\omega)$ over a broader range of $\mathbf{k}$ values.

Remark 65 *Note that the condition $\xi/\xi_{th} \gg 1$, necessary to obtain a large scattering rate, is in general harder to satisfy than the condition that corresponds to being in the renormalized classical regime. Indeed, $\xi/\xi_{th} \gg 1$ corresponds $T/v_F \gg \xi^{-1}$ while the condition $\omega_{sp} \ll T$ for the renormalized classical regime corresponds to $T \gg \xi^{-2}$, with appropriate scale factors, because ω_{sp} scales as ξ^{-2} as we saw in Eq. (??) and below.*

To understand the splitting into two peaks seen in Figs. 15-4 and 16-1 consider the singular renormalized contribution coming from the spin fluctuations in Eq. (16.4) at frequencies $\omega \gg v_F \xi^{-1}$. Taking into account that contributions to the integral come mostly from a region $q \leq \xi^{-1}$, one finds

$$\begin{aligned} \Sigma'^R(\mathbf{k}_F, \omega) &= \left(T \int q^{d-1} dq \frac{1}{q^2 + \xi^{-2}} \right) \frac{1}{ik_n - \varepsilon_{\mathbf{k}_F+\mathbf{Q}}} \\ &\equiv \frac{\Delta^2}{\omega - \varepsilon_{\mathbf{k}_F+\mathbf{Q}}} \end{aligned} \tag{16.8}$$

which, when substituted in the expression for the spectral weight (16.7) leads to large contributions when

$$\omega - \varepsilon_{\mathbf{k}} - \frac{\Delta^2}{\omega - \varepsilon_{\mathbf{k}_F+\mathbf{Q}}} = 0 \tag{16.9}$$

[2] This formula is similar to one that appeared in Ref.[43]

or, equivalently,

$$\omega = \frac{(\varepsilon_{\mathbf{k}} + \varepsilon_{\mathbf{k}_F+\mathbf{Q}}) \pm \sqrt{(\varepsilon_{\mathbf{k}} - \varepsilon_{\mathbf{k}_F+\mathbf{Q}})^2 + 4\Delta^2}}{2}, \tag{16.10}$$

which, at $\omega = 0$, corresponds to the position of the hot spots[3]. At finite frequencies, this turns into the dispersion relation for the antiferromagnet [76].

It is important to understand that analogous arguments hold for any fluctuation that becomes soft because of the Mermin-Wagner theorem,[97, 21] including superconducting ones [97, 3, 38]. The wave vector $\mathbf{Q}$ would be different in each case.

To understand better when Fermi liquid theory is valid and when it is replaced by the pseudogap instead, it is useful to perform the calculations that lead to $\Sigma''^R(\mathbf{k}_F, 0) \propto \xi/\xi_{th}$ in the real frequency formalism. The details may be found in Appendix D of Ref. [97].

16.2 Pseudogap in electron-doped cuprates

High-temperature superconductors are made of layers of CuO_2 planes. The rest of the structure is commonly considered as providing either electron or hole doping of these planes depending on chemistry. At half-filling, or zero-doping, the ground state is an antiferromagnet. As one dopes the planes, one reaches a doping, so-called optimal doping, where the superconducting transition temperature T_c is maximum. Let us start from optimal hole or electron doping and decrease doping towards half-filling. That is the underdoped regime. In that regime, one observes a curious phenomenon, the pseudogap. What this means is that as temperature decreases, physical quantities behave as if the density of states near the Fermi level was decreasing. Finding an explanation for this phenomenon has been one of the major challenges of the field [85, 67].

To make progress, we need a microscopic model for high-temperature superconductors. Band structure calculations [5, 70] reveal that a single band crosses the Fermi level. Hence, it is a common assumption that these materials can be modeled by the one-band Hubbard model. Whether this is an oversimplification is still a subject of controversy [71, 44, 72, 81, 47, 27]. Indeed, spectroscopic studies [18, 71] show that hole doping occurs on the oxygen atoms. The resulting hole behaves as a copper excitation because of Zhang-Rice [100] singlet formation. In addition, the phase diagram [79, 50, 2, 1, 29, 34] and many properties of the hole-doped cuprates can be described by the one-band Hubbard model. Typically, the band parameters that are used are: nearest-neighbor hopping $t = 350$ to 400 meV and next-nearest-neighbor hopping $t' = -0.15$ to $-0.3t$ depending on the compound [5, 70]. Third-nearest-neighbor hopping $t'' = -0.5t'$ is sometimes added to fit finer details of the band structure [70]. The hoppings beyond nearest-neighbor mean that particle-hole symmetry is lost even at the band structure level.

In electron-doped cuprates, the doping occurs on the copper, hence there is little doubt that the single-band Hubbard model is even a better starting point in this case. Band parameters [55] are similar to those of hole-doped cuprates. It is sometimes claimed that there is a pseudogap only in the hole-doped cuprates. The origin of the pseudogap is indeed probably different in the hole-doped cuprates.

[3] For comparisons with paramagnon theory see [74].

But even though the standard signature of a pseudogap is absent in nuclear magnetic resonance [101] (NMR) there is definitely a pseudogap in the electron-doped case as well [7], as can be seen in optical conductivity [68] and in Angle Resolved Photoemission Spectroscopy (ARPES) [8]. As we show in the rest of this section, in electron-doped cuprates strong evidence for the origin of the pseudogap is provided by detailed comparisons of TPSC with ARPES as well as by verification with neutron scattering [64] that the TPSC condition for a pseudogap, namely $\xi > \xi_{th}$, is satisfied. The latter length makes sense from weak to intermediate coupling when quasi-particles exist above the pseudogap temperature. In strong coupling, i.e. for values of U larger than that necessary for the Mott transition, there is evidence that there is another mechanism for the formation of a pseudogap. This is discussed at length in Refs. [80, 28] [4]. The recent discovery [83] that at sufficiently large U there is a first order transition in the paramagnetic state between two kinds of metals, one of which is highly anomalous, gives a sharper meaning to what is meant by strong-coupling pseudogap.

Let us come back to modeling of electron-doped cuprates. Evidence that these are less strongly coupled than their hole-doped counterparts comes from the fact that a) The value of the optical gap at half-filling, ~ 1.5 eV, is smaller than for hole doping, ~ 2.0 eV [86]. b) In a simple Thomas-Fermi picture, the screened interaction scales like $\partial\mu/\partial n$. Quantum cluster calculations [80] show that $\partial\mu/\partial n$ is smaller on the electron-doped side, hence U should be smaller. c) Mechanisms based on the exchange of antiferromagnetic calculations with U/t at weak to intermediate coupling [12, 41] predict that the superconducting T_c increases with U/t. Hence T_c should decrease with increasing pressure in the simplest model where pressure increases hopping t while leaving U essentially unchanged. The opposite behavior, expected at strong coupling where $J = 4t^2/U$ is relevant [34, 36], is observed in the hole-doped cuprates. d) Finally and most importantly, there is detailed agreement between TPSC calculations [39, 28, 88] and measurements such as ARPES [8, 56], optical conductivity [68] and neutron [64] scattering.

To illustrate the last point, consider Fig. 16-2 that compares TPSC calculations with experimental results for ARPES. Apart from a tail in the experimental results, the agreement is striking. [5]. In particular, if there was no interaction, the Fermi surface would be a line (red) on the momentum distribution curve (MDC). Instead, it seems to disappear at symmetrical points displaced from $(\pi/2, \pi/2)$. These points, so-called hot spots, are linked by the wave vector (π, π) to other points on the Fermi surface. This is where the antiferromagnetic gap would open first if there was long-range order. The pull back of the weight from $\omega = 0$ at the hot spots is close to the experimental value: 100 meV for the 15% doping shown, and 300 meV for 10% doping (not shown). More detailed ARPES spectra and comparisons with experiment are shown in Ref. [88]. The value of the temperature T^* at which the pseudogap appears [39] is also close to that observed in optical spectroscopy [68]. In addition, the size of the pseudogap is about ten times T^* in the calculation as well as in the experiments. For optical spectroscopy, vertex corrections (see Sect. **??**) have to be added to be more quantitative. Experimentally, the value of T^* is about twice the antiferromagnetic transition temperature up to $x = 0.13$. That can be obtained [39] by taking $t_z = 0.03t$ for hopping in the third direction. Recall that in strictly two dimensions, there is no long-range order. Antiferromagnetism appears on a much larger range of dopings for electron-doped than for hole-doped cuprates.

These TPSC calculations have predicted the value of the pseudogap temperature at $x = 0.13$ before it was observed experimentally [56] by a group unaware

[4] See also conclusion of Ref.[88].

[5] Such tails tend to disappear in more recent laser ARPES measurements on hole-doped compounds [35].

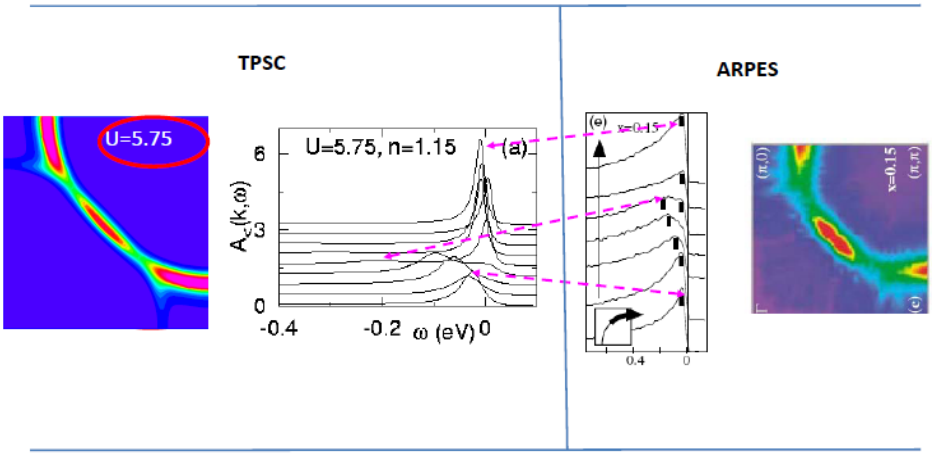

Figure 16-2 On the left, results of TPSC calculations [39, 88] at optimal doping, $x = 0.15$, corresponding to filling 1.15, for $t = 350$ meV, $t' = -0.175t$, $t_J = 0.05t$, $U = 5.75t$, $T = 1/20$. The left-most panel is the magnitude of the spectral weight times a Fermi function, $A(\mathbf{k},\omega) f(\omega)$ at $\omega = 0$, so-called momentum-distribution curve (MDC). Red (dark black) indicates larger value and purple (light grey) smaller value. The next panel is $A(\mathbf{k},\omega) f(\omega)$ for a set of fixed $\mathbf{k}$ values along the Fermi surface. These are so-called energy-dispersion curves (EDC). The two panels to the right are the corresponding experimental results [8] for $Nd_{2-x}Ce_xCuO_4$. Dotted arrows show the correspondence between TPSC and experiment.

of the theoretical prediction in Fig.16.2. In addition, the prediction that ξ should scale like ξ_{th} at the pseudogap temperature has been verified in neutron scattering experiments [64] in the range $x = 0.04$ to $x = 0.15$. The range of temperatures and doping explored in that work is shown in Fig. 16.2. Note that the antiferromagnetic phase boundary, that occurs here because of coupling in the third dimension, is at a location different from earlier estimates that appear in Fig. 16.2. However, the location of the pseudogp temperature has not changed. At the doping that corresponds to optimal doping, T^* becomes of the order of 100 K, more than four times lower than at $x = 0.04$. The antiferromagnetic correlation length ξ beyond optimal doping begins to decrease and violate the scaling of ξ with ξ_{th}. In that doping range, T^* and the superconducting transition temperature are close. Hence it is likely that there is interference between the two phenomena [17], an effect that has not yet been taken into account in TPSC.

An important prediction that one should verify is that inelastic neutron scattering will find over-damped spin fluctuations in the pseudogap regime and that the characteristic spin fluctuation energy will be smaller than k_BT whenever a pseudogap is present. Equality should occur above T^*.

Finally, note that the agreement found in Fig. 16-2 between ARPES and TPSC is for $U \sim 6t$. At smaller values of U the antiferromagnetic correlations are not strong enough to produce a pseudogap in that temperature range. For larger U, the weight near $(\pi/2, \pi/2)$ disappears, in disagreement with experiments. The same value of U is found for the same reasons in strong coupling calculations with Cluster Perturbation Theory (CPT) [80] and with slave boson methods [98]. Recent first principle calculations [96] find essentially the same value of U. In that approach, the value of U is fixed, whereas in TPSC it was necessary to increase U by about 10% moving towards half-filling to get the best agreement with experiment. In any case, it is quite satisfying that weak and strong coupling

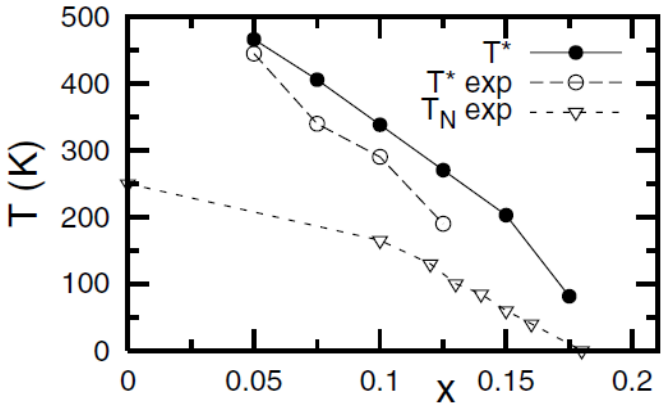
500
400
300
200
100
0
T (K)
0
0.05
0.1
0.15
0.2
x
T*
T* exp
T_N exp

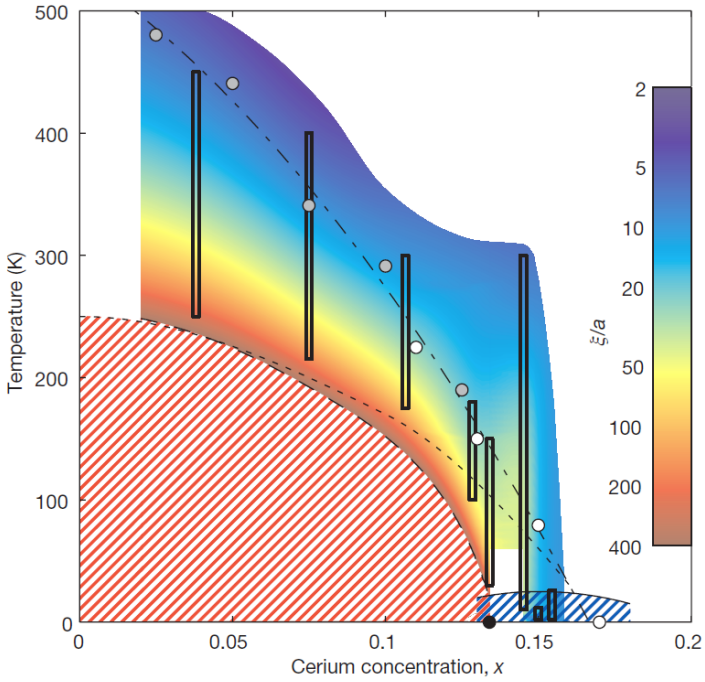
500
400
300
200
100
0
Temperature (K)
0
0.05
0.1
0.15
0.2
Cerium concentration, x
2
5
10
20
50
100
200
400
ξ/a

methods agree on the value of U for electron-doped cuprates. This value of U is very near the critical value for the Mott transition at half-filling [69]. Hence, antiferromagnetic fluctuations at finite doping can be very well described by Slater-like physics (nesting) in electron-doped cuprates.

For recent calculations including the effect of the third dimension on the pseudogap see [78]. Finally, note that the analog of the above mechanism for the pseudogap has also been seen in two-dimensional charge-density wave dichalcogenides [15].

17. DEFINITIONS

1. Dirac's delta $\delta(\omega)$ and Heaviside's theta

$$\theta(\omega) = \begin{cases} 1 \text{ if } \omega > 0 \\ \frac{1}{2} \text{ if } \omega = 0 \\ 0 \text{ if } \omega < 0 \end{cases} \tag{17.1}$$

2. Grand-canonical average

$$\frac{\sum_i e^{-\beta(E_i-\mu N_i)} \langle i| \mathcal{O} |i\rangle}{\sum_i e^{-\beta(E_i-\mu N_i)}} = \frac{\sum_i \langle i| e^{-\beta(H-\mu N)} \mathcal{O} |i\rangle}{\sum_i e^{-\beta(E_i-\mu N_i)}} = \frac{Tr\left[e^{-\beta(H-\mu N)}\mathcal{O}\right]}{Tr\left[e^{-\beta(H-\mu N)}\right]} = \langle \mathcal{O} \rangle \tag{17.2}$$

3. We often define the density matrix by

$$\widehat{\varrho} = e^{-\beta H} / \mathrm{Tr}\left[e^{-\beta H}\right]. \tag{17.3}$$

Then, we can write

$$\langle A_s(t) A_s \rangle = \mathrm{Tr}\left[\widehat{\varrho} A_s(t) A_s\right] \tag{17.4}$$

4. Conductivity sum rule

$$\int_{-\infty}^{\infty} \frac{d\omega}{2\pi} \mathrm{Re}\left[\sigma_{xx}(q_x,\omega)\right] = \frac{ne^2}{2m} = \frac{\omega_p^2}{8\pi} \tag{17.5}$$

5. Dielectric constants

$$\overleftrightarrow{\epsilon^T}(\mathbf{q},\omega) = \left(1 - \frac{\omega_p^2}{(\omega+i\eta)^2}\right) \overleftrightarrow{I} + \frac{4\pi}{(\omega+i\eta)^2} \left(\overleftrightarrow{\chi^R_{\mathbf{jj}}}(\mathbf{q},\omega)\right)^T. \tag{17.6}$$

$$\frac{1}{\epsilon^L(\mathbf{q},\omega)} = 1 - \frac{4\pi}{q^2} \chi^R_{\rho\rho}(\mathbf{q},\omega). \tag{17.7}$$

6. Equalities.

$$\approx \text{ Asymptotically equal to} \tag{17.8}$$

$$\sim \text{ Scales as} \tag{17.9}$$

$$\equiv \text{ Is equal by definition} \tag{17.10}$$

$$\simeq \text{ Is approximately equal to} \tag{17.11}$$

7. f sum rule

$$\int_{-\infty}^{\infty} \frac{d\omega}{\pi} \omega \chi"_{nn}(\mathbf{k},\omega) = \frac{n\mathbf{k}^2}{m}. \tag{17.12}$$

8. Fluctuation-dissipation theorem

$$S_{A_iA_j}(\omega) = \frac{2\hbar}{1 - e^{-\beta\hbar\omega}} \chi"_{A_iA_j}(\omega) \tag{17.13}$$

9. Fourier transforms

$$f_{\mathbf{k}} = \int d^3r\ f(\mathbf{r})\mathbf{e}^{-i\mathbf{k}\cdot\mathbf{r}}$$

$$f(\mathbf{r}) = \int \frac{d^3k}{(2\pi)^3} f_{\mathbf{k}}\mathbf{e}^{i\mathbf{k}\cdot\mathbf{r}}$$

$$g_\omega = \int dt\ g(t)e^{i\omega t}$$

$$g(t) = \int \frac{d\omega}{2\pi} g_\omega e^{-i\omega t}$$

(note the difference in sign in the exponent for space and time Fourier transforms.)

Convolution theorem:

$$\int dt e^{i\omega t}\left[\int dt' a(t')b(t-t')\right] \equiv a_\omega b_\omega$$

Parseval's theorem is obtained by taking $\int \frac{d\omega}{2\pi}$ on both sides of the previous equality

$$\int dt' a(t')b(-t') \equiv \int \frac{d\omega}{2\pi} a_\omega b_\omega$$

The above two theorems may also be written in a reciprocal manner

$$\int \frac{d\omega}{2\pi} e^{-i\omega t}\left[\int \frac{d\omega'}{2\pi} a_{\omega'} b_{\omega-\omega'}\right] = a(t)b(t)$$

$$\int \frac{d\omega'}{2\pi} a_{\omega'} b_{-\omega'} = \int dt e^{i\omega t} a(t)b(t)$$

For a translationally invariant system, note that with $\mathcal{V}$ the volume,

$$\int d\left(\mathbf{r}-\mathbf{r}'\right) e^{-i\mathbf{q}\cdot\left(\mathbf{r}-\mathbf{r}'\right)} f(\mathbf{r}-\mathbf{r}') = \frac{1}{\mathcal{V}}\int d\mathbf{r} e^{-i\mathbf{q}\cdot r}\int d\mathbf{r}' e^{-i\mathbf{q}\cdot r'} f(\mathbf{r}-\mathbf{r}') \tag{17.14}$$

10. Heisenberg representation

$$\mathcal{O}(t) = e^{iHt/\hbar}\mathcal{O}e^{-iHt/\hbar}$$

11. Interaction representation

$$\begin{aligned} \mathcal{O}_I(t) &= e^{iH_0t/\hbar}\mathcal{O}_S e^{-iH_0t/\hbar} \\ i\hbar\frac{\partial}{\partial t}U_I(t,t_0) &= \mathcal{H}_I(t)U_I(t,t_0) \\ U_I(t,0) &= T_c e^{-i\int_0^t \mathcal{H}_I(t')dt'} \end{aligned} \tag{17.15}$$

$$U_I(t_0,t_0) = 1$$

1. Kramers-Krönig relations

$$\mathrm{Re}\left[\chi^R_{A_iA_j}(\omega)\right] = \mathcal{P}\int \frac{d\omega'}{\pi}\frac{\mathrm{Im}\left[\chi^R_{A_iA_j}(\omega')\right]}{\omega'-\omega}$$

$$\mathrm{Im}\left[\chi^R_{A_iA_j}(\omega)\right] = -\mathcal{P}\int \frac{d\omega'}{\pi}\frac{\mathrm{Re}\left[\chi^R_{A_iA_j}(\omega')\right]}{\omega'-\omega}.$$

2. Kubo formula for longitudinal conductivity

$$\sigma_{xx}(q_x,\omega)=\frac{1}{i(\omega+i\eta)}\left[\chi^R_{j_xj_x}(q_x,\omega)-\frac{ne^2}{m}\right]=\left[\frac{1}{iq_x}\chi^R_{j_\mu\rho}(q_x,\omega)\right]. \quad (17.16)$$

for transverse conductivity

$$\sigma_{yy}(q_x,\omega)=\frac{1}{i(\omega+i\eta)}\left[\chi^R_{j_yj_y}(q_x,\omega)-\frac{ne^2}{m}\right]. \quad (17.17)$$

3. Mathematical identities (Sokhatsky-Weierstrass formula)

$$\lim_{\eta\to0}\frac{1}{\omega+i\eta}=\lim_{\eta\to0}\frac{\omega-i\eta}{\omega^2+\eta^2}=\lim_{\eta\to0}\left[\frac{\omega}{\omega^2+\eta^2}-\frac{i\eta}{\omega^2+\eta^2}\right]=\mathcal{P}\frac{1}{\omega}-i\pi\delta(\omega)$$

$$\lim_{\eta\to0}\frac{1}{\omega-i\eta}=\lim_{\eta\to0}\frac{\omega+i\eta}{\omega^2+\eta^2}=\lim_{\eta\to0}\left[\frac{\omega}{\omega^2+\eta^2}+\frac{i\eta}{\omega^2+\eta^2}\right]=\mathcal{P}\frac{1}{\omega}+i\pi\delta(\omega)$$

4. Normalization:

Continuum normalization for plane waves:

$$\langle\mathbf{R}\,|\mathbf{k}_i\rangle=\frac{1}{\Omega^{1/2}}e^{i\mathbf{k}_i\cdot\mathbf{R}} \quad (17.18)$$

$$\int\frac{d\mathbf{k}}{(2\pi)^3}=\frac{1}{\mathcal{V}}\sum_{\mathbf{k}}\quad;\quad\mathcal{V}=L_xL_yL_z\quad;\quad k_x=\frac{\pi n_x}{L_x}...\quad;\quad n_x=-\frac{L_x}{a}+1,...,-1,0,1,...,\frac{L_x}{a} \quad (17.19)$$

This is another consistent normalization

$$\int d\mathbf{r}\,|\mathbf{r}\rangle\langle\mathbf{r}|=1 \quad (17.20)$$

$$\langle\mathbf{r}\,|\mathbf{r}'\rangle=\delta(\mathbf{r}-\mathbf{r}') \quad (17.21)$$

$$\langle\mathbf{r}\,|\mathbf{k}\rangle=e^{i\mathbf{k}\cdot\mathbf{r}} \quad (17.22)$$

$$\int\frac{d\mathbf{k}}{(2\pi)^3}\,|\mathbf{k}\rangle\langle\mathbf{k}|=1 \quad (17.23)$$

$$\langle\mathbf{k}\,|\mathbf{k}'\rangle=(2\pi)^3\delta\left(\mathbf{k}-\mathbf{k}'\right) \quad (17.24)$$

1. Plasma frequency

$$\omega_p^2=\frac{4\pi ne^2}{m} \quad (17.25)$$

2. Response function (Susceptibility)

$$\chi^R_{AB}(\mathbf{r},\mathbf{r}';t,t')=\frac{i}{\hbar}\langle[A(\mathbf{r},t),B(\mathbf{r}',t')]\rangle\,\theta(t-t')$$

or in short hand,

$$\chi"_{A_iA_j}(t-t')=\frac{1}{2\hbar}\langle[A_i(t),A_j(t')]\rangle.$$

$$\chi^R_{A_iA_j}(t-t')=2i\chi"_{A_iA_j}(t-t')\theta(t-t').$$

For operators with the same signature under time reversal,

$$\mathrm{Im}\left[\chi^R_{A_iA_j}(\omega)\right] = \chi"_{A_iA_j}(\omega)$$

while two operators A_i, A_j with opposite signatures under time reversal

$$\mathrm{Re}\left[\chi^R_{A_iA_j}(\omega)\right] = \chi"_{A_iA_j}(\omega).$$

Spectral representation

$$\chi_{A_iA_j}(z) = \int \frac{d\omega'}{\pi} \frac{\chi"_{A_iA_j}(\omega')}{\omega' - z} \tag{17.26}$$

3. Minimal coupling to the electromagnetic field. N.B. e is the charge of the particle. It can be positive or negative

$$\mathbf{p}_\alpha = \frac{\hbar}{i}\nabla_\alpha \to \frac{\hbar}{i}\nabla_\alpha - e\mathbf{A}(\mathbf{r}_\alpha, t) \tag{17.27}$$

$$i\hbar\frac{\partial}{\partial t} \to i\hbar\frac{\partial}{\partial t} - e\phi(\mathbf{r}_\alpha, t). \tag{17.28}$$

4. Tensors. Multiplication by a vector

$$\left(\overleftrightarrow{\sigma^T} \cdot \mathbf{A}\right)_\mu = \sum_\nu \sigma^T_{\mu\nu} A_\nu. \tag{17.29}$$

Unit vector

$$\widehat{\mathbf{q}} = \mathbf{q}/\left|\mathbf{q}\right|$$

Transverse part

$$\overleftrightarrow{\sigma^T}(\mathbf{q},\omega) = \left(\overleftrightarrow{\mathbf{I}} - \widehat{\mathbf{q}}\widehat{\mathbf{q}}\right) \cdot \overleftrightarrow{\sigma}(\mathbf{q},\omega) \cdot \left(\overleftrightarrow{\mathbf{I}} - \widehat{\mathbf{q}}\widehat{\mathbf{q}}\right) \tag{17.30}$$

Dyadic product represention of a matrix

$$(\widehat{\mathbf{q}}\widehat{\mathbf{q}})_{ab} = \widehat{q}_a \widehat{q}_b \tag{17.31}$$

Longitudinal part

$$\overleftrightarrow{\sigma^L}(\mathbf{q},\omega) = \widehat{\mathbf{q}}\widehat{\mathbf{q}} \cdot \overleftrightarrow{\sigma}(\mathbf{q},\omega) \cdot \widehat{\mathbf{q}}\widehat{\mathbf{q}} \tag{17.32}$$

5. Thermal average (see canonical average)

6. Theta function (Heaviside function)

$$\theta(t) = \frac{1 \text{ if } t > 0}{0 \text{ if } t < 0} \tag{17.33}$$

7. Kronecker delta function

$$\delta_{k,0} = \frac{1 \text{ if } k = 0}{0 \text{ otherwise}} \tag{17.34}$$

8. Electromagnetic constants: $\varepsilon_0 = 8.85\times10^{-12}$ farad/meter is the permittivity of vacuum and $\mu_0 = 4\pi \times 10^{-7}$ henry/meter its permeability.

$$\varepsilon_0\mu_0 = \frac{1}{c^2}.$$

BIBLIOGRAPHY

[1] M. Aichhorn, E. Arrigoni, Z. B. Huang, and W. Hanke. Superconducting gap in the hubbard model and the two-gap energy scales of high-t_c cuprate superconductors. *Phys. Rev. Lett.*, 99(25):257002, Dec 2007.

[2] M. Aichhorn, E. Arrigoni, M. Potthoff, and W. Hanke. Variational cluster approach to the hubbard model: Phase-separation tendency and finite-size effects. *Phys. Rev. B*, 74(23):235117, Dec 2006.

[3] S. Allen and A.-M. S. Tremblay. Nonperturbative approach to the attractive hubbard model. *Phys. Rev. B*, 64:075115 – 1, 2001.

[4] S. Allen, A.-M. S. Tremblay, and Y. M. Vilk. Conserving approximations vs two-particle self-consistent approach. In D. Sénéchal, C. Bourbonnais, and A.-M. S. Tremblay, editors, *Theoretical Methods for Strongly Correlated Electrons*, 2003.

[5] O. K. Andersen, A. I. Liechtenstein, O. Jepsen, and F. Paulsen. Lda energy bands, low-energy hamiltonians t', t'', $t_\perp(\mathbf{k})$ and $j_\perp$. *Journal of the Physics and Chemistry of Solids*, 56:1573, 1995.

[6] Ryotaro Arita, Shigeki Onoda, Kazuhiko Kuroki, and Hideo Aoki. Magnetic properties of the hubbard model
on three-dimensional lattices:
fluctuation-exchange and two-particle self-consistent studies. *Journal of the Physical Society of Japan*, 69(3):785–795, 2000.

[7] N. P. Armitage, P. Fournier, and R. L. Greene. Progress and perspectives on electron-doped cuprates. *Rev. Mod. Phys.*, 82(3):2421–2487, Sep 2010.

[8] N. P. Armitage, F. Ronning, D. H. Lu, C. Kim, A. Damascelli, K. M. Shen, D. L. Feng, H. Eisaki, Z.-X. Shen, P. K. Mang, N. Kaneko, M. Greven, Y. Onose, Y. Taguchi, and Y. Tokura. Doping dependence of an n-type cuprate superconductor investigated by angle-resolved photoemission spectroscopy. *Phys. Rev. Lett.*, 88(25):257001, Jun 2002.

[9] Gordon Baym. Self-consistent approximations in many-body systems. *Phys. Rev.*, 127:1391–1401, Aug 1962.

[10] N. F. Berk and J. R. Schrieffer. Effect of ferromagnetic spin correlations on superconductivity. *Phys. Rev. Lett.*, 17(8):433–435, Aug 1966.

[11] N. E. Bickers and D. J. Scalapino. Conserving approximations for strongly fluctuating electron systems. i. formalism and calculational approach. *Ann. Phys. (USA)*, 193(1):206 – 51, 1989.

[12] N. E. Bickers, D. J. Scalapino, and S. R. White. Conserving approximations for strongly correlated electron systems: Bethe-salpeter equation and dynamics for the two-dimensional hubbard model. *Phys. Rev. Lett.*, 62:961, 1989.

[13] N. E. Bickers and S. R. White. Conserving approximations for strongly fluctuating electron systems. ii. numerical results and parquet extension. *Phys. Rev. B*, 43(10):8044–8064, Apr 1991.

[14] K. Borejsza and N. Dupuis. Antiferromagnetism and single-particle properties in the two-dimensional half-filled hubbard model: A nonlinear sigma model approach. *Phys. Rev. B*, 69(8):085119, Feb 2004.

[15] S. V. Borisenko, A. A. Kordyuk, A. N. Yaresko, V. B. Zabolotnyy, D. S. Inosov, R. Schuster, B. Büchner, R. Weber, R. Follath, L. Patthey, and H. Berger. Pseudogap and charge density waves in two dimensions. *Phys. Rev. Lett.*, 100(19):196402, May 2008.

[16] C. Bourbonnais. The dimensionality crossover in quasi-1d conductors. *Mol. Crys. Liq. Crys.*, 119:11, 1985.

[17] C. Bourbonnais and A. Sedeki. Link between antiferromagnetism and superconductivity probed by nuclear spin relaxation in organic conductors. *Phys. Rev. B*, 80(8):085105, Aug 2009.

[18] C. T. Chen, F. Sette, Y. Ma, M. S. Hybertsen, E. B. Stechel, W. M. C. Foulkes, M. Schulter, S-W. Cheong, A. S. Cooper, L. W. Rupp, B. Batlogg, Y. L. Soo, Z. H. Ming, A. Krol, and Y. H. Kao. Electronic states in $la_{2-x}sr_xcuo_{4+\delta}$ probed by soft-x-ray absorption. *Phys. Rev. Lett.*, 66(1):104–107, Jan 1991.

[19] A. Damascelli, D. H. Lu, K. M. Shen, N. P. Armitage, F. Ronning, D. L. Feng, C. Kim, Z.-X. Shen, T. Kimura, Y. Tokura, Z. Q. Mao, and Y. Maeno. Fermi surface, surface states, and surface reconstruction in sr_2ruo_4. *Phys. Rev. Lett.*, 85:5194–5197, Dec 2000.

[20] A.-M. Daré, L. Raymond, G. Albinet, and A.-M. S. Tremblay. Interaction-induced adiabatic cooling for antiferromagnetism in optical lattices. *Phys. Rev. B*, 76(6):064402, Aug 2007.

[21] B. Davoudi, S. R. Hassan, and A.-M. S. Tremblay. Competition between charge and spin order in the $t - u - v$ extended hubbard model on the triangular lattice. *Phys. Rev. B*, 77(21):214408, Jun 2008.

[22] J. J. Deisz, D. W. Hess, and J. W. Serene. Incipient antiferromagnetism and low-energy excitations in the half-filled two-dimensional hubbard model. *Phys. Rev. Lett.*, 76(8):1312–1315, Feb 1996.

[23] I. Dzyaloshinskii. *Sov. Phys. JETP*, 66:848, 1987.

[24] C. Gauvin-Ndiaye, C. Lahaie, Y. M. Vilk, and A.-M. S. Tremblay. Improved two-particle self-consistent approach for the single-band hubbard model in two dimensions. *Physical Review B*, 108(7):075144, August 2023.

[25] C. Gauvin-Ndiaye, J. Leblanc, S. Marin, N. Martin, D. Lessnich, and A.-M. S. Tremblay. Two-particle self-consistent approach for multiorbital models: Application to the emery model. *Physical Review B*, 109(16):165111, April 2024.

[26] A. Georges, G. Kotliar, W. Krauth, and M. J. Rozenberg. Dynamical mean-field theory of strongly correlated fermion systems and the limit of infinite dimensions. *Rev. Mod. Phys.*, 68:13 – 25, 1996.

[27] W. Hanke, M.L. Kiesel, M. Aichhorn, S. Brehm, and E. Arrigoni. The 3-band hubbard-model <i>versus</i> the 1-band model for the high-t_c cuprates: Pairing dynamics, superconductivity and the ground-state phase diagram. *The European Physical Journal - Special Topics*, 188:15–32, 2010. 10.1140/epjst/e2010-01294-y.

[28] V. Hankevych, B. Kyung, A.-M. Daré, D. Sénéchal, and A.-M. S. Tremblay. Strong- and weak-coupling mechanisms for pseudogap in electron-doped cuprates. *Journal of Physics and Chemistry of Solids*, 67(1Ãćâ Ćňâ ĂIJ3):189 – 192, 2006. Spectroscopies in Novel Superconductors 2004.

[29] Kristjan Haule and Gabriel Kotliar. Strongly correlated superconductivity: A plaquette dynamical mean-field theory study. *Physical Review B (Condensed Matter and Materials Physics)*, 76(10):104509, 2007.

[30] Lars Hedin. On correlation effects in electron spectroscopies and the gw approximation. *Journal of Physics: Condensed Matter*, 11(42):R489, 1999.

[31] P. C. Hohenberg. Existence of long-range order in one and two dimensions. *Phys. Rev.*, 158(2):383–386, Jun 1967.

[32] C. Honerkamp and M. Salmhofer. Magnetic and superconducting instabilities of the hubbard model at the van hove filling. *Phys. Rev. Lett.*, 87:187004, 2001.

[33] V. Janis. Green functions in the renormalized many-body perturbation theory for correlated and disordered electrons. *Condensed Matter Physics*, 9:499–518, 2006.

[34] S. S. Kancharla, B. Kyung, D. Senechal, M. Civelli, M. Capone, G. Kotliar, and A.-M. S. Tremblay. Anomalous superconductivity and its competition with antiferromagnetism in doped mott insulators. *Phys. Rev. B*, 77(18):184516, 2008.

[35] J. D. Koralek, J. F. Douglas, N. C. Plumb, Z. Sun, A. V. Fedorov, M. M. Murnane, H. C. Kapteyn, S. T. Cundiff, Y. Aiura, K. Oka, H. Eisaki, and D. S. Dessau. Laser based angle-resolved photoemission, the sudden approximation, and quasiparticle-like spectral peaks in $bi_2sr_2cacu_2o_{8+\delta}$. *Phys. Rev. Lett.*, 96(1):017005, Jan 2006.

[36] G. Kotliar and J. Liu. Superconducting instabilities in the large-u limit of a generalized hubbard model. *Phys. Rev. Lett.*, 61:1784 – 7, 1988.

[37] Evgeny Kozik, Michel Ferrero, and Antoine Georges. Nonexistence of the luttinger-ward functional and misleading convergence of skeleton diagrammatic series for hubbard-like models. *Physical Review Letters*, 114(15):156402, Apr 2015.

[38] B. Kyung, S. Allen, and A.-M. S. Tremblay. Pairing fluctuations and pseudogaps in the attractive hubbard model. *Phys. Rev. B*, 64:075116 – 1, 2001.

[39] B. Kyung, V. Hankevych, A.-M. Daré, and A.-M. S. Tremblay. Pseudogap and spin fluctuations in the normal state of the electron-doped cuprates. *Phys. Rev. Lett.*, 93:147004, Sep 2004.

[40] B. Kyung, J. S. Landry, D. Poulin, and A.-M. S. Tremblay. Comment on ""absence of a slater transition in the two-dimensional hubbard model"". *Phys. Rev. Lett.*, 90:099702 – 1, 2003.

[41] B. Kyung, J.-S. Landry, and A. M. S. Tremblay. Antiferromagnetic fluctuations and d-wave superconductivity in electron-doped high-temperature superconductors. *Phys. Rev. B*, 68:174502, 2003.

[42] P. Lederer, G. Montambaux, and D. Poilblanc. *J. Phys.*, 48:1613, 1987.

[43] P. A. Lee, T. M. Rice, and P. W. Anderson. Fluctuation effects at a peierls transition. *Phys. Rev. Lett.*, 31(7):462–465, Aug 1973.

[44] Ansgar Liebsch. Spectral weight of doping-induced states in the two-dimensional hubbard model. *Phys. Rev. B*, 81(23):235133, Jun 2010.

[45] G. G. Lonzarich and L. Taillefer. *J. Phys. C*, 18:4339, 1985.

[46] J. M. Luttinger and J. C. Ward. Ground-state energy of a many-fermion system. ii. *Phys. Rev.*, 118:1417–1427, Jun 1960.

[47] A. Macridin, Th. A. Maier, M. S. Jarrell, and G. A. Sawatzky. Physics of cuprates with the two-band hubbard model - the validity of the one-band hubbard model. *Phys. Rev. B*, 71:134527, 2005.

[48] G. D. Mahan. *Many-Particle Physics*. Kluwer Academic - Plenum publishers, New-York, 2000.

[49] G. D. Mahan. *Many-Particle Physics, 3rd edition, Section 6.4.4.* Kluwer/Plenum, 2000.

[50] T. A. Maier, M. Jarrell, T. C. Schulthess, P. R. C. Kent, and J. B. White. Systematic study of d-wave superconductivity in the 2d repulsive hubbard model. *Physical Review Letters*, 95(23):237001, 2005.

[51] Avella A. Mancini, F. Equation of motion method for composite field operators. *European Physical Journal B*, 36(1):37–56, 2003. cited By (since 1996) 21.

[52] Avella A. Mancini, F. The hubbard model within the equations of motion approach. *Advances in Physics*, 53(5-6), 2004. cited By (since 1996) 1.

[53] Avella A. Mancini, F. Green's function formalism for highly correlated systems. *Condensed Matter Physics*, 9(3):569–586, 2006. cited By (since 1996) 1.

[54] N. Martin, C. Gauvin-Ndiaye, and A.-M. S. Tremblay. Nonlocal corrections to dynamical mean-field theory from the two-particle self-consistent method. *Physical Review B*, 107(7):075158, February 2023.

[55] S. Massidda, N. Hamada, Jaejun Yu, and A. J. Freeman. Electronic structure of nd-ce-cu-o, a fermi liquid superconductor. *Physica C: Superconductivity*, 157(3):571 – 574, 1989.

[56] H. Matsui, K. Terashima, T. Sato, T. Takahashi, S.-C. Wang, H.-B. Yang, H. Ding, T. Uefuji, and K. Yamada. Angle-resolved photoemission spectroscopy of the antiferromagnetic superconductor nd[sub 1.87]ce[sub 0.13]cuo[sub 4]: Anisotropic spin-correlation gap, pseudogap, and the induced quasiparticle mass enhancement. *Phys. Rev. Lett.*, 94:047005, 2005.

[57] Jianqiao Meng, Guodong Liu, Wentao Zhang, Lin Zhao, Haiyun Liu, Xiaowen Jia, Daixiang Mu, Shanyu Liu, Xiaoli Dong, Jun Zhang, and et al. Coexistence of fermi arcs and fermi pockets in a high-tc copper oxide superconductor. *Nature*, 462(7271):335âĂŞ338, Nov 2009.

[58] N. Menyhard and J. Solyom. *J. Low Temp. Phys.*, 12:529, 1973.

[59] N. D. Mermin and H. Wagner. Absence of ferromagnetism or antiferromagnetism in one- or two-dimensional isotropic heisenberg models. *Phys. Rev. Lett.*, 17(22):1133–1136, Nov 1966.

[60] K Miyake, T Matsuura, and CM Varma. Relation between resistivity and effective mass in heavy-fermion and a15 compounds. *Solid state communications*, 71(12):1149–1153, 1989.

[61] P. Monthoux. Migdal's theorem and the pseudogap. *Phys. Rev. B*, 68(6):064408, Aug 2003.

[62] T. Moriya and K. Ueda. Antiferromagnetic spin fluctuation and superconductivity. *Rep. Prog. Phys.*, 66(8):1299–1341, 2003.

[63] TÃtru Moriya. *Spin Fluctuations in Itinerant Electron Magnetism*. Springer Series in Solid State Sciences, 1985.

[64] E. M. Motoyama, G. Yu, I. M. Vishik, O. P. Vajk, P. K. Mang, and M. Greven. Spin correlations in the electron-doped high-transition-temperature superconductor ncco. *Nature*, 445:186, 2007.

[65] S. Moukouri, S. Allen, F. Lemay, B. Kyung, D. Poulin, Y. M. Vilk, and A.-M. S. Tremblay. Many-body theory versus simulations for the pseudogap in the hubbard model. *Phys. Rev. B*, 61:7887–7892, Mar 2000.

[66] H. Nélisse, C. Bourbonnais, H. Touchette, Y. M. Vilk, and A.-M. S. Tremblay. Spin susceptibility of interacting electrons in one dimension: Luttinger liquid and lattice effects. *Eur. Phys. J. B (France)*, 12:351 – 65, 1999/12/.

[67] M. R. Norman, D. Pines, and C. Kallin. The pseudogap: friend or foe of high t c ? *Advances in Physics*, 54(8):715–733, 2005.

[68] Y. Onose, Y. Taguchi, K. Ishizaka, and Y. Tokura. Doping dependence of pseudogap and related charge dynamics in nd2-xcexcuo. *Phys. Rev. Lett.*, 87:217001, 2001.

[69] H. Park, K. Haule, and G. Kotliar. Cluster dynamical mean field theory of the mott transition. *Physical Review Letters*, 101(18):186403, 2008.

[70] E. Pavarini, I. Dasgupta, T. Saha-Dasgupta, O. Jepsen, and O. K. Andersen. Band-structure trend in hole-doped cuprates and correlation with t_{cmax}. *Phys. Rev. Lett.*, 87(4):047003, Jul 2001.

[71] D. C. Peets, D. G. Hawthorn, K. M. Shen, Young-June Kim, D. S. Ellis, H. Zhang, Seiki Komiya, Yoichi Ando, G. A. Sawatzky, Ruixing Liang, D. A. Bonn, and W. N. Hardy. X-ray absorption spectra reveal the inapplicability of the single-band hubbard model to overdoped cuprate superconductors. *Physical Review Letters*, 103(8):087402, 2009.

[72] P. Phillips and M. Jarrell. Comment on "measurement of x-ray absorption spectra of overdoped high-temperature cuprate superconductors: Inapplicability of the single-band hubbard model". *Phys. Rev. Lett.*, 105:199701, 2010.

[73] Michael Potthoff. Non-perturbative construction of the luttinger-ward functional. *arXiv preprint cond-mat/0406671*, 2004.

[74] T. Saikawa and A. Ferraz. Remnant fermi surface in a pseudogap regime of the two-dimensional hubbard model at finite temperature. *The European Physical Journal B - Condensed Matter and Complex Systems*, 20:65–74, 2001. 10.1007/PL00011093.

[75] Thomas Schaefer, Nils Wentzell, Fedor Åăimkovic, Yuan-Yao He, Cornelia Hille, Marcel Klett, Christian J. Eckhardt, Behnam Arzhang, Viktor Harkov, FranÃğois-Marie Le RÃľgent, and et al. Tracking the footprints of spin fluctuations: A multimethod, multimessenger study of the two-dimensional hubbard model. *Physical Review X*, 11(1):011058, Mar 2021.

[76] J. R. Schrieffer, X. G. Wen, and S. C. Zhang. Dynamic spin fluctuations and the bag mechanism of high-t_c superconductivity. *Phys. Rev. B*, 39(16):11663–11679, Jun 1989.

[77] H. J. Schulz. *Europhys. Lett.*, 4:609, 1987.

[78] Tigran A. Sedrakyan and Andrey V. Chubukov. Pseudogap in underdoped cuprates and spin-density-wave fluctuations. *Phys. Rev. B*, 81(17):174536, May 2010.

[79] David Sénéchal, P.-L. Lavertu, M.-A. Marois, and A.-M. S. Tremblay. Competition between antiferromagnetism and superconductivity in high-t[sub c] cuprates. *Phys. Rev. Lett.*, 94:156404, 2005.

[80] David Sénéchal and A.-M. S. Tremblay. Hot spots and pseudogaps for hole- and electron-doped high-temperature superconductors. *Phys. Rev. Lett.*, 92:126401, 2004.

[81] A. Shekhter and C. M. Varma. Considerations on the symmetry of loop order in cuprates. *Phys. Rev. B*, 80(21):214501, Dec 2009.

[82] K. S. Singwi and M.P. Tosi. *Solid State Physics*. Academic, New York, 1981.

[83] G. Sordi, K. Haule, and A. M. S. Tremblay. Finite doping signatures of the mott transition in the two-dimensional hubbard model. *Phys. Rev. Lett.*, 104(22):226402, Jun 2010.

[84] A. Tamai, M. Zingl, E. Rozbicki, E. Cappelli, S. RiccÃš, A. de la Torre, S. McKeown Walker, F.âĂĽY. Bruno, P.âĂĽD.âĂĽC. King, W. Meevasana, and et al. High-resolution photoemission on sr_2ruo_4 reveals correlation-enhanced effective spin-orbit coupling and dominantly local self-energies. *Physical Review X*, 9(2):021048, Jun 2019.

[85] Tom Timusk and Bryan Statt. The pseudogap in high-temperature superconductors: an experimental survey. *Reports on Progress in Physics*, 62(1):61, 1999.

[86] Y. Tokura, S. Koshihara, T. Arima, H. Takagi, S. Ishibashi, T. Ido, and S. Uchida. Cu-o network dependence of optical charge-transfer gaps and spin-pair excitations in single-cuo_2-layer compounds. *Phys. Rev. B*, 41(16):11657–11660, Jun 1990.

[87] A. M. S. Tremblay. Two-particle-self-consistent approach for the hubbard model. In F. Mancini and A. Avella, editors, *Strongly Correlated Systems: Theoretical Methods*, chapter 13, pages 409–455. Springer series, 2011.

[88] A. M. S. Tremblay, B. Kyung, and D. Sénéchal. Pseudogap and high-temperature superconductivity from weak to strong coupling. towards a quantitative theory. *Low Temp. Phys.*, 32(4-5):424–451, 2006.

[89] Michael A. Tusch, Yolande H. Szczech, and David E. Logan. Magnetism in the hubbard model: An effective spin hamiltonian approach. *Phys. Rev. B*, 53(9):5505–5517, Mar 1996.

[90] A. F. Veilleux. Master's thesis, Université de Sherbrooke, 1994.

[91] A. F. Veilleux, A.-M. Dare, Liang Chen, Y. M. Vilk, and A.-M. S. Tremblay. Magnetic and pair correlations of the hubbard model with next-nearest-neighbor hopping. *Phys. Rev. B*, 52:16255 – 63, 1995.

[92] Y. M. Vilk. Shadow features and shadow bands in the paramagnetic state of cuprate superconductors. *Phys. Rev. B*, 55(6):3870–3875, Feb 1997.

[93] Y. M. Vilk, Liang Chen, and A.-M. S. Tremblay. Theory of spin and charge fluctuations in the hubbard model. *Phys. Rev. B*, 49:13267–13270, May 1994.

[94] Y. M. Vilk and A.-M. S. Tremblay. Destruction of the fermi liquid by spin fluctuations in two dimensions. *J. Phys. Chem. Solids (UK)*, 56(12):1769 – 71, 1995.

[95] Y. M. Vilk and A.-M. S. Tremblay. Destruction of fermi-liquid quasiparticles in two dimensions by critical fluctuations. *EPL (Europhysics Letters)*, 33(2):159, 1996.

[96] C. Weber, K. Haule, and G. Kotliar. Strength of correlations in electron- and hole-doped cuprates. *Nature Physics*, 6(8):574–578, 2010.

[97] Y.M. Vilk and A.-M.S. Tremblay. Non-perturbative many-body approach to the hubbard model and single-particle pseudogap. *J. Phys. I France*, 7(11):1309–1368, 1997.

[98] Qingshan Yuan, Feng Yuan, and C. S. Ting. Doping dependence of the electron-doped cuprate superconductors from the antiferromagnetic properties of the hubbard model. *Phys. Rev. B*, 72(5):054504, Aug 2005.

[99] D. Zanchi. Angle-resolved loss of landau quansiparticles in 2d hubbard model. *Euophys. Lett.*, 55:376, 2001.

[100] F. C. Zhang and T. M. Rice. Effective hamiltonian for the superconducting cu oxides. *Phys. Rev. B*, 37:3759, 1988.

[101] Guo-qing Zheng, T. Sato, Y. Kitaoka, M. Fujita, and K. Yamada. Fermi-liquid ground state in the n-type $pr_{0.91}lace_{0.09}cuo_{4-y}$ copper-oxide superconductor. *Phys. Rev. Lett.*, 90(19):197005, May 2003.

Index